Sex-specific hippocampal metabolic signatures at the onset of systemic inflammation with lipopolysaccharide in the APPswe/PS1dE9 mouse model of Alzheimer's disease

Alessandra Agostini[1], Ding Yuchun[2,3], Bai Li[3], David A. Kendall[1,4], Marie-Christine Pardon[1]

[1]School of Life Sciences, Division of Physiology, Pharmacology and Neuroscience, Medical School, Queens Medical Centre, Nottingham, NG7 2UH, UK

[2]School of Computer Sciences, University of Nottingham, Jubilee Campus, Wollaton Road, Nottingham, NG8 1BB, UK

[3]Present address: School of Computing Science, Urban Sciences Building, Newcastle University, 1 Science Square, Science Central, Newcastle upon Tyne, NE4 5TG, UK

[4]Present address: PharmNovo UK Ltd, Woodlands Lane, CH488DA, UK

* Corresponding author: **Marie-Christine Pardon, PhD**

School of Life Sciences
Division of Physiology, Pharmacology and Neuroscience
University of Nottingham Medical School
Queen's Medical Centre
Nottingham, NG7 2UH, United Kingdom
Ph: +44 115 82 30149
FAX: +44 11582 30142
email: marie.pardon@nottingham.ac.uk

Number of figures: **8**
Number of tables: **1**
Number of words in the abstract: **287**
Number of words in the manuscript (including tables and figure legends): **12,395**
Number of words in the introduction: **1,275**
Number of words in the discussion: **4,251**

Abstract:

Systemic inflammation enhances the risk and progression of Alzheimer's disease (AD). Lipopolysaccharide (LPS), a potent pro-inflammatory endotoxin produced by the gut, is found in excess levels in AD where it associates with neurological hallmarks of pathology. Sex differences in susceptibility to inflammation and AD progression have been reported, but how this impacts on LPS responses remains under investigated. We previously reported in an APP/PS1 model of AD that systemic LPS administration rapidly altered hippocampal metabolism in males. Here, we used untargeted metabolomics to comprehensively identify hippocampal metabolic processes occurring at onset of systemic inflammation with LPS (100µg/kg, i.v.) in APP/PS1 mice, at an early pathological stage, and investigated the sexual dimorphism in this response. Four hours after LPS administration, pathways regulating energy metabolism, immune and oxidative stress responses were simultaneously recruited in the hippocampi of 4.5-month-old mice with a more protective response in females despite their pro-inflammatory and pro-oxidant metabolic signature in the absence of immune stimulation. LPS induced comparable behavioural sickness responses in male and female wild-type and APP/PS1 mice and comparable activation of both the serotonin and nicotinamide pathways of tryptophan metabolism in their hippocampi. Elevations in *N*-methyl-2-pyridone-5-carboxamide, a major toxic metabolite of nicotinamide, correlated with behavioural sickness regardless of sex, as well as with the LPS-induced hypothermia seen in males. Males also exhibited a pro-inflammatory-like downregulation of pyruvate metabolism, exacerbated in APP/PS1 males, and methionine metabolism whereas females showed a greater cytokine response and anti-inflammatory-like downregulation of hippocampal methylglyoxal and methionine metabolism. Metabolic changes were not associated with morphological markers of immune cell activation suggesting that they constitute an early event in the development of LPS-induced neuroinflammation and AD exacerbation. These data suggest that the female hippocampus is more tolerant to acute systemic inflammation.

Keywords: Inflammation, Lipopolysaccharide, Alzheimer's disease, APP/PS1 mouse model, sex differences, hippocampus, microglia, metabolomics, serotonin, methionine.

1. Introduction

Alzheimer's disease (AD), the most common senile dementia, is characterised by a progressive cognitive decline accompanied by the accumulation of aggregated amyloid beta (Aβ) plaques, neurofibrillary tangles made of hyperphosphorylated tau protein, severe brain atrophy and neuroinflammation. The causes of AD are far from being understood, but systemic infection and inflammation have emerged as key modulators of its risk and progression. A number of genes conferring susceptibility to inflammatory conditions have indeed been found to be associated with a predisposition to AD (Karch and Goate, 2015; Malik et al., 2015; Yokoyama et al., 2016), whereas circulating levels of acute phase proteins or pro-inflammatory cytokines were found to be elevated in non-demented subjects presenting with a higher risk of developing late-onset AD (Eikelenboom et al., 2012; Koyama et al., 2013), and in patients in the prodromal, mild cognitive impairment (MCI) phase of AD (Bettcher and Kramer, 2014; King et al., 2018; Trollor et al., 2010). Infection-induced systemic inflammation has been proposed as a mechanistic driver of AD pathogenesis (Ashraf et al., 2019; Giridharan et al., 2019), and the presence of acute inflammatory events, such as respiratory infections or delirium have also been associated with exacerbations of clinical presentation and precipitous cognitive decline in AD patients (Holmer et al., 2018; Holmes et al., 2009; Ide et al., 2016). Altogether, this suggests that AD patients and people at risk of developing the disease are more susceptible to inflammatory conditions, and that such vulnerability contributes to the development of clinical features of AD. The incidence and prevalence of AD are generally higher in women, and although this may be due to their longer life expectancy, they exhibit faster cognitive decline and brain atrophy than men (Ferretti et al., 2018; Podcasy and Epperson, 2016) and are also thought to produce higher inflammatory responses and be more susceptible to inflammatory conditions (Klein and Flanagan, 2016; Roved et al., 2017). Some sex differences in the association between specific pro-inflammatory mediators and clinical outcomes have been noted (Trollor et al., 2010), but this has not been investigated in detail.

Systemic inflammation is thought to be the mechanism whereby acute, accumulative or chronic infections can trigger AD pathogenesis (Ashraf et al., 2019; Giridharan et al., 2019). In preclinical mouse models, lipopolysaccharide (LPS), mimicking gram-negative bacterial infection, and other acute systemic inflammatory stimuli have been found to exacerbate cognitive dysfunction, Aβ plaque load and tau phosphorylation (Barron et al., 2017; Cunningham and Hennessy, 2015; Nazem et al., 2015). While the use of LPS to model systemic inflammation has been debated, in part because of the high doses used which are more relevant to sepsis than to the chronic low grade inflammation associated with ageing, MCI and AD (Barron et al., 2017; Cunningham and Hennessy,

2015; Varatharaj and Galea, 2017), a comparison of three models yielded the conclusion that LPS is a suitable model for studying the impact of new therapies for acute systemic inflammation (Seemann et al., 2017). But importantly, this endotoxin is produced by the gut microbiota in response to systemic infections, and its subsequent release in the systemic circulation plays a key role in the development and persistence of systemic inflammation (Maldonado et al., 2016; Thorburn et al., 2018). Circulating LPS levels are elevated in AD patients (Zhang et al., 2009) and the recent discoveries of LPS infiltration in the post-mortem AD brain where it associates with Aβ plaques, highlights the clinical relevance of this immune model (Zhan et al., 2018; Zhan et al., 2016; Zhao et al., 2017). This has led to the proposal that endogenous LPS accumulation could play a critical role in the pathophysiology of the common, sporadic form of AD (Pistollato et al., 2016; Sochocka et al., 2019; Zhan et al., 2018). To the best of our knowledge, endogenous LPS levels have not been quantified in AD models. Differences in gut microbiota composition between genetic models of AD and their wild type control, consistent with endotoxemia and susceptibility to LPS, have been reported and found associated with the progression of cerebral amyloidosis (Brandscheid et al., 2017; Harach et al., 2017; Zhang et al., 2017). Removal of microbiota from a humanized AD model delayed substantially Aβ plaque deposition, while colonisation of these mice with gut microbiota from a conventional AD model, but not from their wild type control, accelerated Aβ deposition (Harach et al., 2017). There is, therefore, a need to better understand the mechanisms whereby systemic LPS affects the brain and contributes to AD progression.

LPS, is an agonist of the toll-like receptor 4, which in the brain, is almost exclusively expressed by microglia (Hanke and Kielian, 2011), the resident immune cell in the central nervous system. Microglia play a critical role in the clearance of Aβ and tau aggregates, and their dysfunction is associated with the genetic risk of developing AD (Hansen et al., 2018; Perea et al., 2018). At low doses able to induce physiologically relevant low grade inflammation, penetration of LPS in the mouse brain is limited in the absence of blood brain barrier dysfunction (Banks and Robinson, 2010; Varatharaj and Galea, 2017). However, pro-inflammatory changes in microglia can be seen as early as 4 hours post-inoculation depending on the disease status (Murray et al., 2011; Pardon et al., 2016). Using magnetic resonance spectroscopy, we previously observed that mild systemic inflammation, induced with the low 100µg/kg dose of LPS, rapidly altered hippocampal metabolism in the APPswe/PS1dE9 (APP/PS1) mouse model of amyloidosis and its wild-type (WT) littermates at early to advanced pathological stages (Pardon et al., 2016). The metabolic changes occurring within 4 hours of immune stimulation also discriminated the microglial response of WT and APP/PS1 mice (Pardon et al., 2016). Variations in brain metabolism and substrate availability are thought to influence microglial function, although the mechanisms involved are not clear (Ghosh et al., 2018). In the same APP/PS1 mouse

model of amyloidosis used in our previous study, age- and region-specific metabolic perturbations have been reported in the brain of males and females, but sex differences have not been systematically tested (Gonzalez-Dominguez et al., 2014; Maroof et al., 2014), although they have been seen with brain aging in WT mice and are thought to contribute to differential susceptibility to AD-like pathology (Zhao et al., 2016). Preclinical data from genetically altered mouse models of AD indeed confirm that cerebral amyloidosis indeed develops faster in females than in males (Li et al., 2016; Wang et al., 2003). Thus, metabolic responses to systemic inflammation could mediate exacerbation of AD-like pathology and the impact of sex on disease progression.

In this context, we aimed, in the present study, to gain further understanding of the metabolic processes occurring at onset of systemic inflammation with LPS, and used untargeted metabolomics to comprehensively identify pathways that rapidly respond to immune stimulation in WT and APP/PS1 mice of both sexes. We tested the hypothesis that APP/PS1 mice would be more susceptible to the metabolic effects of LPS, and postulated a sexual dimorphism in the hippocampal metabolic response to systemic inflammation. As reviewed above, systemic inflammation is expected to be an early event in the pathogenesis of AD; we therefore used 4.5-month-old mice, an age characterised by the appearance of the first plaques and subtle cognitive deficits (Bonardi et al., 2011; Malm et al., 2011; Maroof et al., 2014). Our results indicate that pathways regulating energy metabolism, immune and oxidative stress responses are simultaneously recruited 4 hours after systemic LPS, and comparably in the hippocampus of both WT and APP/PS1 mice, whose hippocampal metabolism was similar in the absence of immune stimulation. While unchallenged females exhibited a pro-inflammatory and pro-oxidant hippocampal metabolic signature compared to males, the recruitment of some pathways at onset of systemic inflammation was sex-dependent with the metabolic response of females shifting towards a more pronounced anti-inflammatory and neuroprotective component than males, which also showed more severe sickness symptoms at this time point.

2. Material and methods

2.1. Ethics statement

All procedures were carried out in accordance with the UK Animals (Scientific Procedures) Act of 1986 under project license 40/3601, approved by the University of Nottingham Ethical Review Committee and are reported according to the ARRIVE guidelines (Kilkenny et al., 2010). All analyses were performed in blind.

2.2. Animals

Forty-four 4.5-month-old male and female APPswe/PS1dE9 (APP/PS1, (Jankowsky et al., 2004)) mice and their wild-type (WT) littermates were used (n=5-6 per sex, genotype and treatment). All experimental animals were bred and maintained in the University of Nottingham Biomedical Service Unit as previously described (Pardon et al., 2016). Genotyping was performed by Transnetyx (Cordova, TN, USA). Mice were maintained group-housed in individually vented cages (3-4 per cage) under standard husbandry conditions with *ad libitum* access to food and water, and were provided with nesting material and a play tube. The room was on a 12/12 h light cycle with lights on at 07:00 h; temperature, relative humidity and air exchange were automatically controlled.

2.3. Drug treatment

Lipopolysaccharide (LPS, Escherichia coli serotype Sigma0111:B4, Sigma Aldrich) was dissolved in phosphate buffered saline (PBS, Sigma Aldrich) at a concentration of 200 µg/ml, and stored in aliquots at −20°C until use. On the day of the experiment, LPS was further diluted 1:2 in PBS to a final concentration of 100 µg/ml. Mice were injected intravenously (i.v.) in the lateral tail vein with 100 µg/kg of LPS, or an equivalent volume of its vehicle PBS, as previously described (Pardon et al., 2016).

2.4. Study design

The timeline of the experiment is represented in Fig. 1A. 4.5-month-old male and female APP/PS1 and WT mice were randomly allocated to the LPS or PBS treatment groups (n=5-6). Baseline behavioural assessment was carried out on days 1 & 2. Mice were first tested for spatial working memory performance and exploratory drive in the spontaneous alternation test (Day 1). They were then trained to burrow food in groups overnight in their home cage (Deacon, 2012) and on Day 2, underwent baseline food burrowing testing over 4 hours while singly housed. On Day 3, mice were challenged with LPS (100µg/kg i.v.) or PBS (1µl/g of body weight). Post-treatment sickness effects were assessed 4 hours after injection in the food burrowing and spontaneous alternation tests, by monitoring changes in body weight and assessing body temperature taken using a rectal probe at the time of culling. Immediately after the spontaneous alternation task, mice were culled by cervical dislocation and trunk blood was collected. Their brains were removed; the hippocampi were dissected from one hemisphere, snap frozen and stored at -80°C until use for metabolomics. The second hemisphere was post-fixed by immersion in 4% paraformaldehyde, stored at 4–8 °C for a minimum of 24 hours, and then embedded in paraffin wax on a tissue embedding station (Leica TP1020).

2.5. Behavioural assessment

2.5.1. Food Burrowing

Food burrowing is a species-specific behaviour largely, dependent of the integrity of the hippocampus (Deacon et al., 2002), which is suppressed in response to systemic inflammation (Teeling et al., 2007). The protocol was adapted from one previously described (Geiszler et al., 2016). A glass jar containing 30g of food pellets broken into small pieces was added to the home cage overnight for training in groups, or in individual cages for the two test sessions, with *ad libitum* access to food and water. The amount of food displaced from the jar was recorded, expressed as a percentage from the 30g provided, and used as a measure of food burrowing performance. To assess sickness effects, the difference between pre- and post-injection burrowing performance was calculated.

2.5.2. Spontaneous Alternation

Spontaneous alternation was used as previously described (Geiszler et al., 2016; Maroof et al., 2014) to assess spatial working memory and exploratory drive. The latter is suppressed in response to LPS-induced sickness and is a potential confounding factor for the assessment of cognitive effects (Cunningham and Sanderson, 2008). The Y-shaped maze comprised three identical transparent Plexiglas® arms at a 120° angle from each other (41.5 cm in length and 6 cm in width surrounded by 15 cm high transparent Perspex walls). The start point (6 cm x 7.5 cm) was located in the center of the maze, and the mice were allowed to freely explore the three arms over five minutes. The number of alternations was recorded manually and expressed as a percentage of alternations to estimate spatial working memory performance, while the number of arms visited was used as an indication of exploratory drive. To assess sickness effects, the difference between pre- and post-injection performance was calculated. Mice that entered only one arm after the LPS challenge (1 WT female, 1 WT male and 2 APP/PS1 males) were excluded from sickness data as their alternation rate post-injection could not be calculated, but remained included in the analysis of baseline performance.

2.6. Immunohistochemical analyses

2.6.1. Immunohistochemistry

7 µm-thick coronal sections were cut throughout the hippocampus using a microtome (Microtome Slee Cut 4060), mounted on APES-coated slides and dried

overnight at 40 °C. Immunostaining of the microglial marker Ionized calcium binding adaptor molecule 1 (Iba1) and the astrocyte marker glial fibrillary acidic protein (GFAP) was carried out using standard protocols as previously described (Pardon et al., 2016), in 6-8 brain slices per brain. Incubation with rabbit anti-Iba1 [Wako, cat. nr. 019–19741; 1:6000 in PBS-Tween (0.05% Tween-20 in PBS)] or anti-GFAP (Biogenix, cat. nr. AM020-5M, 1:4000 in PBS-T) antibodies was carried out for 1 h at room temperature. Biotinylated secondary antibody (Vectastain Elite ABC Kit, Rabbit IgG, Vector Labs, Burlingame, CA cat. nr. PK-6101, 1:200 in PBS-T) was applied for 30 min. Tissue was washed, exposed to ABC-HRP (Vectastain Elite ABC Kit R.T.U, Vector Labs, cat. nr. PK-7100), labelled with DAB peroxidase substrate (Vector Labs cat. SK-4100) according to manufacturer's instructions, and counterstained using a haematoxylin and eosin protocol. Digital focused photo-scanning images were then acquired using a Hamamatsu NanoZoomer-XR 2.0-RS C10730 digital scanning system with TDI camera technology a NanoZoomer (Hamamatsu Photonics K.K. Systems, Japan) at 20× magnification and visualised using NDP.view2 (NanoZoomer Digital Photography).

2.6.2. Semi-automated quantification of Iba1 and GFAP immunostaining

For segmentation of microglia and astrocytes, and extraction of microglial morphometric features, we used custom made software (Matlab) adapted from our previous studies (Ding et al., 2016; Pardon et al., 2016) and applied to the following regions of interest: whole hippocampus, hippocampal CA1, CA2, CA3 and dentate gyrus (DG) subfields. Examples of the semi-automated extraction of regions of interest selection are shown in Suppl. Fig. 5A. This provided the percentage area occupied by glial cells, the number of Iba1- and GFAP- positive cells, used as a measure of microglial and astrocyte density, respectively, and the size of microglial soma, used as a morphometric marker of microglia activation and known to be sensitive to LPS (Kozlowski and Weimer, 2012; Kreisel et al., 2014; Pardon et al., 2016).

2.7. Multiplex

Plasma levels of interleukin 1 beta (IL-1β), IL-6, IL-10, interferon gamma (IFN-γ) and tumour necrosis factor alpha (TNF-α) were determined using the Bio-Plex ProTM Mouse Cytokine 23-Plex, Group I assay and Bio-Plex array reader, and analysed using the Bio-Plex Manager Software (Bio-Rad Laboratories, Berkeley, CA, USA) according to the manufacturer's instructions. The cytokine panel was designed to provide a measure of key cytokines known to respond to LPS and to play a role in AD. IL-1β data were deemed unreliable and were excluded from the results section.

2.8. Mass spectrometry

2.8.1. Metabolomic profiling by LC-MS

Hippocampal tissues were weighed and then homogenised with chloroform/methanol/water (1:3:1, 10 µl/mg) using Retsch MM301 ball mill equipment for 3 min. The extraction solvent and sample rack for the ball mill were pre-cooled at -20 °C. The homogenised tissues were mixed vigorously for 1 h at 4 °C and then centrifuged at 15,000×g for 10 min at 4 °C. After centrifugation, the supernatant was collected and stored at -80 °C prior to LC-MS analysis. A quality control sample was prepared by mixing an equal volume of all samples in order to assess instrument performance (Pereira et al., 2010). Chromatographic separation was performed using a ZIC-pHILIC column (150 mm × 4.6 mm, 5 µm, Merck Sequant). The column was maintained at 45 °C with a flow rate of 300 µl/min as previously described (Surrati et al., 2016). Briefly, the mobile phase consisted of 20 mM ammonium carbonate in water (A) and 100% acetonitrile (B), and the tissue extracts were eluted with a linear gradient over 24 min as follows: 80% B (0 min) to 5% B over 15 min to 5% B with a 2 min linear gradient, followed by re-equilibration with 80% B. A 10 µl injection of each extract was employed for LC-MS analysis. An Exactive MS (Thermo Fisher Scientific, Hemel Hempstead, UK) was used to acquire spectral data in full scan (*m/z* 70-1400, resolution 50 000) and both positive and negative electrospray ion modes. The capillary temperature and probe temperature were maintained at 275 and 150 °C, respectively as previously described (Creek et al., 2011).

2.8.2. LC-MS data processing

XCMS was used to pre-process raw LC-MS data for untargeted peak-picking (Tautenhahn et al., 2008) and mzMatch was employed for peak matching and annotation of related peaks (Scheltema et al., 2011). The processed data was then imported into IDEOM for noise filtering and putative metabolite identification (Creek et al., 2012). Metabolite identification was carried out by matching accurate masses and retention times of authentic standards but when standards were not available, accurate masses and predicted retention times were used (Sumner et al., 2007). Metabolites were filtered in IDEOM to have retention time errors of below 35% and mass errors below three parts per million (Vincent et al., 2014).

2.9. Data analysis

Data are presented as mean ± SEM (standard error of the mean) and were analysed using InVivoStat (Clark et al., 2012), unless otherwise stated. Baseline behavioural and body weight data, sickness scores, histological and cytokine data were all subjected to 3-way ANOVAs with genotype, sex and treatment, followed, where appropriate, by planned comparisons. To assess the effect of the PBS and LPS challenges on behavioural data and to compare baseline and post-injection data, we used 3-way ANOVAs with genotype, sex

and treatment and repeated measure over time, followed, when appropriate, by planned comparisons. The following pairwise comparisons were decided a priori: i) PBS-treated WT *vs* APP/PS1 mice within each sex to test for genotype differences; ii) PBS-treated males *vs* females within each genotype to test for sex differences; ii) PBS- *vs* LPS-treated mice within each sex and genotype condition to test for differences caused by systemic inflammation with LPS and, where appropriate, iv) baseline *vs* post-injection data within each experimental group to test for the effect of the PBS or LPS challenge. Cytokine and food burrowing data were rank-transformed to normalise the distribution, but presented as non-normalised responses (Deacon, 2012). The number of arm entries was used as a covariate for the analysis of spontaneous alternation performance, in order to control for confounding effects of LPS-induced behavioural suppression.

For LC-MS data, variable selection was performed as a by-product of a classification model. Data were first subjected to multivariate analyses by principal component analysis-class (PCA) and orthogonal partial least squares-discriminant analysis (OPLS-DA), using SIMCA-P version 15.02 (Umetrics AB, Umea, Sweden), in order to detect global metabolic differences between experimental conditions. This was followed by OPLS-DAs applied to models including 2 classes: i) WT *vs* APP/PS1 PBS-treated mice, to identify potential metabolic differences due to the genotype in the absence of immune stimulation, ii) male *vs* female PBS-treated mice, to identify sex-dependent metabolic differences; iii) LPS *vs* PBS for all mice to identify effects global effects of LPS; iv) LPS *vs* PBS for each sex separately to identify sex-dependent metabolic responses to LPS. Mass ions which contributed to separations and clusters were selected according to the variable importance in projection (VIP), a weighted sum of the PLS weight which indicates the importance of the model. VIP values greater than 1.5 were first considered indicative of significant differences between groups. Next, these metabolites were subjected to three-way ANOVAs with genotype, sex and treatment as between subject factors, to confirm the statistical significance of these factors and test for significant interactions between them. Metabolites from this list for which significant overall effects of treatment, or sex X treatment interaction were found, were also considered as potential discriminant of the LPS response within each sex if VIP values from the OPLS-DA models testing the effect of LPS within each sex were greater than 1. This was followed, where appropriate, by planned comparisons, as defined above.

Relationships between behavioural, cytokine, glial and metabolic data, and whether these associations were dependent upon the genotype, sex or treatment, were tested using the Pearson correlation coefficient, for which statistically significant values above 0.7 were considered as strong associations.

$P \leq 0.05$ was considered statistically significant for all analyses.

3. Results

3.1. Systemic LPS-induced sickness

To assess whether APP/PS1 mice responded more strongly to LPS in the early hours after systemic injection than their WT littermates, and to explore the sex dependency of this response, we assessed LPS-induced sickness using physiological measures and by monitoring behavioural suppression from baseline pre-injection performance in two tasks. Results of the three-way ANOVAs on these measures are presented in Suppl. Table 1.

3.1.1. Body mass and rectal temperature

Body mass was overall lower in females regardless of their genotype ($F_{(1,36)}$ = 152.67, p=0.005; Suppl. Fig 1A). Within APP/PS1 mice, females (p<0.0001), but not males (p=0.87), weighed less than their WT littermates (Genotype x Sex: $F_{(1,36)}$ = 12.22, p=0.0013) but none of the experimental groups showed significant weight loss 4 hours after the LPS or PBS challenge (Suppl. Fig 1A). Rectal body temperature was overall reduced by LPS ($F_{(1,34)}$=17.09, p=0.0002), but partial comparisons showed that this decrease was only significant in males (minus ~1.2-1.5°C, p<0.05 for both WT and APP/PS1 males compared to PBS-treated males, Fig. 1B).

3.1.1. LPS suppressed food burrowing activity

Food borrowing behaviour was overall suppressed by systemic LPS (p<0.0001) but unaffected by PBS (p=0.52; Treatment x Time: $F_{(1,36)}$=9.47, p=0.004, Fig. 1C). Significant reductions in food burrowing behaviour 4 hours after injection of LPS were seen in WT males (p=0.008), WT females (p=0.002) and APP/PS1 females (p=0.04), but not in APP/PS1 males (p=0.10) whose baseline performance was lower than of WT males females and more variable than of APP/PS1 females (Fig. 1C).

3.1.2. LPS suppressed exploratory drive without altering spatial working memory performance

Exploration of the Y maze, assessed through the number of arm visits, did not differ between any experimental groups at baseline (Fig. 1D) but was suppressed by LPS, regardless of the genotype (p<0.0001 compared to baseline in all cases, Fig. 1E, and p<0.01 compared to PBS-treated mice in all cases, Suppl. Fig 1B; Treatment: $F_{(1,36)}$=20.66, p<0.0001). All PBS-treated groups, but female APP/PS1, also showed a milder reduction in Y maze exploration 4 hours after injection (p<0.05 in all cases, Fig. 1E; Treatment x Time: $F_{(1,36)}$=58.55, p<0.0001), reflecting habituation to the apparatus. Spontaneous alternation performance was overall lower in females compared to males

($F_{(1,35)}$=4.25, p=0.048, Fig. 1F) at baseline but not following PBS or LPS administration (Suppl. Fig 1B), and none of the treatments altered the alternation rate (Fig. 1G).

3.2. Systemic LPS-induced circulating cytokines

We assessed systemic inflammation 4 hours after inoculation with LPS by quantifying plasma levels of 5 pro- or anti-inflammatory cytokines. Results of the three-way ANOVAs applied to circulating cytokine levels are presented in Suppl. Table 2.

We found that, regardless of sex and genotype, LPS led to significant increases in plasma levels of IL-6 ($F_{(1,30)}$=116.2, p<0.0001, post-hoc tests: p<0.0002 compared to PBS-treated mice in all cases, Fig. 2A), a cytokine known to exert both pro-and anti-inflammatory effects. Elevated levels of the pro-inflammatory cytokine TNF-α after LPS ($F_{(1,30)}$=7.82, p=0.009) were only significant in WT females (p=0.02 compared to PBS-treated mice, Fig. 2B), whereas LPS-treated females also exhibited significantly higher levels of the anti-inflammatory cytokine IL-10 (Treatment x Sex: $F_{(1,30)}$=4.54, p=0.04), regardless of their genotype (WT: p=0.0004 and APP/PS1: p=0.007, compared to PBS-treated mice, Fig. 2D). Circulating INF-γ ($F_{(1,30)}$=2.70, p=0.11, Fig. 2C) levels were unaltered by LPS.

3.3. Hippocampal metabolic profiles

3.3.1. Identification of discriminant metabolites

To investigate LPS-induced metabolic changes in the hippocampus, and whether this was dependent upon the genotype and/or and sex of the mice, we used LC-MS analysis. Metabolic data from all hippocampal extracts were first subjected to PCA, to identify trends, and OPLS-DA to detect global metabolic differences between experimental conditions. Then, OPLS-DAs applied to models including 2 classes were carried out in order to identify metabolites differentially expressed in response to LPS or as a function of sex or genotype. The quality of these models was assessed by the R^2 and Q^2 parameters which indicate the variance explained by the model and predicted variance after cross-validation, respectively and range between 0 and 1, with Q2 values above 0.5 (50% of variance predicted) revealing good separation between the classes tested.

Metabolites were considered to contribute to the separations and clusters associated with each experimental condition when their VIP values from OPLS-DA models was greater than 1.5 if subsequent 3-way ANOVAs confirmed their ability to discriminate genotypes, sexes, treatment conditions and/or interactions between these factors. As shown in Table 1, 98 metabolites were identified as potential discriminators of the disease status, sex and/or LPS response, after confirmation with ANOVAs. Their function in the brain and potential implication in sex differences in brain function, AD progression and/or inflammatory processes, when known, is presented in Suppl. Table 3.

3.3.1.1. Global metabolic differences reveal distinct clustering between PBS- and LPS treated mice

PCA analysis preformed on all animals gave 6 components explaining 59.6% of the variance. The plots pertaining to the first two components revealed, as the major trend, a separation between LPS-treated males and females (Fig. 3A). This was confirmed by the global OPLS-DA which gave 5 components (1 predictive and 4 orthogonal) with a variance explained (R2) of 99.4% and predictive variance (Q2) of 88.6%. As shown on Fig.3B a clear separation was found between PBS- and LPS-treated male and female WT and APP/PS1 mice 4 hours after the immune challenge, indicating that metabolic changes rapidly occurred in response to LPS, regardless of sex or disease status. Within LPS-treated mice, some separation between sexes was also seen, regardless of genotype (Fig. 3B), suggesting that the response to LPS was in part, sex-dependent. Metabolic differences between genotypes were not apparent. Thirty-seven metabolites with VIP values above 1.5 were identified from the global OPLS-DA model. Thirty-two of them showed statistically significant overall effects of treatment, revealing major changes in amino acids, carbohydrate, nucleotide, lipid and energy metabolism in response to LPS, regardless of sex and genotype (Table 1).

Subsequent 2-class OPLS-DAs between PBS- and LPS-treated mice within each sex, also gave strong models with a variance explained of 100% and a predicted variance above 85%. Five components were identified in males (1 predictive + 4 orthogonal; R^2= 1.00, Q^2 = 0.857) and 7 in females (1 predictive and 6 orthogonal; R^2= 1.00, Q^2 = 0.863). Loading plots of predictive *vs* first orthogonal components revealed a clear separation between treatment groups, regardless of genotype, in both sexes (Fig. 3C&D, for males and females, respectively). The hippocampal metabolic response of males to LPS was characterised by significant changes in 53 metabolites (Table 1). Thirty-six discriminant metabolites with VIP values above 1.5 were identified from the 2-class OPLS-DA between PBS- and LPS-treated males, and confirmed with ANOVAs. Statistical significance between these groups was also confirmed for another 13 metabolites identified from the global OPLS-DA model, and for 4 the 11 metabolites with confirmed Sex X Treatment interaction effects. The hippocampal metabolic response to LPS in females was characterised by statistically significant changes in 50 metabolites (Table 1). Twenty discriminant metabolites with VIP values above 1.5 were identified from the 2-class OPLS-DA model, and confirmed with ANOVAs. Statistical significance between PBS- and LPS-treated females was also confirmed for another 20 metabolites identified from the global OPLS-DA model, and for 9 of the 11 metabolites showing sexually dimorphic responses to LPS.

3.3.1.2. Discriminant metabolites between sexes in PBS-treated mice

Since the metabolic response to LPS was found to be, at least in part, sex-dependent, a 2-class OPLS-DA was also carried out between PBS-treated males and females in order to identify whether the hippocampal metabolic profile of males and females differs in the absence of immune stimulation. This gave a strong model with 1 predictive and 2 orthogonal components (R^2= 0.985, Q^2 = 0.809) and clear separation between sexes, regardless of genotype (Fig. 3E). Sex differences in hippocampal metabolism were characterised by significant changes in the levels of 40 metabolites, showing major differences in amino acids, carbohydrate and fatty acyls metabolism (Table 1). While forty-three metabolites with VIP values above 1.5 were identified from the 2-class OPLS-DA model, 36 were confirmed with statistically significant sex effects in PBS-treated mice. Sex differences in PBS-treated mice were also confirmed for another 4 metabolites for which significant effects of sex or sex X treatment interaction were revealed by individual ANOVAs.

3.3.1.2. Lack of major metabolic perturbations in the hippocampus of 4.5-month-old APP/PS1 mice

Next we carried out a 2-class OPLS-DA between genotypes in PBS-treated mice to confirm the lack of apparent differences in the hippocampal metabolic profile of WT and APP/PS1 mice. This gave a weak model explaining 24.4% of the variance between genotypes (3 predictive, 0 orthogonal components; R^2= 0.697, Q^2 = 0.244), revealing a lack of complete separation between WT and APP/PS1 mice (Fig. 3F). This indicates that the metabolic profile of PBS-treated WT and APP/PS1 mice was not strongly influenced by the disease status, consistent with our previous study in males showing a lack of clear differences in hippocampal metabolism between WT and APP/PS1 mice at 4 and 8 months of age (Maroof et al., 2014).

Accordingly, only 2 metabolites with VIP values above 1.5 could be identified with this 2-class OPLS-DA model and confirmed with ANOVAs. Significant genotype effects were also found for another 3 out of the 98 validated metabolites, with confirmed statistical significance within PBS-treated mice (Table 1). Although some separation in hippocampal metabolism appear to be emerging between 4.5-months-old WT and APP/PS1 males (Fig. 3F), statistically significant genotype differences were predominantly seen in females (Suppl. metabolomics results and Suppl. Fig. 2). This apparent distinct clustering, which cannot be explained by orthogonal variation within males, may be due to a combination of borderline differences that are not sufficiently severe to reach statistical significance in individual ANOVAs. Indeed, 59 additional metabolites showed VIP values comprised between 1 and 1.5 (Table1).

3.3.2. Metabolic pathways with sex differences and responsive to systemic LPS

The analyses revealed that regardless of sex and disease status, LPS predominantly affected the activity of four metabolic pathways: tryptophan (Fig. 4) and methionine (Fig. 5), regardless of sex and disease status, pyruvate in males (Fig. 6) and methylglyoxal in females (Fig. 7); while sex differences were also found in the absence of immune stimulation within the methionine (Fig. 5) and pyruvate (Fig. 6) metabolic pathways.

Changes in other metabolites as well as their role in brain function and implications in sex differences, AD progression and immune processes, are reported in Suppl. metabolomics results, Suppl. Fig. 3 and Suppl. Table 3, respectively.

3.3.2.1 LPS-induced tryptophan metabolism regardless of sex and disease status

Tryptophan metabolic pathways are represented Fig.4. Tryptophan is an essential amino acid involved in protein synthesis and substrate of a number of bioactive substances. It is the precursor of the monoaminergic neurotransmitter serotonin which plays a critical beneficial role in modulating behaviour, cognition, mood, stress and inflammatory responses (Hoglund et al., 2019). The majority of tryptophan is, however, catabolised by the kynurenine pathway, the first part of the tryptophan nicotinamide pathway (Fukuwatari and Shibata, 2013), which has been linked to impaired behavioural and stress responses, and proinflammatory changes to the brain (Hoglund et al., 2019). Kynurenine metabolism leads to activation of nicotinamide adenine dinucleotide (NAD) metabolism, an important regulator of various energy metabolism pathways and cellular homeostasis, *via* the biosynthesis of quinolinic acid, forming the second part of the tryptophan-nicotinamide pathway (Fukuwatari and Shibata, 2013; Yaku et al., 2018).

Both the serotonin and nicotinamide pathways of tryptophan metabolism, illustrated Fig. 4, were found to be stimulated in the hippocampus of LPS-treated mice. This was reflected by elevated L-tryptophan levels (Fig. 4A), associated with higher levels of 5-Hydroxylindoleacetate (5-HIAA), the end product of the serotonin pathway of tryptophan metabolism, as well as of N1-methyl-2-pyridone-5-carboxamide (2PY, Fig. 4B&C), a toxic degradation product of nicotinamide (Lenglet et al., 2016) whose levels reflect the amount of nicotinamide biosynthesized from tryptophan (Shibata and Matsuo, 1990) and correlate with upstream activation of the kynurenine pathway of tryptophan metabolism (Mayneris-Perxachs et al., 2016).

Correlation analyses indicated that fluctuations in 2PY levels were associated with a number of parameters related to the sickness response to LPS. We found negative associations between 2PY levels and i) rectal temperature (Fig. 4D) in males, which exhibited LPS-induced hypothermia (males: $r = -0.718$, $p = 0.0004$; females: $r = -0.21$, $p = 0.37$); ii) the number of arms visited in the spontaneous alternation test 4 hours after the injection ($r = -0.80$, $p < 0.0001$; Fig. 4E), in both males ($r = -0.837$, $p < 0.0001$) and females ($r = -0.791$, $p < 0.0001$); and iii) sickness scores for arm visits

($r = -0.773$, $p < 0.0001$; Fig. 4F) in both males ($r = -0.741$, $p < 0.0001$) and females ($r = -0.824$, $p < 0.0001$).

3.3.2.2. LPS-induced alterations in methionine metabolism are in part sex-dependent

Methionine is an essential amino acid involved in protein synthesis and required for growth and tissue repair, immune responses, protection against oxidative stress as well as epigenetic regulation in the brain (Martinez et al., 2017; McGowan et al., 2008). It is also a substrate for other key amino acids, such as taurine and cysteine, as well as the antioxidant molecule glutathione (Fig. 5).

Significant reductions in L-methionine (Fig. 5A), L-methionine S-oxide (Fig. 5B), a toxic oxidation product of methionine (Stadtman et al., 2005), and 5'-methylthioadenosine (Fig. 5C), a methionine precursor in the salvage pathway (Christa et al., 1986), indicated that LPS attenuated the production and metabolism of L-methionine, regardless of sex and disease status.

Levels of S-adenosy-L-homocysteine, an intermediate in methionine biosynthesis and degradation by the recycling and transsulfuration pathways, respectively, were increased by LPS in APP/PS1 males with opposite effects seen in APP/PS1 females (Genotype X Sex X Treatment: $F_{(1,34)}=4.13$, $p=0.49$; Fig. 5E). Methionine is a substrate for the anti-oxidant molecule glutathione whose toxic oxidation product glutathione disulfide (Stadtman et al., 2005) was more found more abundant in the hippocampus of LPS-treated males, regardless of genotype, but less abundant in the hippocampus of WT females (Sex X Treatment: $F_{(1,34)}=14.52$, $p=0.0006$, Fig. 5H).

Effects of LPS were more pronounced in females which also showed downregulation of other metabolites involved in the synthesis of methionine *via* both the salvage and recycling pathways. LPS-treated females exhibited reduced hippocampal levels of S-adenosy-L-methionine (Fig. 5D), an intermediate in methionine salvage also involved in the synthesis of homocysteine, key intermediate in methionine metabolism located at the branch point between the recycling pathway and transsulfuration pathway, as well as of O-succinyl-L-homoserine (Fig. 5F), also involved in L-methionine recycling and degradation *via* modulation of homocysteine biosynthesis (Flavin and Slaughter, 1967).

In the absence of immune stimulation, females also presented with reduced levels of L- 5'-methylthioadenosine (Fig. 5C), the first step in the methionine salvage pathway, as well as L-cystathionine and hypotaurine (Fig. 5G&I, respectively), two methionine derivatives and key intermediates in the synthesis of taurine, an amino acid found in very high concentrations in most cells (Schaffer and Kim, 2018); but L-methionine levels were not affected by sex differences (Fig. 5A).

3.3.2.3. LPS lowers pyruvate metabolism in APP/PS1males

Pyruvate is a key metabolite in several metabolic pathways important for glucose and energy homeostasis, with potent anti-oxidant and anti-inflammatory properties (Das, 2006). It is made from glucose and is the end-product of glycolysis (Fig. 6).

In males, and more specifically APP/PS1 males, LPS rapidly lowered pyruvate metabolism by downregulating several intermediates in the glycolysis pathway. D-fructose 1,6-bisphosphate (Fig.6A), and downstream metabolites, D-glyceraldehyde 3-phosphate (Fig.6B), 3-Phospho-D-glycerate (Fig. 6C), phosphoenolpyruvate (Fig. 6D) and ultimately of pyruvate (Fig. 6E) were all significantly less abundant in the hippocampus of LPS-treated APP/PS1 males 4 hours after LPS administration. A baseline, however, there was a trend for these metabolites to be more abundant in the hippocampi of APP/PS1 males, explaining the greater effect of LPS, but post-LPS levels of these intermediates in pyruvate metabolism were similar in males from both genotypes. This was associated with reduced levels of 2-phosphoglycolate (Sex X Treatment: $F_{(1,34)}$=7.63, p=0.009, Fig. 6G), which can be converted into the glycolytic intermediate 3-phospho-D-glycerate (Fig. 6C) *via* activation of glycolate metabolism. Conversion of glucose into fructose is a two-step process in which glucose is reduced to sorbitol, which is then converted to fructose. LPS-treated APP/PS1 males also failed to show the decreased in D-sorbitol contents observed in all other LPS-treated groups (WT males, WT and APP/PS1 females, Fig.6F). In females of both genotypes, LPS also reduced the levels of S-malate (Sex X Treatment: $F_{(1,34)}$=11.62, p=0.0017, Fig. 6I), a metabolite of the KREBS cycle, which can be recycled into pyruvate.

3.3.2.4. LPS lowers methylglyoxal metabolism in females

Methylglyoxal is a neurotoxic by-product of glycolysis, fructose, fatty acid and protein metabolism and potent inducer of inflammation and oxidative stress which can be detoxified by degradation in D-lactate *via* conversion into D-S-lactoylglutathione [(Allaman et al., 2015; Desai et al., 2010), Fig. 7].

In females, LPS induced a downregulation a number of metabolites upstream and downstream of methylglyoxal production. This includes D-sorbitol, which is involved in fructose metabolism (Fig.6F), metabolites involved in the biosynthesis of unsaturated fatty acids, particularly APP/PS1 females [hexadecanoic acid, octadecanoic acid, icosatrienoic acid (Sex X Treatment: $F_{(1,34)}$=10.67, p=0.002), Fig. 7A-C, respectively], the fatty acid and conjugate [FA (20:4)] 5Z,8Z,11Z,14Z-eicosatetraenoic acid (Sex X Treatment: $F_{(1,34)}$=11.42, p=0.0018, Fig. 7D) as well as sn-glycerol 3-phosphate (Sex X Treatment: $F_{(1,34)}$=10.94, p=0.002, Fig. 7E), which is synthesised by both glycerol and sn-glycero-3-phosphoethanolamine (Sex X Treatment: $F_{(1,34)}$=18.49, p=0.002, Fig. 7F) to form dihydroxyacetone phosphate and ultimately, methylglyoxal. This was associated with

reduced levels of its degradation product (D)-S-lactoylglutathione and (D)-lactate (Sex X Treatment: $F_{(1,34)}$=6.17, p=0.02 & $F_{(1,34)}$=5.62, p=0.02; Fig. 7G&H, respectively).

3.4. Lack of glial response to LPS at 4 hours post-injection

We used immunohistochemistry to detect Iba-1 positive cells, quantify their number, the area they occupied and the size of their soma (used as a morphological marker of microglial activation) and to determine the area occupied by GFAP-positive astrocytes, in the hippocampus of 4.5-month-old male and female WT and APP/PS1 mice 4 hours after LPS or PBS administration. Results of the three-way ANOVAs applied to these measures are presented in Suppl. table 4.

We report that the area occupied by Iba-1 positive microglia was lower in the hippocampus of WT female mice compared to WT males and APP/PS1 females (Genotype X Sex: $F_{(1,35)}$=4.14, p=0.049, Fig. 8A&F), with significant reductions being particularly evident in the CA2 (Genotype X Sex: $F_{(1,34)}$=4.24, p=0.047, Fig. 8C&H) and CA3 (Genotype X Sex: $F_{(1,36)}$=7.37, p=0.01, Fig. 8D&I) subfields. The smaller area covered by microglia seen in WT females was particularly evident in PBS-treated mice for both the whole hippocampus (p =0.02 vs WT males and APP/PS1 females, Fig. 8F) and CA3 subfield (p=0.01 *vs* WT males and p=0.007 APP/PS1 females, Fig. 8I). LPS caused non-significant reductions in the area covered by Iba-1 throughout the hippocampus of APP/PS1 females, as well as of males from both genotypes (Fig. 8F-J). We also found a lower number of Iba1 positive cells in the DG of PBS-treated females compared to PBS-treated WT males (p=0.008, Fig. 8O) and APP/PS1 females (p=0.03, Genotype X Sex: $F_{(1,36)}$=5.02, p=0.03, Fig. 8O). The area of microglial somas did not differ between the sex, genotype and treatment conditions in any of the hippocampal subfields (Suppl. Fig 5B-F), and there were very few microglial clusters, albeit significantly more in the hippocampi of APP/PS1 mice compared to their WT littermates ($F_{(1,35)}$=10.05, p=0.003; Suppl. Fig 5G), consistent with the relatively low Aβ plaque load at 4.5 months of age (Suppl. Fig 5H&I).

We did not detect differences in the area occupied by GFAP after LPS in discrete hippocampal regions of 4.5-month-old male and female WT and APP/PS1 mice and there was no genotype or sex dependency in this measure (Suppl. Fig 6A-J).

4. Discussion

Given the role of systemic inflammation in AD pathogenesis and known sex differences in the risk of AD and immune responses, we tested whether the behavioural and hippocampal metabolic responses to a systemic challenge with LPS would be exacerbated in young APP/PS1 female in the early hours post-inoculation. Here, we first show that the hippocampal metabolic signature of APP/PS1 mice, in the absence of

immune stimulation, did not clearly differ from that of WT mice, at this early pathological stage, revealing only subtle differences, but predominantly in females. This is consistent with our previous study in males (Maroof et al., 2014). Differences in hippocampal metabolism have been previously reported in this model at 6 months of age, and in comparison to C57BL/6j mice rather than WT littermates, but without testing for potential sex differences although both males and females were included in that study (Gonzalez-Dominguez et al., 2014). Second, we also show in the absence of immune stimulation, a sexual dimorphism in the hippocampal metabolic profile of 4.5-month-old mice, particularly affecting methionine and pyruvate metabolism, but independent of the genotype. The major finding, however, was that 4 hours after onset of systemic inflammation, several aspects of the LPS response were also sex-dependent. Importantly, we found at this time point that males and females exhibited comparable behavioural responses to LPS, regardless of the genotype, but the temperature change was greater in males and the cytokine response, particularly the secretion of IL-10, was greater in females. Metabolic data indicated that LPS induced a comparable activation of both the serotonin and nicotinamide pathways of tryptophan metabolism in the hippocampus of WT and APP/PS1 mice of both sexes, with hippocampal levels of the toxic nicotinamide metabolite 2PY being positively associated with the severity of the sickness response. And while all LPS-treated mice exhibited a downregulation in methionine levels, reversible oxidation and salvage, sex-differences were observed in the response of the recycling and transsulfuration pathways of methionine metabolism. Males also exhibited a downregulation of pyruvate metabolism after LPS, exacerbated in APP/PS1 males, while females showed downregulation of methylglyoxal metabolism.

Sex differences in hippocampal metabolism in the absence of immune stimulation

Spontaneous alternation was preserved in APP/PS1 mice regardless of sex, in agreement with our previous findings in both males and females at the same pathological stage (Bonardi et al., 2011; Maroof et al., 2014). In the present study, however, we observed an overall reduction in spontaneous alternation performance in females, suggesting a lower spatial working memory ability as was also previously reported in C57BL/6j mice (Tucker et al., 2016), the genetic background of our APP/PS1 mice. Males are indeed generally found to outperform females for spatial working memory, and this has been related to differences in hippocampal morphology and function (Koss and Frick, 2017). Accordingly, we have also shown that the hippocampal metabolic profile of females differed from that of males for 41 metabolites, but similarly in WT and APP/PS1 mice.

The most significant changes affected the metabolism of methionine, an essential amino acid for protein synthesis and epigenetic regulation in the brain, and key regulator

of antioxidant protection and immune responses at physiological levels (Martinez et al., 2017; McGowan et al., 2008). Sex differences were seen in the salvage and transsulfuration pathways of methionine metabolism, with robustly downregulated levels of 5'-methylthioadenosine and hypotaurine, respectively. Methionine levels are in part regulated by the salvage pathway which recycles 5'-methylthioadenosine back in methionine (Albers, 2009). Reduced levels of 5'-methylthioadenosine in females were not associated with altered methionine levels, suggesting that they could be maintained *via* an alternative biosynthetic route and/or through reduced catabolism. The latter hypothesis is supported by the associated reduced levels of L-cystathionine and hypotaurine in females, two key intermediates in the synthesis of taurine from the methionine derivative homocysteine, during their degradation of *via* the transsulfuration pathway (Stipanuk and Ueki, 2011). While methionine levels were preserved in females, the specific changes observed in downstream metabolites in females may predispose them to immune dysfunction and cell damage. 5'-methylthioadenosine, is indeed now seen as a key regulator of immune responses to inflammation and systemic infections (Albers, 2009; Wang et al., 2017), proven to mediate protection against LPS-induced inflammation *in vitro* (Hevia et al., 2004) but also to inhibit inflammation and reduce brain damage in animal models of neuroinflammation (Moreno et al., 2006). Furthermore, hypotaurine which has well established antioxidant properties (Fontana et al., 2004), was also found to effectively suppress inflammatory and neuropathic pain (Hara et al., 2012). Taurine and hypotaurine are present in elevated levels in the brain of the long-lived Snell Dwarf mouse (Vitvitsky et al., 2013), which exhibits reduced oxidative damage to the brain (Brown-Borg, 2006) and hypothalamic inflammation (Sadagurski et al., 2015). Taurine also plays a protective role against age-related cognitive decline (El Idrissi, 2008), and therefore, the downregulated transsulfuration pathway of methionine metabolism could, in part, contribute to the lower spatial working memory performance seen in females.

Increased abundance in members of the glycolytic metabolic pathway, which provides energy for cellular metabolism in the form of pyruvate and ATP, was also observed in female hippocampi with particularly elevated levels of 3-phosphoglycerate and phosphoenolpyruvate in WT females. This was accompanied by unaltered pyruvate and ATP levels, but reduced levels of 2—phosphoglycolate, regardless of the genotype, possibly reflecting a metabolic shift towards enhanced regeneration of 3-phosphoglycerate from 2-phosphoglycolate, at the expense of glyoxylate metabolism, as suggested by the associated downregulation in 3-oxalomalate levels. Glycolate and glyoxylate metabolism have been linked to oxidative stress in peroxisomes (Schrader and Fahimi, 2006), essential organelles mediating biosynthetic and biodegradative reactions in a variety of cells (Terlecky et al., 2012). 2-phosphoglycolate is produced as a by-product of oxidative DNA damage (Segerer et al., 2016), and is also toxic for cells as a source of glycolate

accumulation (Flugel et al., 2017). Conversion of glycolate into glyoxylate, a precursor of 3-oxalomate (Irace et al., 2007), is reduced in rats subjected to oxidative stress (Recalcati et al., 2003). This may lead to adverse effects as oxalomalate is known to prevent LPS-induced production of nitric oxide by activated macrophages (Irace et al., 2007). Peroxisome-associated oxidative stress is a mechanism thought to contribute to neurotoxicity, inflammation, cognitive dysfunction, and accelerated brain aging (Moruno-Manchon et al., 2018; Terlecky et al., 2012), but whether the metabolic changes seen in females reflect a pro- or anti-oxidant status will need to be addressed in further studies.

In PBS-treated mice, metabolic differences were not associated with significant sex differences in the number of astrocytes and microglia, or microglial soma size, a morphological activation marker. The area covered by microglia was, however, lower in the hippocampus of WT females, which could reflect reduced ramification per cell, as previously reported in females (Young et al., 2018). This reduction was not seen in APP/PS1 female mice, consistent with recent observations. Microglia of APP/PS1 mice was indeed found to develop ramifications in the presence of Aβ plaques, regardless of sex, but this response occurs earlier in females than in males (Frigerio et al., 2019), which can be related to the faster progression of cerebral amyloidosis consistently seen in females from this genotype (Frigerio et al., 2019; Li et al., 2016; Wang et al., 2003). APP/PS1 female mice also slightly differed from WT mice in their hippocampal metabolic profile, as well as with their reduced body weight and lack of habituation to repeated exposure to the Y-maze. But, while sex differences in brain metabolism seen in the ageing WT mouse brain have been hypothesised to contribute to the greater susceptibility of females to AD-like pathology (Zhao et al., 2016), our data do not support a link between differences in hippocampal metabolism and early-stage amyloidosis. The implication of the few metabolites found to be less abundant in the hippocampus of female APP/PS1 mice in Aβ plaques deposition is currently unknown. In contrast, global differences in hippocampal metabolism appeared to be emerging at 4.5 months of age between WT and APP/PS1 males, expected to develop the pathology at a slower rate than female, but in the absence of behavioural and/or physiological changes. Furthermore, the role of the metabolites found altered in female APP/PS1 mice in microglial morphology or function is also unknown, and we did not found any association between metabolite levels and microglial density and/or activation.

Metabolic effects of LPS independent of sex and disease status.

4.5-month-old WT and APP/PS1 mice, regardless of their sex, exhibited a robust behavioural suppression 4 hours after inoculation with a low systemic LPS dose of 100ug/kg, without concomitant changes in the number and morphology of glial cells in the hippocampus. This is consistent with findings in 4-month-old C57BL/6J females (Hart et

al., 2012), but the discrepancy with our previous data showing enlargement of microglial soma in WT, but not APP/PS1 males at the same time point (Pardon et al., 2016), could be due to the exacerbating impact of anaesthesia (Ye et al., 2013), as previously discussed (Pardon et al., 2016). Indeed, morphological activation of microglia would generally occur 6 hours after systemic administration of higher doses of LPS in the healthy brain (Hoogland et al., 2015), but within 4 hours in the primed hippocampus (Murray et al., 2011). Thus, the fact that we did not find differences in microglial number and morphology between sexes and genotypes is consistent with the lack of microglial response at 4 hours post-LPS, and published reports showing that changes in microglial phenotypes, occurring with the progression of amyloidosis in this APP/PS1 model, manifest after the age of 5 months (Martin et al., 2017). A subset of microglia, however, shows signs of activated morphology and phenotype prior to that, when clustering around Aβ plaques (Martin et al., 2017; Ruan et al., 2009), but our data show that both are rare in 4.5-month-old APP/PS1 mice.

As consistently reported with a range of systemic LPS doses, hippocampal tryptophan levels rapidly increased in the hippocampus of LPS-treated mice, independently of sex and disease status. This was associated with elevated levels of degradation products of both the serotonin and nicotinamide pathways of tryptophan metabolism, suggesting their co-activation, as seen previously (Guo et al., 2016; O'Connor et al., 2009; Parrott et al., 2016). A shift in the balance of brain tryptophan metabolism towards the kynurenine pathway is thought to be a major mediator of pro-inflammatory changes following systemic inflammation, and to ultimately cause serotonin deficiency (Kim and Jeon, 2018). Although serotonin levels were not measured here, as this would require the optimisation of a single LC/MS method specifically designed to address behavioural and structural differences between tryptophan metabolites and related monoamines (Fuertig et al., 2016), increased levels of its degradation product 5-HIAA could instead suggest an increase in serotonin turnover. Several studies have shown that elevated hippocampal 5-HIAA occurring in the first 24 hours after inoculation with systemic LPS were associated with stable serotonin levels (Pitychoutis et al., 2009; Sens et al., 2017), suggesting an increased rate of serotonin synthesis (Brodie et al., 1966). Transient region-specific increases in the activity of enzymes involved in serotonin synthesis were indeed seen 2 hours after systemic LPS in the frontal cortex and midbrain of rats challenged with the same 100ug/kg dose, but returning to baseline levels by the 6th hour post-inoculation (Nolan et al., 2000). In agreement with this, a time course microdialysis study showed that systemic LPS-induced a gradual increase in extracellular hippocampal tryptophan and 5-HIAA levels over 8 hours, which was associated with a transient increase in serotonin levels, peaking 3-4 hours after administration (Guo et al., 2016). Interestingly, the subsequent decline towards baseline serotonin levels was associated with a downregulation of the serotonin/tryptophan ratio and concomitant upregulation of the

kynurenine/tryptophan ratio, indicating a metabolic shift towards kynurenine metabolism (Guo et al., 2016). Increased 2PY levels, reflecting the amount of nicotinamide biosynthesized from tryptophan (Shibata and Matsuo, 1990), have been linked to activation of tryptophan metabolism through the kynurenine pathway and associated with systemic inflammation in malnutrition (Guerrant et al., 2016; Mayneris-Perxachs et al., 2016). We can, therefore, hypothesise that the elevated hippocampal 2PY levels we saw 4 hours after LPS administration would reflect an activation of the tryptophan-nicotinamide pathway, but whether or not its association with elevated hippocampal 5-HIAA levels predict a metabolic shift towards kynurenine metabolism will need to be determined in future studies, by measuring the levels of serotonin and key intermediates of the kynurenine pathway at later points. This is particularly important because activation of the serotonin pathway of tryptophan metabolism is protective to the brain whereas activation of the kynurenine pathway leads to detrimental effects, the former being anti-inflammatory (Dominguez-Soto et al., 2017) and latter pro-inflammatory (Davis and Liu, 2015) and a major driver of LPS-induced sickness (O'Connor et al., 2009). This is also consistent with our observed association between 2PY levels and the severity of the behavioural and temperature response to LPS. The time course of changes in tryptophan metabolic pathways also has implication for our understanding of the mechanisms underlying the precipitating influence of systemic infection and inflammation in AD. Recent findings indeed suggest that reduced serotonin neurotransmission contributes to the development of early cognitive symptoms of AD (Smith et al., 2017), while upregulation of key components of the kynurenine pathway are associated with Aβ plaques and neurofibrillary tangles in the brain of AD patients (Wu et al., 2013).

We also showed, for the first time, that systemic LPS rapidly inhibited the synthesis and metabolism of methionine in the hippocampus, illustrated by the lowering of both L-methionine and its downstream metabolites. Regardless of sex, LPS altered methionine reversible oxidation and salvage. Methionine reversible oxidation, the process whereby methionine is oxidized into methionine sulfoxide, which is then reduced back to methionine, is thought to play a key regulatory role in mediating activity-dependent plastic changes in cellular excitability (Hoshi and Heinemann, 2001). The reduction in the levels of the methionine oxidation product L-methionine S-oxide by LPS could be seen as a protective response since reversible methionine oxidation becomes impaired in ageing and related diseases, leading to the accumulation of toxic methionine oxidation products, oxidative damage to cells (Stadtman et al., 2005) and Aβ accumulation (Moskovitz et al., 2016). Methionine sulfoxide reductase, the antioxidant enzyme which reduces methionine sulfoxide back to methionine, is also known to alleviate LPS-induced inflammation in microglia (Fan et al., 2015). However, we found here that this was associated with reduced abundance of L-methionine, suggesting that the lack of L-methionine availability, rather

than enhanced reversible oxidation, caused the lowering of L-methionine S-oxide levels. The salvage pathway plays a critical role in maintaining optimal methionine levels as proven by the ability of 5'-methylthioadenosine to replenish the cellular methionine pool within 24 hours of methionine deprivation (Shiraki et al., 2014). Reduced levels of both S-adenosyl-L-methionine and 5'-methylthioadenosine, as we saw here associated with methionine deficiency 4 hours after LPS administration, are thought to be early events reflecting the activation of the salvage pathway for the rescue of methionine levels, but this could only confirmed by looking at later time points (Shiraki et al., 2014). A failure of this mechanism would lead to detrimental effects, by compromising cell differentiation, growth and survival (Shiraki et al., 2014) as well as protein synthesis and epigenetic reactions. The methionine salvage pathway indeed recycles the sulphur of 5'-methylthioadenosine back into methionine, which is critically needed for protein synthesis (Kabil et al., 2014). S-adenosyl-L-methionine, whose levels were particularly decreased by LPS in female mice, is a precursor for this reaction but also a methyl donor for epigenetic reactions and key regulator of metabolism, proliferation, and apoptosis (Albers, 2009). Persistent downregulation of the salvage pathway could also be damaging due to the anti-inflammatory properties of both S-adenosyl-L-methionine and 5'-methylthioadenosine (Ge et al., 2018; Hevia et al., 2004; Moreno et al., 2006; Pfalzer et al., 2014), whose levels were also found reduced in the AD brain (Morrison et al., 1996). However, while methionine deficiency, if persistent, can impair multiple aspects of cell function, and ultimately cell viability (Shiraki et al., 2014), and as such contribute to the development of AD, its excess is also neurotoxic leading to inflammation and exacerbation of behavioural and neurological markers of AD (Tapia-Rojas et al., 2015), perhaps questioning the functional significance of our findings. Reduced availability and metabolism of methionine is indeed thought to be the main driver of lifespan and healthspan enhancement by dietary restriction through improved lipid metabolism as well as reduced oxidative stress, inflammation and susceptibility to immune and central nervous disorders (Martinez et al., 2017; Orgeron et al., 2014). Methionine metabolism is indeed reduced in the long-lived naked-mole rat (Lewis et al., 2018) but it is enhanced in the long-lived Ames dwarf mouse (Uthus and Brown-Borg, 2003), and both show activation of anti-inflammatory pathways (Cheng et al., 2017; Dhahbi et al., 2007).

Thus, whether our observed rapid downregulation of methionine metabolism by LPS constitutes a beneficial or detrimental response in the brain cannot be fully answered in this study and our data also suggest that this may be, in part, sex-dependent. Indeed, O-succinyl-L-homoserine contributes to the synthesis of both homocysteine and L-methionine (Flavin and Slaughter, 1967), and in the present study, it was less abundant in LPS-treated females. This is particularly relevant to the link between immune responses and AD progression, since homocysteine can trigger neuroinflammation and microglial

activation (Chen et al., 2017) and its levels are positively associated with the risk of dementia (Smith et al., 2018), therefore suggesting a protective downregulation of methionine metabolism in females. In contrast, in LPS-treated males instead presented with increased levels of glutathione disulfide, a toxic oxidized form of glutathione and an end product of methionine metabolism, whose circulating levels were found to be elevated in inflammatory conditions (Ikegami et al., 1994), and reduced in the long-lived naked-mole rat (Lewis et al., 2018), suggesting a more damaging downregulation of methionine metabolism.

Sexual dimorphism in the hippocampal metabolic response to LPS.

Changes in body temperature, pyruvate and methylglyoxal metabolism 4 hours after onset of systemic inflammation were clearly sex-dependent. Thermoregulatory responses to LPS in rodents are made of one to three phases of hyperthermia and/or hypothermia, although fever is less likely to occur in mice than in rats (Blanque et al., 1996; Romanovsky et al., 2005). LPS-induced hypothermia is seen as a thermoregulatory "failure", thought to reflect the inability of the brain to regulate body temperature in shock (Romanovsky et al., 2005). It is also an indicator of the severity of LPS responses, as it was found to be dose-dependent and more pronounced in mouse strains susceptible to this endotoxin (Blanque et al., 1996). Consistent with our findings, LPS-induced hypothermia is generally found to be more severe in male than female mice (Cai et al., 2016; Card et al., 2006), suggesting that they experience more severe acute effects of LPS. Hypothermia is thought to be in part induced in response to changes in the brain as it did not appear to be related to variations in circulating levels of IL-1β, IL-6 or IL-10 (Blanque et al., 1996; Skelly et al., 2013). Our data showing that LPS-induced hypothermia is correlated with increased 2PY levels, thought to reflect an activation of the tryptophan-nicotinamide pathway, are consistent with previous reports showing that sickness responses to LPS are in part mediated by activation of the kynurenine pathway (O'Connor et al., 2009) and the ability of kynurenine and its metabolites to potentiate drug-induced hypothermic responses (Lapin, 2003). Here, hypothermia was sex-dependent and this was also associated with a reduction in hippocampal pyruvate metabolism particularly affecting APP/PS1 males. A possible link cannot be ruled out as hypothermia was found to cause a progressive decrease in cerebral pyruvate contents in the rat (Nilsson et al., 1975), although central administration of pyruvate did not significantly alter body temperature (Soto et al., 2018). Pyruvate is an intermediate energy metabolite of glucose with potent anti-oxidant and anti-inflammatory actions (Das, 2006). Sex differences in pyruvate metabolism have been associated with a higher mitochondrial respiration rate and reduced oxidative stress in females (Gaignard et al., 2015), as well as protection against oxidative damage induced by excitotoxic injury

whereby the ratio of lipid peroxidation markers over pyruvate increased in males but decreased in females in response to an ischemic insult (Wagner et al., 2004). Evidence of anti-inflammatory effects of pyruvate in the brain include the demonstration that treatment with its ethyl pyruvate derivatives exerts robust neuroprotective effects, in both the post-ischemic brain and LPS-treated animals, by alleviating microglial activation and neutrophil infiltrations *in vivo*, and inhibiting LPS-induced pro-inflammatory changes in these cells *in vitro* (Lee et al., 2017; Lee et al., 2013). In addition, dietary supplementation with pyruvate was found to improve spatial memory impairments and brain energy metabolism in males of the same APP/PS1 mouse line as used here (Koivisto et al., 2016) as well as in male and female 3xTg-AD mice, while also reducing oxidative stress, albeit without effects on Aβ and tau pathology (Isopi et al., 2015). Although systemic inflammation has been linked to cognitive decline and AD progression in both males and females (Holmes et al., 2009; Trollor et al., 2010), sex-specific differences were found in the association between pro-inflammatory mediators and cognitive function in mild cognitively impaired patients (Trollor et al., 2010). Thus, the present finding that male APP/PS1 mice were more susceptible to downregulation of pyruvate metabolism in the early hours post-inoculation with LPS could constitute a male-specific mechanism underlying exacerbation of cognitive and neurodegenerative changes after systemic inflammation.

In contrast, females displayed a downregulation of methylglyoxal metabolism illustrated by reduced levels of its upstream regulators, with the exception of glycolysis, and of its reduction product D-lactate. Methylglyoxal is a cytotoxic and pro-inflammatory glycotoxin whose deleterious effects are due to its role as a major precursor of advanced glycation end-products, and have been associated with several pathologies including diabetes, ageing and neurodegenerative diseases (Allaman et al., 2015; Angeloni et al., 2014; Beeri et al., 2011). Cerebrospinal fluid as well as serum methylglyoxal concentrations are increased in AD patients (Beeri et al., 2011; Kuhla et al., 2005) and the latter has been found to be associated with cognitive decline regardless of sex (Beeri et al., 2011). Direct administration of methylglyoxal was also found to cause cognitive deficits in rats (Hansen et al., 2016) and its accumulation promotes inflammation (Vulesevic et al., 2016) as well as Aβ aggregation (Woltjer et al., 2003). Methylglyoxal is also produced by Aβ, contributing to cell death (Tajes et al., 2014), providing a link between inflammation and AD exacerbation. In this context, we can hypothesise that the inhibition of methylglyoxal metabolism seen in females in response to systemic inflammation would constitute a protective response that, if persistent, may limit inflammation-induced exacerbation of AD-like pathology. The mechanism behind a sexual dimorphism in this response, is however unknown. Females were found to be more

susceptible to the acute toxicity of methylglyoxal (Peters et al., 1978), but the present study is the first show a sex-dependent response of this metabolic pathway to immune stimulation. Nevertheless, methylglyoxal metabolism has been implicated in obesity and diabetes (Matafome et al., 2013), the risk of which is exacerbated by systemic inflammation (Esser et al., 2014), and females have been found less susceptible to diet-induced obesity and its metabolic and pro-inflammatory consequences (Dorfman et al., 2017). Our finding is, however, consistent with the elevated levels of the anti-inflammatory cytokine IL-10 that we found in LPS-treated females, but not males, at the 4 hour time point. Indeed, methylglyoxal was found to particularly inhibit the secretion of IL-10 and TNFα by myeloid cells (Price et al., 2010), whereas IL-10 can suppress pro-inflammatory and toxic effects of methylglyoxal (Onishi et al., 2015).

5. Conclusions

Taken together, our data indicate that while hippocampal metabolism in females, compared to males, may reflect a shift towards a pro-inflammatory and pro-oxidant signature, and while subtle metabolic differences in APP/PS1 mice compared to their WT littermates were only seen in females, in the early hours following inoculation with LPS, the physiological and metabolic responses of males are more pronounced, regardless of the genotype. This is consistent with recent findings in a model of traumatic brain injury, whereby males exhibited a more aggressive neuroinflammatory profile than female mice during the acute and subacute phases post-injury (Villapol et al., 2017), and also with the recently established sexual dimorphism in microglia. The molecular signature of male microglia was indeed found to be skewed towards pro-inflammatory activation and that of females found to be neuroprotective, expressing proteins related to the inhibition of inflammatory responses and promotion of repair mechanisms (Guneykaya et al., 2018; Villa et al., 2018a; Villa et al., 2018b). Metabolic changes in the hippocampus occurred in the present study before morphological signs of microglial activation could be detected, affecting pathways known to modulate microglial activation. This provides insights into how systemic LPS, whose brain penetration is poor at low dose and in the absence of blood brain barrier dysfunction (Banks and Robinson, 2010; Varatharaj and Galea, 2017), can trigger rapid inflammatory responses in the brain. Importantly, we have found here that some of the metabolic changes are sex-specific, highlighting the importance of taking gender into consideration when studying susceptibility to inflammatory conditions and AD exacerbation. Moreover, this study is the first to show an association between onset of systemic inflammation and downregulation of hippocampal methionine metabolism, but the protective or detrimental nature of this change needs to be determined in future studies. No major differences in the response to LPS were seen here between WT and

APP/PS1 mice, which can be due to the early pathological stages under investigation, since differences in microglial activation are subtle before the age of 4 months (Martin et al., 2017; Ruan et al., 2009), and/or the early time point, as the resolution of neuroinflammation is an active process particularly impaired in neurodegenerative diseases (Schwartz and Baruch, 2014). However, some of the metabolic changes that we saw here in the hippocampus, a brain area critically affected by AD, 4 hours after induction of systemic inflammation with LPS, are relevant to AD pathogenesis, particularly the activation of the tryptophan-nicotinamide pathway, reduced methionine availability and salvage as well as the reduction in pyruvate metabolism in male The extent to which a single infectious episode is sufficient to drive the progression of AD in susceptible individuals is not currently known. Looking at the persistence of these metabolic alterations in relation to the progression of behavioural and neurological hallmarks of AD may help answering into this question.

6. Acknowledgements

This work was supported by UNICAS – a University of Nottingham initiative to fund interdisciplinary equipment based research (UNICAS-A2B177) and a MRC Confidence in Concepts award (CiC2014029). Alessandra Agostini was supported by a University of Nottingham European Union Masters Scholarship and Vice-Chancellor's PhD Scholarship for Research Excellence. Thanks are due to Dr Dong-Hyun Kim, School of Pharmacy, University of Nottingham, for technical contributions to the acquisition of metabolomics data, and to Dr Simon Bates, statistician, for his helpful advices and comments on data analysis.

7. Author Contributions

Conceived and designed the experiments: M-CP, DAK. Performed the experiments: AA. Analysed the data: AA. M-CP. Contributed to the development of analysis tools: DY, BL. Supervised the experiments: M-CP. Wrote the paper: M-CP.

8. Conflicts of interest: none

Appendix A. Supplementary data

Figure captions.

Figure 1. LPS-induced behavioural suppression at 4 hours post-injection is independent of sex or genotype. A) Timeline of the experiment. 4.5-month-old male and female APP/PS1 mice and their wild-type (WT) littermates (n=5-6) were subjected to baseline assessment of spatial working memory performance and exploratory drive in the spontaneous test as well as food burrowing behaviour prior to receiving a tail vein injection of lipopolysaccharide (LPS, 100 µg/kg) or its vehicle (phosphate buffer saline, PBS). Induced sickness effects were tested at 4 hours post-injection in the same tests, prior to blood and tissue collection. At this time point, a significant decrease in core body temperature was observed in males, regardless of their genotype (B). LPS also suppressed food burrowing activity (C) and exploratory drive in the spontaneous alternation test, assessed through the number of arms visits (E), regardless of sex and genotype, but baseline performance for these behavioural measures did not differ between groups (C,D). Female mice overall exhibited lower spontaneous alternation performance than their male counterparts at baseline (F), but LPS had no significant impact on this measure (G). Parametric data are expressed as Means $\pm$ SEM. Dots represent individual animals. Post-hoc tests: * $p< 0.05$; ** $p<0.01$, *** $p<0.0001$ *vs* PBS or baseline. Food burrowing data were rank-transformed for statistical analysis but represented as non-normalised responses and expressed as Median $\pm$ interquartile range. Sickness scores are represented as the difference between pre- and post-injection performance. Within-subjects pairwise comparisons following 3-way ANOVAs: $^{\#}$ $p<0.05$; $^{\#\#}$ $p<0.01$, $^{\#\#\#}$ $p<0.0001$ compared to baseline performance (E).

Figure 2. LPS-induced plasma cytokine at 4 hours post-injection. 4.5-month-old male and female APP/PS1 mice and their wild-type (WT) littermates were challenged with LPS (100µ/kg *i.v.*) or its vehicle PBS. Their plasma was collected 4 hours later, immediately after behavioural assessment, for measurement of induced levels of pro- and anti-inflammatory cytokines. At this time point, a significant increase in circulating Interleukin 6 (IL-6, A), which has both pro- and anti-inflammatory effects, was observed regardless of sex and genotype (A). Levels of the pro-inflammatory cytokine tumour necrosis factor alpha (TNF-α) were increased by LPS in females, particularly WT females (B), but the levels of the other pro-inflammatory mediator, interferon gamma (IFN-γ), were unaltered (C). A significant increase in circulating levels of the anti-inflammatory cytokine IL-10, was also observed in females, regardless of genotype (E). Data were rank-transformed for statistical analyses but are expressed as Median $\pm$ interquartile range of non-normalised responses. Dots represent individual animals. Pairwise comparisons: * $p<0.05$; ** $p<0.01$, *** $p<0.0001$ *vs* PBS.

Figure 3. Score plots of Principal Component Analysis (PCA) and two-class Orthogonal Partial Least Square Discriminant Analysis (OPLS-DA) models for hippocampal metabolism at 4 hours post-injection with LPS or PBS. R^2: variance explained, Q^2: variance predicted. Dots represent individual animals. A). PCA analysis reveals global metabolic differences between LPS-treated males and females regardless of genotype [PC1 (X axis): $R^2X[1] = 0.232$, $Q^2 = 0.115$; PC2 (Y axis): $R^2X[2] = 0.123$, $Q^2 = 0.082$). B) Global OPLS-DA model ($R^2= 0.994$, Q2 = 0.886) revealing clear separations between PBS- and LPS-treated mice (X axis: predictive component), but also some separation between LPS-treated male and female mice (Y axis: first orthogonal component), regardless of genotype. C) Accordingly, the class OPLS-DA model comparing genotypes in PBS-treated mice confirmed the lack of clear separation between WT and APP/PS1 mice ($R^2= 0.697$, $Q^2 = 0.244$). Predictive component 1 (X axis) *vs* 2 (Y axis). 2-class OPLS-DA models confirmed the strong differences in hippocampal metabolism due to sex in the absence of immune stimulation, ($R^2= 0.985$, $Q^2 = 0.809$; D) as well as the excellent separation between PBS- and LPS-treated mice males ($R^2= 1.00$, $Q^2 = 0.857$; E) and females ($R^2= 1.00$, Q2 = 0.863, F). D-F: Predictive (X axis) *vs* 1st orthogonal (Y axis) component.

Figure 4. Increased hippocampal tryptophan metabolism 4 hours after systemic LPS administration. 4.5-month-old male and female APP/PS1 mice and their wild-type (WT) littermates were challenged with LPS (100µ/kg *i.v.*) or its vehicle PBS. Schematic representation of the anti-inflammatory serotonin, and pro-inflammatory kynurenine, pathways of tryptophan metabolism. At 4 hours post-injection, LPS-treated mice showed significant upregulation of L-tryptophan (A) as well as of 5-Hydroxylindoleacetic acid (B) and N1-Methyl-2-pyridone-5-carboxamide (2PY, C), the end metabolites of the serotonin and kynurenine pathways, respectively. Changes in 2PY levels were negatively correlated to D) rectal temperature in males ($r = -0.718$, $p = 0.0004$) which exhibited an hypothermic response to LPS but not females 9$r = -0.21$, $p = 0.37$); E) the number of arms visited in the spontaneous alternation test 4 hours after the injection in both males ($r = -0.837$, $p < 0.0001$) and females ($r = -0.791$, $p < 0.0001$); and F) sickness scores for arm visits in both males ($r = -0.741$, $p < 0.0001$) and females ($r = -0.824$, $p < 0.0001$), suggesting that increased 2PY levels is associated with the severity of LPS-induced sickness. Data are expressed as Means $\pm$ SEM. Dots represent individual animals. Discriminant metabolites are highlighted by grey text boxes. Pairwise comparisons following 3-way ANOVAs: *, $p<0.05$; **, $p<0.01$; **, $p<0.0001$ compared to PBS-treated mice of same sex and genotype.

Figure 5. Reduced hippocampal methionine metabolism 4 hours after systemic LPS administration. 4.5-month-old male and female APP/PS1 mice and their wild-type (WT) littermates were challenged with LPS (100µ/kg *i.v.*) or its vehicle PBS. Schematic representation of methionine metabolism showing downregulation of 4 key metabolites of this pathway in LPS-treated mice, at 4 hours post-injection, regardless of sex or genotype (A-D). Two of these metabolites, L-methionine-S-Oxide (B) and 5'-Methylthioadenosine (D), as well as 2 methionine derivatives involved in taurine metabolism, L-Cystathionine (E) and hypotaurine (F), were also found in significantly reduced levels in females compared to males. Data are expressed as Means ± SEM. Dots represent individual animals. Discriminant metabolites are highlighted by grey text boxes. Pairwise comparisons following 3-way ANOVAs: *, $p<0.05$; **, $p<0.01$; **, $p<0.0001$ compared to PBS-treated mice of same sex and genotype; $^{++}$, $p<0.01$, $^{+++}$, $p<0.0001$ compared to males. $^{\#}$, $p<0.05$; $^{\#\#}$, $p<0.01$; $^{\#\#\#}$, $p<0.0001$; compared to PBS-treated males of same genotype.

Figure 6. Reduced pyruvate metabolism in the hippocampus of APP/PS1 male 4 hours after systemic LPS administration. 4.5-month-old male and female APP/PS1 mice and their wild-type (WT) littermates were challenged with LPS (100µ/kg *i.v.*) or its vehicle PBS. Schematic representation of the pyruvate metabolic pathway and its links with the sorbitol and glycolate pathways. At 4 hours post-injection, LPS-treated APP/PS1 male mice failed to show a reduction in D-sorbitol levels (A), but in contrast, exhibited downregulation of 4 key metabolites of the pyruvate metabolic pathway: 3-Phospho-D-glycerate (B), 2-phosphoglycolate (C), phosphoenolpyruvate (D) and pyruvate (E). Data are expressed as Means ± SEM. Dots represent individual animals. Discriminant metabolites are highlighted by grey text boxes. Pairwise comparisons following 3-way ANOVAs: *, $p<0.05$; **, $p<0.01$; compared to PBS-treated mice of same sex and genotype. $^{\#}$, $p<0.05$; $^{\#\#}$, $p<0.01$; $^{\#\#\#}$, $p<0.0001$; compared to PBS-treated males of same genotype.

Figure 7. Reduced methylglyoxal metabolism in the hippocampus of WT and APP/PS1 female 4 hours after systemic LPS administration. 4.5-month-old male and female APP/PS1 mice and their wild-type (WT) littermates were challenged with LPS (100µ/kg *i.v.*) or its vehicle PBS. Schematic representation of the main pathways regulating methylglyoxal metabolism. At 4 hours post-injection, LPS-treated APP/PS1 female mice showed a reduction in lipid metabolism, with downregulation of 5 key metabolites involved in fatty acid and glycerolipid metabolism: hexadecanoic acid (A), octadecanoic acid (B), Icosatrienoic acid (C) and [FA (17:0)] heptadecanoic acid (D) and sn-Glycerol 3-phosphate (E). This was associated with reduced levels of (D)-S-

Lactoylglutathione (F) and (D)-Lactate (G), the reduction products of methylglyoxal. Data are expressed as Means ± SEM. Dots represent individual animals. Discriminant metabolites are highlighted by grey text boxes. Pairwise comparisons following 3-way ANOVAs: *, $p<0.05$; **, $p<0.01$; ***, $p<0.0001$ compared to PBS-treated mice of same sex and genotype. #, $p<0.05$; compared to PBS-treated males of same genotype.

Figure 8. Lack of microglial response to LPS in the hippocampus at 4 hours post-injection. 4.5-month-old male and female APP/PS1 mice and their wild-type (WT) littermates were challenged with LPS (100µ/kg *i.v.*) or its vehicle PBS. Their brain were collected 4 hours later, immediately after behavioural assessment, and one hemisphere was processed for immunostaining of Iba1 positive microglia. Representative images of Iba1 immunostaining in the whole hippocampus (A), CA1 (B), CA2 (C), CA3 (D), and dentate gyrus (DG, E) subfields extracted and analysed using a Matlab tool. LPS had no significant effects on microglial density in any hippocampal areas, estimated through the quantification the percentage area covered by Iba1 positive microglia (F-J) and number of microglial cells per mm^2 (K-O). The area covered by microglia, was, however, significantly lower in the hippocampus of WT females (F), particularly in the CA2 (H) and CA3 (G) subfields, but lower microglial numbers were only observed in the dentate gyrus (O). Data are expressed as Means ± SEM. Dots represent individual animals. Pairwise comparisons: * $p<0.05$; ** $p<0.01$.

References

Albers, E., 2009. Metabolic characteristics and importance of the universal methionine salvage pathway recycling methionine from 5'-methylthioadenosine. IUBMB Life 61, 1132-1142.

Allaman, I., Belanger, M., Magistretti, P.J., 2015. Methylglyoxal, the dark side of glycolysis. Front Neurosci-Switz 9.

Angeloni, C., Zambonin, L., Hrelia, S., 2014. Role of methylglyoxal in Alzheimer's disease. Biomed Res Int 2014, 238485.

Ashraf, G.M., Tarasov, V.V., Makhmutovsmall a, C.A., Chubarev, V.N., Avila-Rodriguez, M., Bachurin, S.O., Aliev, G., 2019. The Possibility of an Infectious Etiology of Alzheimer Disease. Mol Neurobiol 56, 4479-4491.

Banks, W.A., Robinson, S.M., 2010. Minimal penetration of lipopolysaccharide across the murine blood-brain barrier. Brain Behav Immun 24, 102-109.

Barron, M., Gartlon, J., Dawson, L.A., Atkinson, P.J., Pardon, M.C., 2017. A state of delirium: Deciphering the effect of inflammation on tau pathology in Alzheimer's disease. Exp Gerontol 94, 103-107.

Beeri, M.S., Moshier, E., Schmeidler, J., Godbold, J., Uribarri, J., Reddy, S., Sano, M., Grossman, H.T., Cai, W.J., Vlassara, H., Silverman, J.M., 2011. Serum concentration of an inflammatory glycotoxin, methylglyoxal, is associated with increased cognitive decline in elderly individuals. Mech Ageing Dev 132, 583-587.

Bettcher, B.M., Kramer, J.H., 2014. Longitudinal inflammation, cognitive decline, and Alzheimer's disease: a mini-review. Clin Pharmacol Ther 96, 464-469.

Blanque, R., Meakin, C., Millet, S., Gardner, C.R., 1996. Hypothermia as an indicator of the acute effects of lipopolysaccharides: Comparison with serum levels of IL1 beta, IL6 and TNF alpha. Gen Pharmacol 27, 973-977.

Bonardi, C., de Pulford, F., Jennings, D., Pardon, M.C., 2011. A detailed analysis of the early context extinction deficits seen in APPswe/PS1dE9 female mice and their relevance to preclinical Alzheimer's disease. Behav Brain Res 222, 89-97.

Brandscheid, C., Schuck, F., Reinhardt, S., Schafer, K.H., Pietrzik, C.U., Grimm, M., Hartmann, T., Schwiertz, A., Endres, K., 2017. Altered Gut Microbiome Composition and Tryptic Activity of the 5xFAD Alzheimer's Mouse Model. Journal of Alzheimers Disease 56, 775-788.

Brodie, B.B., Costa, E., Dlabac, A., Neff, N.H., Smookler, H.H., 1966. Application of steady state kinetics to the estimation of synthesis rate and turnover time of tissue catecholamines. J Pharmacol Exp Ther 154, 493-498.

Brown-Borg, H.M., 2006. Longevity in mice: is stress resistance a common factor? Age 28, 145-162.

Cai, K.C., van Mil, S., Murray, E., Mallet, J.F., Matar, C., Ismail, N., 2016. Age and sex differences in immune response following LPS treatment in mice. Brain Behav Immun 58, 327-337.

Card, J.W., Carey, M.A., Bradbury, J.A., DeGraff, L.M., Morgan, D.L., Moorman, M.P., Flake, G.P., Zeldin, D.C., 2006. Gender differences in murine airway responsiveness and lipopolysaccharide-induced inflammation. J Immunol 177, 621-630.

Chen, S., Dong, Z.P., Cheng, M., Zhao, Y.Q., Wang, M.Y., Sai, N., Wang, X., Liu, H., Huang, G.W., Zhang, X.M., 2017. Homocysteine exaggerates microglia activation and neuroinflammation through microglia localized STAT3 overactivation following ischemic stroke. J Neuroinflamm 14.

Cheng, J., Yuan, Z., Yang, W., Xu, C., Cong, W., Lin, L., Zhao, S., Sun, W., Bai, X., Cui, S., 2017. Comparative study of macrophages in naked mole rats and ICR mice. Oncotarget 8, 96924-96934.

Christa, L., Kersual, J., Auge, J., Perignon, J.L., 1986. Salvage of 5'-Deoxy-5'-Methylthioadenosine and L-Homocysteine into Methionine in Cells Cultured in a Methionine-Free Medium - a Study of Methionine-Dependence. Biochem Bioph Res Co 135, 131-138.

Clark, R.A., Shoaib, M., Hewitt, K.N., Stanford, S.C., Bate, S.T., 2012. A comparison of InVivoStat with other statistical software packages for analysis of data generated from animal experiments. J Psychopharmacol 26, 1136-1142.

Creek, D.J., Jankevics, A., Breitling, R., Watson, D.G., Barrett, M.P., Burgess, K.E.V., 2011. Toward Global Metabolomics Analysis with Hydrophilic Interaction Liquid Chromatography-Mass Spectrometry: Improved Metabolite Identification by Retention Time Prediction. Analytical Chemistry 83, 8703-8710.
Creek, D.J., Jankevics, A., Burgess, K.E.V., Breitling, R., Barrett, M.P., 2012. IDEOM: an Excel interface for analysis of LC-MS-based metabolomics data. Bioinformatics 28, 1048-1049.
Cunningham, C., Hennessy, E., 2015. Co-morbidity and systemic inflammation as drivers of cognitive decline: new experimental models adopting a broader paradigm in dementia research. Alzheimers Res Ther 7.
Cunningham, C., Sanderson, D.J., 2008. Malaise in the water maze: untangling the effects of LPS and IL-1beta on learning and memory. Brain Behav Immun 22, 1117-1127.
Das, U.N., 2006. Pyruvate is an endogenous anti-inflammatory and anti-oxidant molecule. Med Sci Monitor 12, Ra79-Ra84.
Davis, I., Liu, A.M., 2015. What is the tryptophan kynurenine pathway and why is it important to neurotherapeutics? Expert Rev Neurother 15, 719-721.
Deacon, R., 2012. Assessing Burrowing, Nest Construction, and Hoarding in Mice. Jove-Journal of Visualized Experiments.
Deacon, R.M.J., Croucher, A., Rawlins, J.N.P., 2002. Hippocampal cytotoxic lesion effects on species-typical behaviours in mice. Behav Brain Res 132, 203-213.
Desai, K.M., Chang, T.J., Wang, H., Banigesh, A., Dhar, A., Liu, J.H., Untereiner, A., Wu, L.Y., 2010. Oxidative stress and aging: Is methylglyoxal the hidden enemy? Can J Physiol Pharm 88, 273-284.
Dhahbi, J., Li, X.C., Tran, T., Masternak, M.M., Bartke, A., 2007. Circulating blood leukocyte gene expression profiles: Effects of the Ames dwarf mutation on pathways related to immunity and inflammation. Exp Gerontol 42, 772-788.
Ding, Y., Pardon, M.C., Agostini, A., Faas, H., Duan, J., Ward, W.O., Easton, F., Auer, D., Bai, L., 2016. Novel Methods for Microglia Segmentation, Feature Extraction and Classification. IEEE/ACM Trans Comput Biol Bioinform.
Dominguez-Soto, A., Usategui, A., de las Casas-Engel, M., Simon-Fuentes, M., Nieto, C., Cuevas, V.D., Vega, M.A., Pablos, J.L., Corbi, A.L., 2017. Serotonin drives the acquisition of a profibrotic and anti-inflammatory gene profile through the 5-HT7R-PKA signaling axis. Sci Rep-Uk 7.
Dorfman, M.D., Krull, J.E., Douglass, J.D., Fasnacht, R., Lara-Lince, F., Meek, T.H., Shi, X.G., Damian, V., Nguyen, H.T., Matsen, M.E., Morton, G.J., Thaler, J.P., 2017. Sex differences in microglial CX3CR1 signalling determine obesity susceptibility in mice. Nat Commun 8.
Eikelenboom, P., Hoozemans, J.J.M., Veerhuis, R., van Exel, E., Rozemuller, A.J.M., van Gool, W.A., 2012. Whether, when and how chronic inflammation increases the risk of developing late-onset Alzheimer's disease. Alzheimers Res Ther 4.
El Idrissi, A., 2008. Taurine improves learning and retention in aged mice. Neurosci Lett 436, 19-22.
Esser, N., Legrand-Poels, S., Piette, J., Scheen, A.J., Paquot, N., 2014. Inflammation as a link between obesity, metabolic syndrome and type 2 diabetes. Diabetes Res Clin Pr 105, 141-150.
Fan, H., Wu, P.F., Zhang, L., Hu, Z.L., Wang, W., Guan, X.L., Luo, H., Ni, M., Yang, J.W., Li, M.X., Chen, J.G., Wang, F., 2015. Methionine Sulfoxide Reductase A Negatively Controls Microglia-Mediated Neuroinflammation via Inhibiting ROS/MAPKs/NF-kappa B Signaling Pathways Through a Catalytic Antioxidant Function. Antioxid Redox Sign 22, 832-847.
Ferretti, M.T., Iulita, M.F., Cavedo, E., Chiesa, P.A., Schumacher Dimech, A., Santuccione Chadha, A., Baracchi, F., Girouard, H., Misoch, S., Giacobini, E., Depypere, H., Hampel, H., Women's Brain, P., the Alzheimer Precision Medicine, I., 2018. Sex differences in Alzheimer disease - the gateway to precision medicine. Nat Rev Neurol 14, 457-469.
Flavin, M., Slaughter, C., 1967. Enzymatic synthesis of homocysteine or methionine directly from O-succinyl-homoserine. Biochim Biophys Acta 132, 400-405.

Flugel, F., Timm, S., Arrivault, S., Florian, A., Stitt, M., Fernie, A.R., Bauwe, H., 2017. The Photorespiratory Metabolite 2-Phosphoglycolate Regulates Photosynthesis and Starch Accumulation in Arabidopsis. Plant Cell 29, 2537-2551.
Fontana, M., Pecci, L., Dupre, S., Cavallini, D., 2004. Antioxidant properties of sulfinates: protective effect of hypotaurine on peroxynitrite-dependent damage. Neurochem Res 29, 111-116.
Frigerio, C.S., Wolfs, L., Fattorelli, N., Thrupp, N., Voytyukt, I., Schmidt, I., Mancuso, R., Chen, W.T., Woodbury, M.E., Srivastava, G., Moller, T., Hudry, E., Das, S., Saido, T., Karran, E., Hyman, B., Perry, V.H., Fiers, M., De Strooper, B., 2019. The Major Risk Factors for Alzheimer's Disease: Age, Sex, and Genes Modulate the Microglia Response to A beta Plaques. Cell Rep 27, 1293-+.
Fuertig, R., Ceci, A., Camus, S.M., Bezard, E., Luippold, A.H., Hengerer, B., 2016. LC-MS/MS-based quantification of kynurenine metabolites, tryptophan, monoamines and neopterin in plasma, cerebrospinal fluid and brain. Bioanalysis 8, 1903-1917.
Fukuwatari, T., Shibata, K., 2013. Nutritional aspect of tryptophan metabolism. Int J Tryptophan Res 6, 3-8.
Gaignard, P., Savouroux, S., Liere, P., Pianos, A., Therond, P., Schumacher, M., Slama, A., Guennoun, R., 2015. Effect of Sex Differences on Brain Mitochondrial Function and Its Suppression by Ovariectomy and in Aged Mice. Endocrinology 156, 2893-2904.
Ge, J., Han, T., Li, X.Q., Shan, L.L., Zhang, J.H., Hong, Y., Xia, Y.Q., Wang, J., Hou, M.X., 2018. S-adenosyl methionine regulates calcium channels and inhibits uterine smooth muscle contraction in rats with infectious premature delivery through the transient receptor protein 3/protein kinase C beta/C-kinase-activated protein phosphatase-1 inhibitor of 17 kDa signaling pathway. Exp Ther Med 16, 103-112.
Geiszler, P.C., Barron, M.R., Pardon, M.C., 2016. Impaired Burrowing Is the Most Prominent Behavioral Deficit of Aging Htau Mice. Neuroscience 329, 98-111.
Ghosh, S., Castillo, E., Frias, E.S., Swanson, R.A., 2018. Bioenergetic regulation of microglia. Glia 66, 1200-1212.
Giridharan, V.V., Masud, F., Petronilho, F., Dal-Pizzol, F., Barichello, T., 2019. Infection-Induced Systemic Inflammation Is a Potential Driver of Alzheimer's Disease Progression. Frontiers in Aging Neuroscience 11.
Gonzalez-Dominguez, R., Garcia-Barrera, T., Vitorica, J., Gomez-Ariza, J.L., 2014. Region-specific metabolic alterations in the brain of the APP/PS1 transgenic mice of Alzheimer's disease. Biochim Biophys Acta 1842, 2395-2402.
Guerrant, R.L., Leite, A.M., Pinkerton, R., Medeiros, P.H., Cavalcante, P.A., DeBoer, M., Kosek, M., Duggan, C., Gewirtz, A., Kagan, J.C., Gauthier, A.E., Swann, J., Mayneris-Perxachs, J., Bolick, D.T., Maier, E.A., Guedes, M.M., Moore, S.R., Petri, W.A., Havt, A., Lima, I.F., Prata, M.M., Michaleckyj, J.C., Scharf, R.J., Sturgeon, C., Fasano, A., Lima, A.A., 2016. Biomarkers of Environmental Enteropathy, Inflammation, Stunting, and Impaired Growth in Children in Northeast Brazil. PLoS One 11, e0158772.
Guneykaya, D., Ivanov, A., Hernandez, D.P., Haage, V., Wojtas, B., Meyer, N., Maricos, M., Jordan, P., Buonfiglioli, A., Gielniewski, B., Ochocka, N., Comert, C., Friedrich, C., Artiles, L.S., Kaminska, B., Mertins, P., Beule, D., Kettenmann, H., Wolf, S.A., 2018. Transcriptional and Translational Differences of Microglia from Male and Female Brains. Cell Rep 24, 2773-2783 e2776.
Guo, Y.J., Cai, H.L., Chen, L., Liang, D.L., Yang, R.Y., Dang, R.L., Jiang, P., 2016. Quantitative profiling of neurotransmitter abnormalities in the hippocampus of rats treated with lipopolysaccharide: Focusing on kynurenine pathway and implications for depression. J Neuroimmunol 295, 41-46.
Hanke, M.L., Kielian, T., 2011. Toll-like receptors in health and disease in the brain: mechanisms and therapeutic potential. Clin Sci (Lond) 121, 367-387.
Hansen, D.V., Hanson, J.E., Sheng, M., 2018. Microglia in Alzheimer's disease. J Cell Biol 217, 459-472.
Hansen, F., Pandolfo, P., Galland, F., Torres, F.V., Dutra, M.F., Batassini, C., Guerra, M.C., Leite, M.C., Goncalves, C.A., 2016. Methylglyoxal can mediate behavioral and neurochemical alterations in rat brain. Physiol Behav 164, 93-101.

Hara, K., Nakamura, M., Haranishi, Y., Terada, T., Kataoka, K., Sata, T., 2012. Antinociceptive effect of intrathecal administration of hypotaurine in rat models of inflammatory and neuropathic pain. Amino Acids 43, 397-404.
Harach, T., Marungruang, N., Duthilleul, N., Cheatham, V., Mc Coy, K.D., Frisoni, G., Neher, J.J., Fak, F., Jucker, M., Lasser, T., Bolmont, T., 2017. Reduction of Abeta amyloid pathology in APPPS1 transgenic mice in the absence of gut microbiota. Sci Rep-Uk 7.
Hart, A.D., Wyttenbach, A., Perry, V.H., Teeling, J.L., 2012. Age related changes in microglial phenotype vary between CNS regions: Grey versus white matter differences. Brain Behav Immun 26, 754-765.
Hevia, H., Varela-Rey, M., Corrales, F.J., Berasain, C., Martinez-Chantar, M.L., Latasa, M.U., Lu, S.C., Mato, J.M., Garcia-Trevijano, E.R., Avila, M.A., 2004. 5 '-methylthioadenosine modulates the inflammatory response to endotoxin in mice and in rat hepatocytes. Hepatology 39, 1088-1098.
Hoglund, E., Overli, O., Winberg, S., 2019. Tryptophan Metabolic Pathways and Brain Serotonergic Activity: A Comparative Review. Front Endocrinol (Lausanne) 10, 158.
Holmer, J., Eriksdotter, M., Schultzberg, M., Pussinen, P.J., Buhlin, K., 2018. Association between periodontitis and risk of Alzheimer's disease, mild cognitive impairment and subjective cognitive decline: A case-control study. J Clin Periodontol 45, 1287-1298.
Holmes, C., Cunningham, C., Zotova, E., Woolford, J., Dean, C., Kerr, S., Culliford, D., Perry, V.H., 2009. Systemic inflammation and disease progression in Alzheimer disease. Neurology 73, 768-774.
Hoogland, I.C.M., Houbolt, C., van Westerloo, D.J., van Gool, W.A., van de Beek, D., 2015. Systemic inflammation and microglial activation: systematic review of animal experiments. J Neuroinflamm 12.
Hoshi, T., Heinemann, S., 2001. Regulation of cell function by methionine oxidation and reduction. J Physiol 531, 1-11.
Ide, M., Harris, M., Stevens, A., Sussams, R., Hopkins, V., Culliford, D., Fuller, J., Ibbett, P., Raybould, R., Thomas, R., Puenter, U., Teeling, J., Perry, V.H., Holmes, C., 2016. Periodontitis and Cognitive Decline in Alzheimer's Disease. PLoS One 11, e0151081.
Ikegami, K., Lalonde, C., Youn, Y.K., Picard, L., Demling, R., 1994. Comparison of Plasma Reduced Glutathione and Oxidized Glutathione with Lung and Liver-Tissue Oxidant and Antioxidant Activity during Acute-Inflammation. Shock 1, 307-312.
Irace, C., Esposito, G., Maffettone, C., Rossi, A., Festa, M., Iuvone, T., Santamaria, R., Sautebin, L., Carnuccio, R., Colonna, A., 2007. Oxalomalate affects the inducible nitric oxide synthase expression and activity. Life Sci 80, 1282-1291.
Isopi, E., Granzotto, A., Corona, C., Bomba, M., Ciavardelli, D., Curcio, M., Canzoniero, L.M.T., Navarra, R., Lattanzio, R., Piantelli, M., Sensi, S.L., 2015. Pyruvate prevents the development of age-dependent cognitive deficits in a mouse model of Alzheimer's disease without reducing amyloid and tau pathology. Neurobiology of Disease 81, 214-224.
Jankowsky, J.L., Fadale, D.J., Anderson, J., Xu, G.M., Gonzales, V., Jenkins, N.A., Copeland, N.G., Lee, M.K., Younkin, L.H., Wagner, S.L., Younkin, S.G., Borchelt, D.R., 2004. Mutant presenilins specifically elevate the levels of the 42 residue beta-amyloid peptide in vivo: evidence for augmentation of a 42-specific gamma secretase. Hum Mol Genet 13, 159-170.
Kabil, O., Vitvitsky, V., Banerjee, R., 2014. Sulfur as a Signaling Nutrient Through Hydrogen Sulfide. Annu Rev Nutr 34, 171-205.
Karch, C.M., Goate, A.M., 2015. Alzheimer's disease risk genes and mechanisms of disease pathogenesis. Biol Psychiatry 77, 43-51.
Kilkenny, C., Browne, W.J., Cuthill, I.C., Emerson, M., Altman, D.G., 2010. Improving bioscience research reporting: the ARRIVE guidelines for reporting animal research. PLoS Biol 8, e1000412.
Kim, Y.K., Jeon, S.W., 2018. Neuroinflammation and the Immune-Kynurenine Pathway in Anxiety Disorders. Curr Neuropharmacol 16, 574-582.
King, E., O'Brien, J.T., Donaghy, P., Morris, C., Barnett, N., Olsen, K., Martin-Ruiz, C., Taylor, J.P., Thomas, A.J., 2018. Peripheral inflammation in prodromal Alzheimer's and Lewy body dementias. J Neurol Neurosurg Psychiatry 89, 339-345.

Klein, S.L., Flanagan, K.L., 2016. Sex differences in immune responses. Nat Rev Immunol 16, 626-638.
Koivisto, H., Leinonen, H., Puurula, M., Hafez, H.S., Barrera, G.A., Stridh, M.H., Waagepetersen, H.S., Tiainen, M., Soininen, P., Zilberter, Y., Tanila, H., 2016. Chronic Pyruvate Supplementation Increases Exploratory Activity and Brain Energy Reserves in Young and Middle-Aged Mice. Front Aging Neurosci 8, 41.
Koss, W.A., Frick, K.M., 2017. Sex Differences in Hippocampal Function. J Neurosci Res 95, 539-562.
Koyama, A., O'Brien, J., Weuve, J., Blacker, D., Metti, A.L., Yaffe, K., 2013. The role of peripheral inflammatory markers in dementia and Alzheimer's disease: a meta-analysis. J Gerontol A Biol Sci Med Sci 68, 433-440.
Kozlowski, C., Weimer, R.M., 2012. An automated method to quantify microglia morphology and application to monitor activation state longitudinally in vivo. PLoS One 7, e31814.
Kreisel, T., Frank, M.G., Licht, T., Reshef, R., Ben-Menachem-Zidon, O., Baratta, M.V., Maier, S.F., Yirmiya, R., 2014. Dynamic microglial alterations underlie stress-induced depressive-like behavior and suppressed neurogenesis. Mol Psychiatry 19, 699-709.
Kuhla, B., Luth, H.J., Haferburg, D., Boeck, K., Arendt, T., Munch, G., 2005. Methylglyoxal, glyoxal, and their detoxification in Alzheimer's disease. Ann Ny Acad Sci 1043, 211-216.
Lapin, I.P., 2003. Neurokynurenines (NEKY) as common neurochemical links of stress and anxiety. Adv Exp Med Biol 527, 121-125.
Lee, H.K., Kim, I.D., Kim, S.W., Lee, H., Park, J.Y., Yoon, S.H., Lee, J.K., 2017. Anti-inflammatory and anti-excitoxic effects of diethyl oxopropanamide, an ethyl pyruvate bioisoster, exert robust neuroprotective effects in the postischemic brain. Sci Rep 7, 42891.
Lee, H.K., Kim, S.W., Jin, Y., Kim, I.D., Park, J.Y., Yoon, S.H., Lee, J.K., 2013. Anti-inflammatory effects of OBA-09, a salicylic acid/pyruvate ester, in the postischemic brain. Brain Res 1528, 68-79.
Lenglet, A., Liabeuf, S., Bodeau, S., Louvet, L., Mary, A., Boullier, A., Lemaire-Hurtel, A.S., Jonet, A., Sonnet, P., Kamel, S., Massy, Z.A., 2016. N-methyl-2-pyridone-5-carboxamide (2PY)-Major Metabolite of Nicotinamide: An Update on an Old Uremic Toxin. Toxins 8.
Lewis, K.N., Rubinstein, N.D., Buffenstein, R., 2018. A window into extreme longevity; the circulating metabolomic signature of the naked mole-rat, a mammal that shows negligible senescence (vol 40 pg 105, 2018). Geroscience 40, 357-358.
Li, X., Feng, Y., Wu, W., Zhao, J., Fu, C.M., Li, Y., Ding, Y.N., Wu, B.H., Gong, Y.J., Yang, G.Z., Zhou, X., 2016. Sex differences between APPswePS1dE9 mice in A-beta accumulation and pancreatic islet function during the development of Alzheimer's disease. Lab Anim-Uk 50, 275-285.
Maldonado, R.F., Sa-Correia, I., Valvano, M.A., 2016. Lipopolysaccharide modification in Gram-negative bacteria during chronic infection. FEMS Microbiol Rev 40, 480-493.
Malik, M., Parikh, I., Vasquez, J.B., Smith, C., Tai, L., Bu, G., LaDu, M.J., Fardo, D.W., Rebeck, G.W., Estus, S., 2015. Genetics ignite focus on microglial inflammation in Alzheimer's disease. Mol Neurodegener 10, 52.
Malm, T., Koistinaho, J., Kanninen, K., 2011. Utilization of APPswe/PS1dE9 Transgenic Mice in Research of Alzheimer's Disease: Focus on Gene Therapy and Cell-Based Therapy Applications. Int J Alzheimers Dis 2011, 517160.
Maroof, N., Ravipati, S., Pardon, M.C., Barrett, D.A., Kendall, D.A., 2014. Reductions in Endocannabinoid Levels and Enhanced Coupling of Cannabinoid Receptors in the Striatum are Accompanied by Cognitive Impairments in the A beta PPswe/PS1 Delta E9 Mouse Model of Alzheimer's Disease. Journal of Alzheimers Disease 42, 227-245.
Martin, E., Boucher, C., Fontaine, B., Delarasse, C., 2017. Distinct inflammatory phenotypes of microglia and monocyte-derived macrophages in Alzheimer's disease models: effects of aging and amyloid pathology. Aging Cell 16, 27-38.
Martinez, Y., Li, X., Liu, G., Bin, P., Yan, W., Mas, D., Valdivie, M., Hu, C.A., Ren, W., Yin, Y., 2017. The role of methionine on metabolism, oxidative stress, and diseases. Amino Acids 49, 2091-2098.

Matafome, P., Sena, C., Seica, R., 2013. Methylglyoxal, obesity, and diabetes. Endocrine 43, 472-484.
Mayneris-Perxachs, J., Lima, A.A., Guerrant, R.L., Leite, A.M., Moura, A.F., Lima, N.L., Soares, A.M., Havt, A., Moore, S.R., Pinkerton, R., Swann, J.R., 2016. Urinary N-methylnicotinamide and beta-aminoisobutyric acid predict catch-up growth in undernourished Brazilian children. Sci Rep 6, 19780.
McGowan, P.O., Meaney, M.J., Szyf, M., 2008. Diet and the epigenetic (re)programming of phenotypic differences in behavior. Brain Res 1237, 12-24.
Moreno, B., Hevia, H., Santamaria, M., Sepulcre, J., Munoz, J., Garcia-Trevijano, E.R., Berasain, C., Corrales, F.J., Avila, M.A., Villoslada, P., 2006. Methylthioadenosine reverses brain autoimmune disease. Ann Neurol 60, 323-334.
Morrison, L.D., Smith, D.D., Kish, S.J., 1996. Brain S-adenosylmethionine levels are severely decreased in Alzheimer's disease. J Neurochem 67, 1328-1331.
Moruno-Manchon, J.F., Uzor, N.E., Kesler, S.R., Wefel, J.S., Townley, D.M., Nagaraja, A.S., Pradeep, S., Mangala, L.S., Sood, A.K., Tsvetkov, A.S., 2018. Peroxisomes contribute to oxidative stress in neurons during doxorubicin-based chemotherapy. Mol Cell Neurosci 86, 65-71.
Moskovitz, J., Du, F., Bowman, C.F., Yan, S.S., 2016. Methionine sulfoxide reductase A affects beta-amyloid solubility and mitochondrial function in a mouse model of Alzheimer's disease. Am J Physiol Endocrinol Metab 310, E388-393.
Murray, C.L., Skelly, D.T., Cunningham, C., 2011. Exacerbation of CNS inflammation and neurodegeneration by systemic LPS treatment is independent of circulating IL-1 beta and IL-6. J Neuroinflamm 8.
Nazem, A., Sankowski, R., Bacher, M., Al-Abed, Y., 2015. Rodent models of neuroinflammation for Alzheimer's disease. J Neuroinflamm 12.
Nilsson, L., Kogure, K., Busto, R., 1975. Effects of hypothermia and hyperthermia on brain energy metabolism. Acta Anaesthesiol Scand 19, 199-205.
Nolan, Y., Connor, T.J., Kelly, J.P., Leonard, B.E., 2000. Lipopolysaccharide administration produces time-dependent and region-specific alterations in tryptophan and tyrosine hydroxylase activities in rat brain. J Neural Transm (Vienna) 107, 1393-1401.
O'Connor, J.C., Lawson, M.A., Andre, C., Moreau, M., Lestage, J., Castanon, N., Kelley, K.W., Dantzer, R., 2009. Lipopolysaccharide-induced depressive-like behavior is mediated by indoleamine 2,3-dioxygenase activation in mice. Mol Psychiatr 14, 511-522.
Onishi, A., Akimoto, T., Urabe, M., Hirahara, I., Muto, S., Ozawa, K., Nagata, D., Kusano, E., 2015. Attenuation of methylglyoxal-induced peritoneal fibrosis: immunomodulation by interleukin-10. Lab Invest 95, 1353-1362.
Orgeron, M.L., Stone, K.P., Wanders, D., Cortez, C.C., Van, N.T., Gettys, T.W., 2014. The impact of dietary methionine restriction on biomarkers of metabolic health. Prog Mol Biol Transl Sci 121, 351-376.
Pardon, M.C., Yanez Lopez, M., Yuchun, D., Marjanska, M., Prior, M., Brignell, C., Parhizkar, S., Agostini, A., Bai, L., Auer, D.P., Faas, H.M., 2016. Magnetic Resonance Spectroscopy discriminates the response to microglial stimulation of wild type and Alzheimer's disease models. Sci Rep 6, 19880.
Parrott, J.M., Redus, L., O'Connor, J.C., 2016. Kynurenine metabolic balance is disrupted in the hippocampus following peripheral lipopolysaccharide challenge. J Neuroinflamm 13.
Perea, J.R., Llorens-Martin, M., Avila, J., Bolos, M., 2018. The Role of Microglia in the Spread of Tau: Relevance for Tauopathies. Frontiers in Cellular Neuroscience 12.
Pereira, H., Martin, J.F., Joly, C., Sebedio, J.L., Pujos-Guillot, E., 2010. Development and validation of a UPLC/MS method for a nutritional metabolomic study of human plasma. Metabolomics 6, 207-218.
Peters, M.A., Hudson, P.M., Jurgelske, W., Jr., 1978. The acute toxicity of methylglyoxal in rats: the influence of age, sex, and pregnancy. Ecotoxicol Environ Saf 2, 369-374.
Pfalzer, A.C., Choi, S.W., Tammen, S.A., Park, L.K., Bottiglieri, T., Parnell, L.D., Lamon-Fava, S., 2014. S-adenosylmethionine mediates inhibition of inflammatory response and changes in DNA methylation in human macrophages. Physiol Genomics 46, 617-623.

Pistollato, F., Cano, S.S., Elio, I., Vergara, M.M., Giampieri, F., Battino, M., 2016. Role of gut microbiota and nutrients in amyloid formation and pathogenesis of Alzheimer disease. Nutr Rev 74, 624-634.
Pitychoutis, P.M., Nakamura, K., Tsonis, P.A., Papadopoulou-Daifoti, Z., 2009. Neurochemical and behavioral alterations in an inflammatory model of depression: sex differences exposed. Neuroscience 159, 1216-1232.
Podcasy, J.L., Epperson, C.N., 2016. Considering sex and gender in Alzheimer disease and other dementias. Dialogues Clin Neurosci 18, 437-446.
Price, C.L., Hassi, H.O., English, N.R., Blakemore, A.I., Stagg, A.J., Knight, S.C., 2010. Methylglyoxal modulates immune responses: relevance to diabetes. J Cell Mol Med 14, 1806-1815.
Recalcati, S., Tacchini, L., Alberghini, A., Conte, D., Cairo, G., 2003. Oxidative stress-mediated down-regulation of rat hydroxyacid oxidase 1, a liver-specific peroxisomal enzyme. Hepatology 38, 1159-1166.
Romanovsky, A.A., Almeida, M.C., Aronoff, D.M., Ivanov, A.I., Konsman, J.P., Steiner, A.A., Turek, V.F., 2005. Fever and hypothermia in systemic inflammation: Recent discoveries and revisions. Front Biosci-Landmrk 10, 2193-2216.
Roved, J., Westerdahl, H., Hasselquist, D., 2017. Sex differences in immune responses: Hormonal effects, antagonistic selection, and evolutionary consequences. Horm Behav 88, 95-105.
Ruan, L., Kang, Z., Pei, G., Le, Y., 2009. Amyloid deposition and inflammation in APPswe/PS1dE9 mouse model of Alzheimer's disease. Curr Alzheimer Res 6, 531-540.
Sadagurski, M., Landeryou, T., Cady, G., Kopchick, J.J., List, E.O., Berryman, D.E., Bartke, A., Miller, R.A., 2015. Growth hormone modulates hypothalamic inflammation in long-lived pituitary dwarf mice. Aging Cell 14, 1045-1054.
Schaffer, S., Kim, H.W., 2018. Effects and Mechanisms of Taurine as a Therapeutic Agent. Biomol Ther 26, 225-241.
Scheltema, R.A., Jankevics, A., Jansen, R.C., Swertz, M.A., Breitling, R., 2011. PeakML/mzMatch: A File Format, Java Library, R Library, and Tool-Chain for Mass Spectrometry Data Analysis. Analytical Chemistry 83, 2786-2793.
Schrader, M., Fahimi, H.D., 2006. Peroxisomes and oxidative stress. Bba-Mol Cell Res 1763, 1755-1766.
Schwartz, M., Baruch, K., 2014. The resolution of neuroinflammation in neurodegeneration: leukocyte recruitment via the choroid plexus. EMBO J 33, 7-22.
Seemann, S., Zohles, F., Lupp, A., 2017. Comprehensive comparison of three different animal models for systemic inflammation. J Biomed Sci 24, 60.
Segerer, G., Hadamek, K., Zundler, M., Fekete, A., Seifried, A., Mueller, M.J., Koentgen, F., Gessler, M., Jeanclos, E., Gohla, A., 2016. An essential developmental function for murine phosphoglycolate phosphatase in safeguarding cell proliferation. Sci Rep-Uk 6.
Sens, J., Schneider, E., Mauch, J., Schaffstein, A., Mohamed, S., Fasoli, K., Saurine, J., Britzolaki, A., Thelen, C., Pitychoutis, P.M., 2017. Lipopolysaccharide administration induces sex-dependent behavioural and serotonergic neurochemical signatures in mice. Pharmacol Biochem Behav 153, 168-181.
Shibata, K., Matsuo, H., 1990. Effect of dietary tryptophan levels on the urinary excretion of nicotinamide and its metabolites in rats fed a niacin-free diet or a constant total protein level. J Nutr 120, 1191-1197.
Shiraki, N., Shiraki, Y., Tsuyama, T., Obata, F., Miura, M., Nagae, G., Aburatani, H., Kume, K., Endo, F., Kume, S., 2014. Methionine metabolism regulates maintenance and differentiation of human pluripotent stem cells. Cell Metab 19, 780-794.
Skelly, D.T., Hennessy, E., Dansereau, M.A., Cunningham, C., 2013. A systematic analysis of the peripheral and CNS effects of systemic LPS, IL-1beta, [corrected] TNF-alpha and IL-6 challenges in C57BL/6 mice. PLoS One 8, e69123.
Smith, A.D., Refsum, H., Bottiglieri, T., Fenech, M., Hooshmand, B., McCaddon, A., Miller, J.W., Rosenberg, I.H., Obeid, R., 2018. Homocysteine and Dementia: An International Consensus Statement. Journal of Alzheimers Disease 62, 561-570.
Smith, G.S., Barrett, F.S., Joo, J.H., Nassery, N., Savonenko, A., Sodums, D.J., Marano, C.M., Munro, C.A., Brandt, J., Kraut, M.A., Zhou, Y., Wong, D.F., Workman, C.I., 2017.

Molecular imaging of serotonin degeneration in mild cognitive impairment. Neurobiol Dis 105, 33-41.
Sochocka, M., Donskow-Lysoniewska, K., Diniz, B.S., Kurpas, D., Brzozowska, E., Leszek, J., 2019. The Gut Microbiome Alterations and Inflammation-Driven Pathogenesis of Alzheimer's Diseasea Critical Review. Molecular Neurobiology 56, 1841-1851.
Soto, M., Orliaguet, L., Reyzer, M.L., Manier, M.L., Caprioli, R.M., Kahn, C.R., 2018. Pyruvate induces torpor in obese mice. Proc Natl Acad Sci U S A 115, 810-815.
Stadtman, E.R., Van Remmen, H., Richardson, A., Wehr, N.B., Levine, R.L., 2005. Methionine oxidation and aging. Biochim Biophys Acta 1703, 135-140.
Stipanuk, M.H., Ueki, I., 2011. Dealing with methionine/homocysteine sulfur: cysteine metabolism to taurine and inorganic sulfur. J Inherit Metab Dis 34, 17-32.
Sumner, L.W., Amberg, A., Barrett, D., Beale, M.H., Beger, R., Daykin, C.A., Fan, T.W., Fiehn, O., Goodacre, R., Griffin, J.L., Hankemeier, T., Hardy, N., Harnly, J., Higashi, R., Kopka, J., Lane, A.N., Lindon, J.C., Marriott, P., Nicholls, A.W., Reily, M.D., Thaden, J.J., Viant, M.R., 2007. Proposed minimum reporting standards for chemical analysis Chemical Analysis Working Group (CAWG) Metabolomics Standards Initiative (MSI). Metabolomics 3, 211-221.
Surrati, A., Linforth, R., Fisk, I.D., Sottile, V., Kim, D.H., 2016. Non-destructive characterisation of mesenchymal stem cell differentiation using LC-MS-based metabolite footprinting. Analyst 141, 3776-3787.
Tajes, M., Eraso-Pichot, A., Rubio-Moscardo, F., Guivernau, B., Ramos-Fernandez, E., Bosch-Morato, M., Guix, F.X., Clarimon, J., Miscione, G.P., Boada, M., Gil-Gomez, G., Suzuki, T., Molina, H., Villa-Freixa, J., Vicente, R., Munoz, F.J., 2014. Methylglyoxal produced by amyloid-beta peptide-induced nitrotyrosination of triosephosphate isomerase triggers neuronal death in Alzheimer's disease. J Alzheimers Dis 41, 273-288.
Tapia-Rojas, C., Lindsay, C.B., Montecinos-Oliva, C., Arrazola, M.S., Retamales, R.M., Bunout, D., Hirsch, S., Inestrosa, N.C., 2015. Is L-methionine a trigger factor for Alzheimer's-like neurodegeneration?: Changes in Abeta oligomers, tau phosphorylation, synaptic proteins, Wnt signaling and behavioral impairment in wild-type mice. Mol Neurodegener 10, 62.
Tautenhahn, R., Bottcher, C., Neumann, S., 2008. Highly sensitive feature detection for high resolution LC/MS. Bmc Bioinformatics 9.
Teeling, J.L., Felton, L.M., Deacon, R.M., Cunningham, C., Rawlins, J.N., Perry, V.H., 2007. Sub-pyrogenic systemic inflammation impacts on brain and behavior, independent of cytokines. Brain Behav Immun 21, 836-850.
Terlecky, S.R., Terlecky, L.J., Giordano, C.R., 2012. Peroxisomes, oxidative stress, and inflammation. World J Biol Chem 3, 93-97.
Thorburn, T., Aali, M., Lehmann, C., 2018. Immune response to systemic inflammation in the intestinal microcirculation. Front Biosci (Landmark Ed) 23, 782-795.
Trollor, J.N., Smith, E., Baune, B.T., Kochan, N.A., Campbell, L., Samaras, K., Crawford, J., Brodaty, H., Sachdev, P., 2010. Systemic Inflammation Is Associated with MCI and Its Subtypes: The Sydney Memory and Aging Study. Dement Geriatr Cogn 30, 569-578.
Tucker, L.B., Fu, A.H., McCabe, J.T., 2016. Performance of Male and Female C57BL/6J Mice on Motor and Cognitive Tasks Commonly Used in Pre-Clinical Traumatic Brain Injury Research. J Neurotraum 33, 880-894.
Uthus, E.O., Brown-Borg, H.M., 2003. Altered methionine metabolism in long living Ames dwarf mice. Exp Gerontol 38, 491-498.
Varatharaj, A., Galea, I., 2017. The blood-brain barrier in systemic inflammation. Brain Behav Immun 60, 1-12.
Villa, A., Della Torre, S., Maggi, A., 2018a. Sexual differentiation of microglia. Front Neuroendocrinol.
Villa, A., Gelosa, P., Castiglioni, L., Cimino, M., Rizzi, N., Pepe, G., Lolli, F., Marcello, E., Sironi, L., Vegeto, E., Maggi, A., 2018b. Sex-Specific Features of Microglia from Adult Mice. Cell Rep 23, 3501-3511.
Villapol, S., Loane, D.J., Burns, M.P., 2017. Sexual dimorphism in the inflammatory response to traumatic brain injury. Glia 65, 1423-1438.

Vincent, I.M., Weidt, S., Rivas, L., Burgess, K., Smith, T.K., Ouellette, M., 2014. Untargeted metabolomic analysis of miltefosine action in Leishmania infantum reveals changes to the internal lipid metabolism. Int J Parasitol Drugs Drug Resist 4, 20-27.
Vitvitsky, V., Martinov, M., Ataullakhanov, F., Miller, R.A., Banerjee, R., 2013. Sulfur-based redox alterations in long-lived Snell dwarf mice. Mech Ageing Dev 134, 321-330.
Vulesevic, B., McNeill, B., Giacco, F., Maeda, K., Blackburn, N.J.R., Brownlee, M., Milne, R.W., Suuronen, E.J., 2016. Methylglyoxal-Induced Endothelial Cell Loss and Inflammation Contribute to the Development of Diabetic Cardiomyopathy. Diabetes 65, 1699-1713.
Wagner, A.K., Bayir, H., Ren, D.X., Puccio, A., Zafonte, R.D., Kochanek, P.M., 2004. Relationships between cerebrospinal fluid markers of excitotoxicity, ischemia, and oxidative damage after severe TBI: The impact of gender, age, and hypothermia. J Neurotraum 21, 125-136.
Wang, J., Tanila, H., Puolivali, J., Kadish, I., van Groen, T., 2003. Gender differences in the amount and deposition of amyloidbeta in APPswe and PS1 double transgenic mice. Neurobiol Dis 14, 318-327.
Wang, L., Ko, E.R., Gilchrist, J.J., Pittman, K.J., Rautanen, A., Pirinen, M., Thompson, J.W., Dubois, L.G., Langley, R.J., Jaslow, S.L., Salinas, R.E., Rouse, D.C., Moseley, M.A., Mwarumba, S., Njuguna, P., Mturi, N., Williams, T.N., Scott, J.A.G., Hill, A.V.S., Woods, C.W., Ginsburg, G.S., Tsalik, E.L., Ko, D.C., Control, W.T.C., Grp, K.B.S., 2017. Human genetic and metabolite variation reveals that methylthioadenosine is a prognostic biomarker and an inflammatory regulator in sepsis. Sci Adv 3.
Woltjer, R.L., Maezawa, I., Ou, J.J., Montine, K.S., Montine, T.J., 2003. Advanced glycation endproduct precursor alters intracellular amyloid-beta/A beta PP carboxy-terminal fragment aggregation and cytotoxicity. J Alzheimers Dis 5, 467-476.
Wu, W., Nicolazzo, J.A., Wen, L., Chung, R., Stankovic, R., Bao, S.S.S., Lim, C.K., Brew, B.J., Cullen, K.M., Guillemin, G.J., 2013. Expression of Tryptophan 2,3-Dioxygenase and Production of Kynurenine Pathway Metabolites in Triple Transgenic Mice and Human Alzheimer's Disease Brain. Plos One 8.
Yaku, K., Okabe, K., Nakagawa, T., 2018. NAD metabolism: Implications in aging and longevity. Ageing Res Rev 47, 1-17.
Ye, X.F., Lian, Q.Q., Eckenhoff, M.F., Eckenhoff, R.G., Pan, J.Z., 2013. Differential General Anesthetic Effects on Microglial Cytokine Expression. Plos One 8.
Yokoyama, J.S., Wang, Y.P., Schork, A.J., Thompson, W.K., Karch, C.M., Cruchaga, C., McEvoy, L.K., Witoelar, A., Chen, C.H., Holland, D., Brewer, J.B., Franke, A., Dillon, W.P., Wilson, D.M., Mukherjee, P., Hess, C.P., Miller, Z., Bonham, L.W., Shen, J., Rabinovici, G.D., Rosen, H.J., Miller, B.L., Hyman, B.T., Schellenberg, G.D., Karlsen, T.H., Andreassen, O.A., Dale, A.M., Desikan, R.S., Initi, A.s.D.N., 2016. Association Between Genetic Traits for Immune-Mediated Diseases and Alzheimer Disease. Jama Neurol 73, 691-697.
Young, K., Rothers, J., Castaneda, S., Ritchie, J., E Pottenger, A., Morrison, H., 2018. Sex and regional differences in microglia morphology and complement receptor 3 are independent of constitutive neuroinflammatory protein concentrations in healthy mice.
Zhan, X., Stamova, B., Sharp, F.R., 2018. Lipopolysaccharide Associates with Amyloid Plaques, Neurons and Oligodendrocytes in Alzheimer's Disease Brain: A Review. Front Aging Neurosci 10, 42.
Zhan, X.H., Stamova, B., Jin, L.W., DeCarli, C., Phinney, B., Sharp, F.R., 2016. Gram-negative bacterial molecules associate with Alzheimer disease pathology. Neurology 87, 2324-2332.
Zhang, L., Wang, Y., Xiayu, X., Shi, C., Chen, W., Song, N., Fu, X., Zhou, R., Xu, Y.F., Huang, L., Zhu, H., Han, Y., Qin, C., 2017. Altered Gut Microbiota in a Mouse Model of Alzheimer's Disease. J Alzheimers Dis 60, 1241-1257.
Zhang, R., Miller, R.G., Gascon, R., Champion, S., Katz, J., Lancero, M., Narvaez, A., Honrada, R., Ruvalcaba, D., McGrath, M.S., 2009. Circulating endotoxin and systemic immune activation in sporadic amyotrophic lateral sclerosis (sALS). J Neuroimmunol 206, 121-124.

Zhao, L.Q., Mao, Z.S., Woody, S.K., Brinton, R.D., 2016. Sex differences in metabolic aging of the brain: insights into female susceptibility to Alzheimer's disease. Neurobiol Aging 42, 69-79.
Zhao, Y.H., Cong, L., Jaber, V., Lukiw, W.J., 2017. Microbiome-Derived Lipopolysaccharide Enriched in the Perinuclear Region of Alzheimer's Disease Brain. Front Immunol 8.

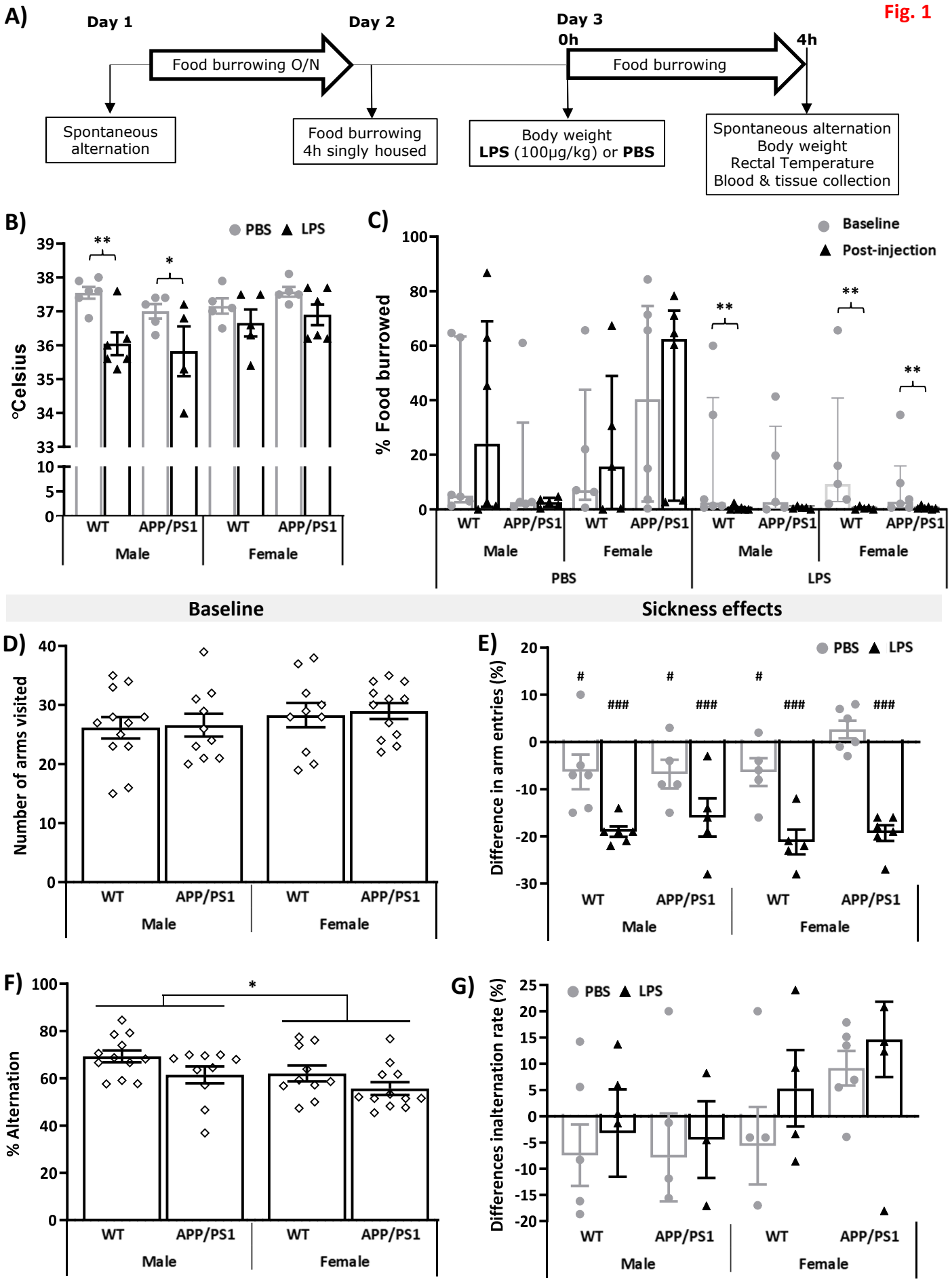
Fig. 1
A)
Day 1
Day 2
Day 3
0h
4h
Food burrowing O/N
Food burrowing
Spontaneous alternation
Food burrowing 4h singly housed
Body weight LPS (100µg/kg) or PBS
Spontaneous alternation
Body weight
Rectal Temperature
Blood & tissue collection
B)
PBS
LPS
°Celsius
WT
APP/PS1
Male
Female
C)
Baseline
Post-injection
% Food burrowed
PBS
LPS
Baseline
Sickness effects
D)
Number of arms visited
E)
Difference in arm entries (%)
F)
% Alternation
G)
Differences inalternation rate (%)

Fig. 2

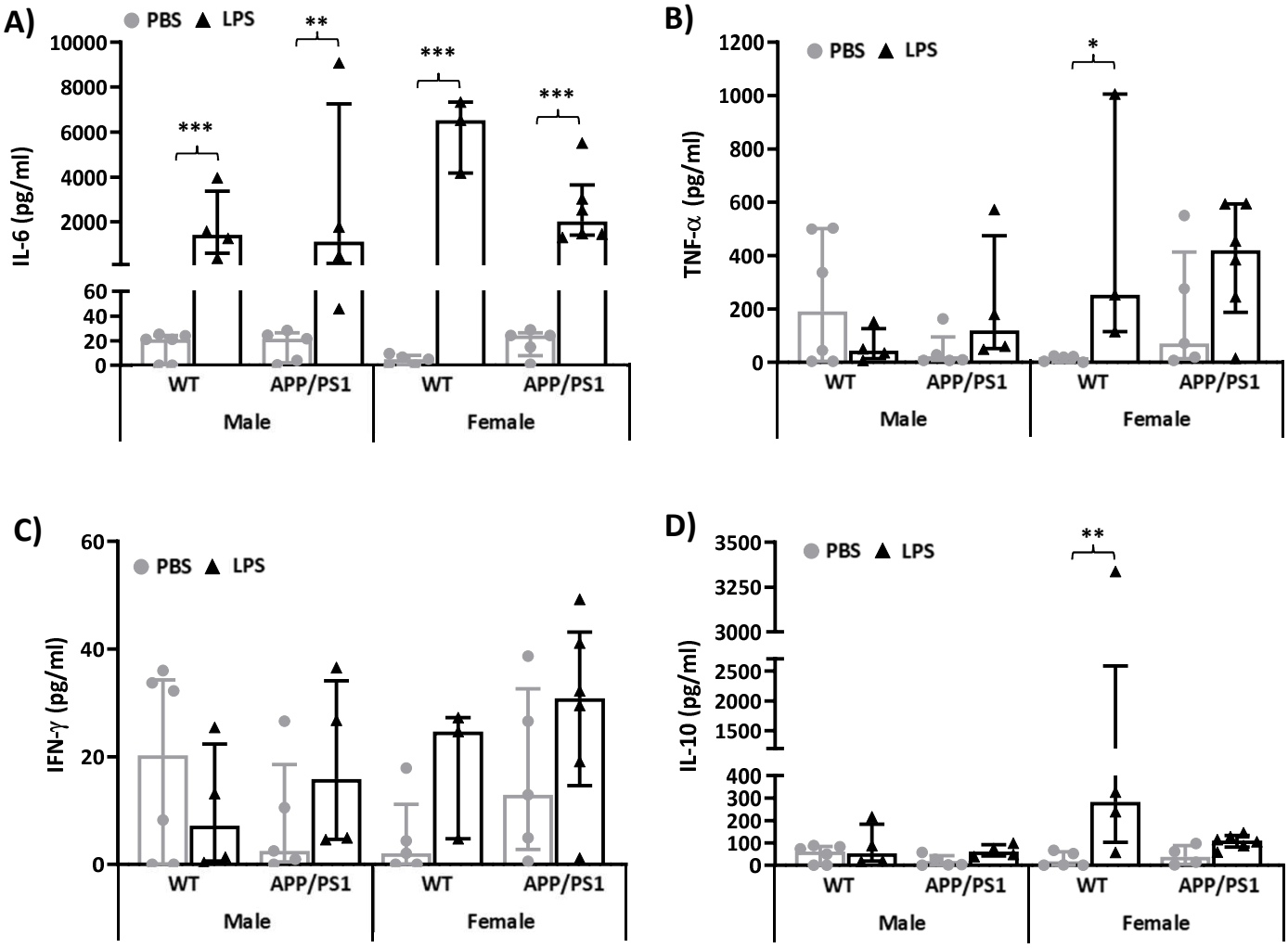
A)
PBS
LPS
IL-6 (pg/ml)
10000
8000
6000
4000
2000
60
40
20
0
***
**
***
***
WT
APP/PS1
WT
APP/PS1
Male
Female
B)
PBS
LPS
TNF-α (pg/ml)
1200
1000
800
600
400
200
0
*
WT
APP/PS1
WT
APP/PS1
Male
Female
C)
PBS
LPS
IFN-γ (pg/ml)
60
40
20
0
WT
APP/PS1
WT
APP/PS1
Male
Female
D)
PBS
LPS
IL-10 (pg/ml)
3500
3250
3000
2500
2000
1500
400
300
200
100
0
**
WT
APP/PS1
WT
APP/PS1
Male
Female

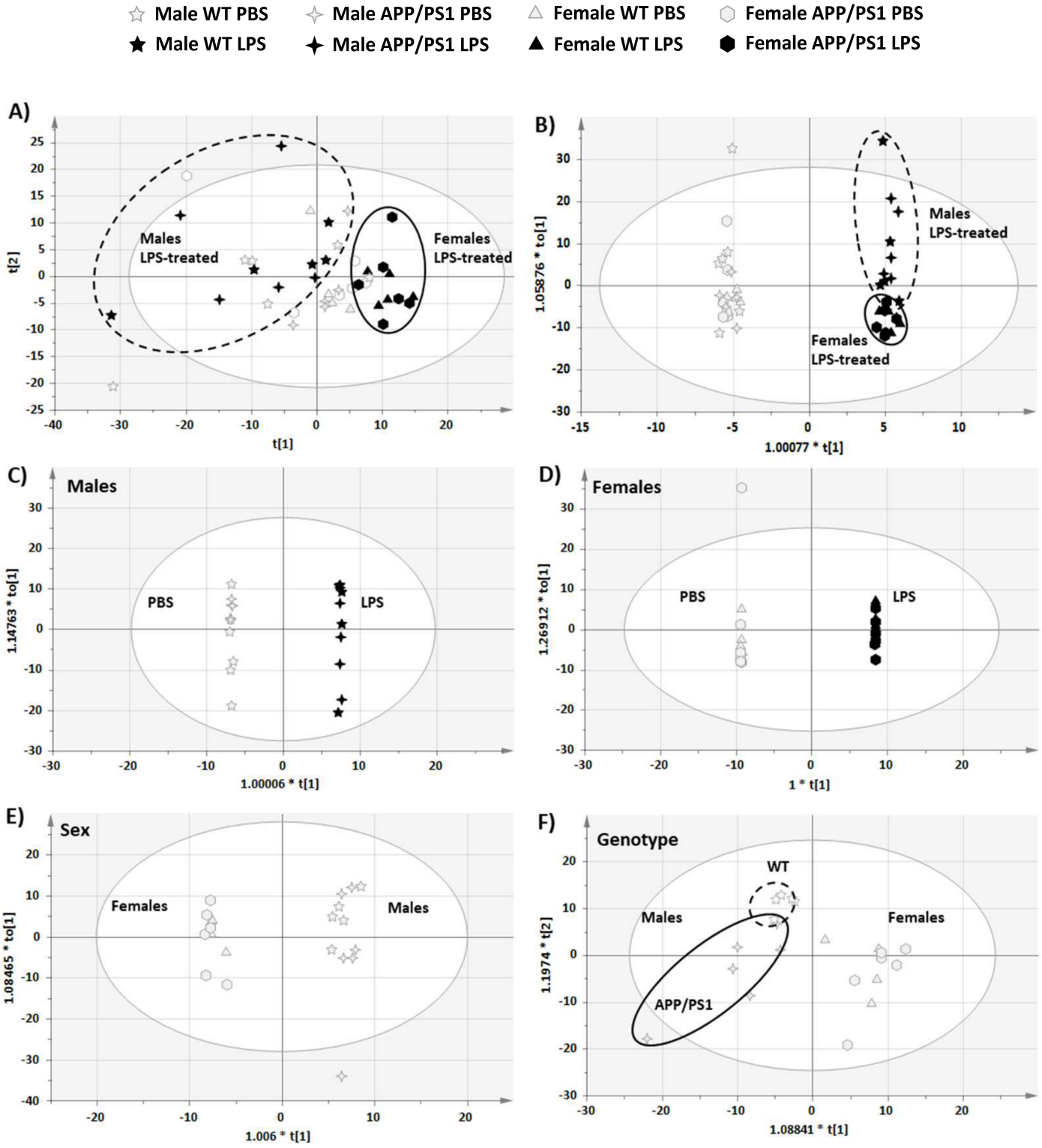
Male WT PBS
Male APP/PS1 PBS
Female WT PBS
Female APP/PS1 PBS
Male WT LPS
Male APP/PS1 LPS
Female WT LPS
Female APP/PS1 LPS
A)
Males
LPS-treated
Females
LPS-treated
t[1]
t[2]
B)
Males
LPS-treated
Females
LPS-treated
1.00077 * t[1]
1.05876 * to[1]
C)
Males
PBS
LPS
1.00006 * t[1]
1.14763 * to[1]
D)
Females
PBS
LPS
1 * t[1]
1.26912 * to[1]
E)
Sex
Females
Males
1.006 * t[1]
1.08465 * to[1]
F)
Genotype
WT
Males
Females
APP/PS1
1.08841 * t[1]
1.1974 * t[2]

Fig 3.

Fig. 4

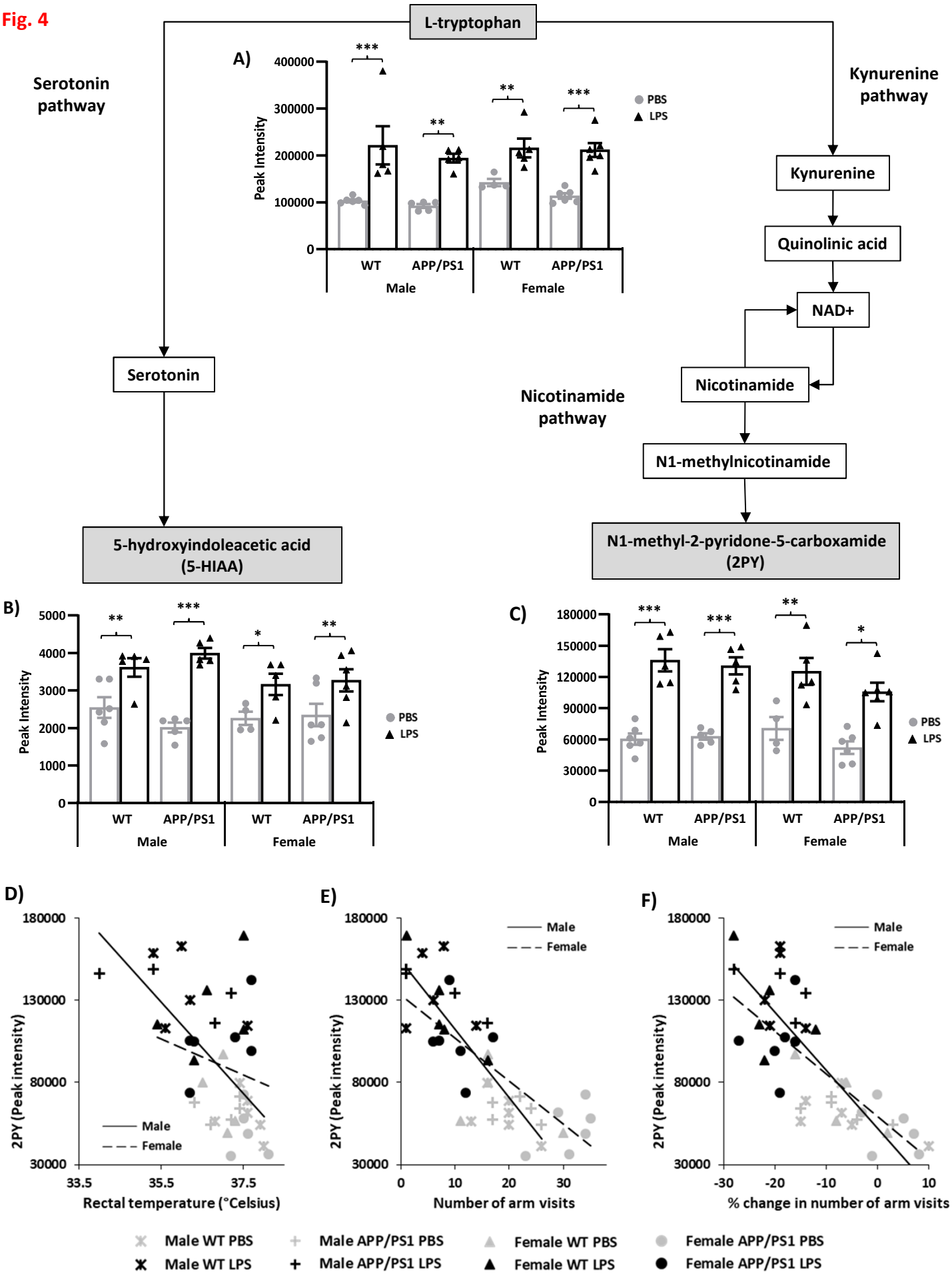
L-tryptophan
Serotonin pathway
Kynurenine pathway
A)
Peak Intensity
PBS
LPS
WT
APP/PS1
Male
Female
Kynurenine
Quinolinic acid
NAD+
Nicotinamide
Nicotinamide pathway
N1-methylnicotinamide
Serotonin
5-hydroxyindoleacetic acid (5-HIAA)
N1-methyl-2-pyridone-5-carboxamide (2PY)
B)
C)
D)
E)
F)
2PY (Peak intensity)
Rectal temperature (°Celsius)
Number of arm visits
% change in number of arm visits
Male
Female
Male WT PBS
Male WT LPS
Male APP/PS1 PBS
Male APP/PS1 LPS
Female WT PBS
Female WT LPS
Female APP/PS1 PBS
Female APP/PS1 LPS

Fig. 5

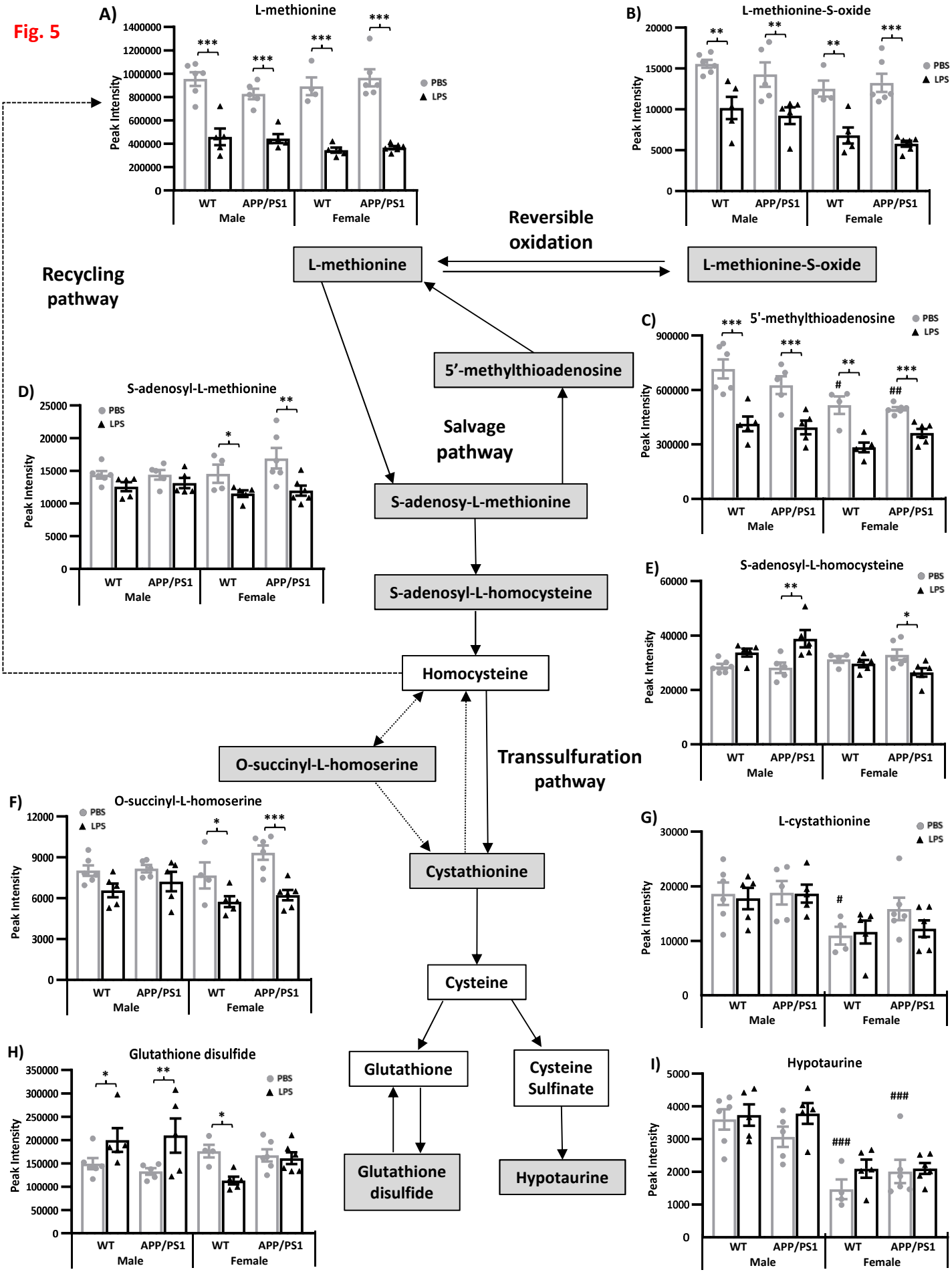
A)
L-methionine
Peak Intensity
PBS
LPS
WT
APP/PS1
Male
Female
B)
L-methionine-S-oxide
Reversible oxidation
L-methionine
L-methionine-S-oxide
Recycling pathway
C)
5'-methylthioadenosine
5'-methylthioadenosine
D)
S-adenosyl-L-methionine
Salvage pathway
S-adenosy-L-methionine
S-adenosyl-L-homocysteine
E)
S-adenosyl-L-homocysteine
Homocysteine
O-succinyl-L-homoserine
Transsulfuration pathway
F)
O-succinyl-L-homoserine
Cystathionine
G)
L-cystathionine
Cysteine
H)
Glutathione disulfide
Glutathione
Cysteine Sulfinate
Glutathione disulfide
Hypotaurine
I)
Hypotaurine

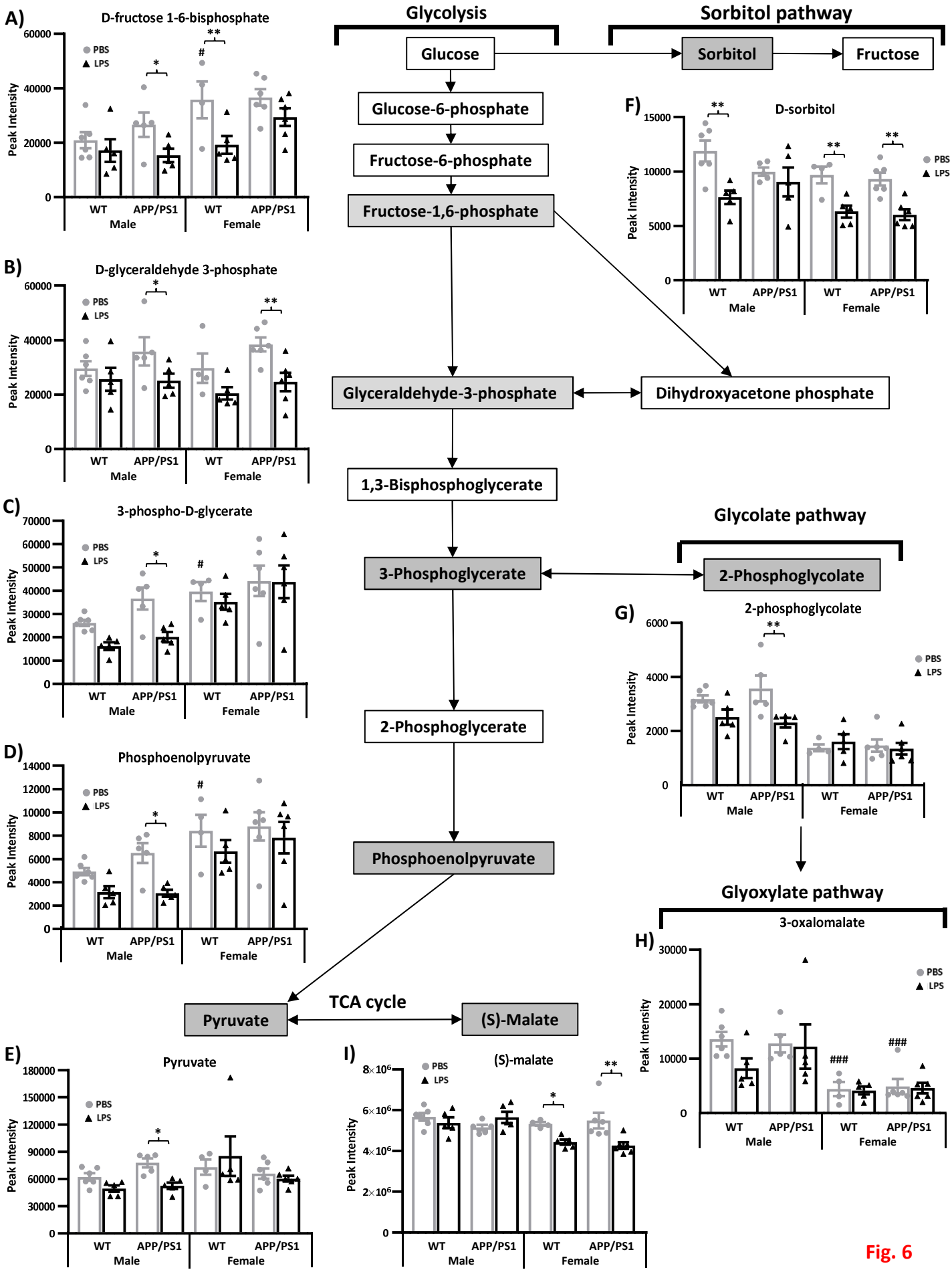
A)
D-fructose 1-6-bisphosphate
Peak Intensity
PBS
LPS
WT
APP/PS1
Male
Female
B)
D-glyceraldehyde 3-phosphate
C)
3-phospho-D-glycerate
D)
Phosphoenolpyruvate
E)
Pyruvate
F)
D-sorbitol
G)
2-phosphoglycolate
H)
3-oxalomalate
I)
(S)-malate
Glycolysis
Sorbitol pathway
Glucose
Sorbitol
Fructose
Glucose-6-phosphate
Fructose-6-phosphate
Fructose-1,6-phosphate
Glyceraldehyde-3-phosphate
Dihydroxyacetone phosphate
1,3-Bisphosphoglycerate
Glycolate pathway
3-Phosphoglycerate
2-Phosphoglycolate
2-Phosphoglycerate
Phosphoenolpyruvate
Glyoxylate pathway
Pyruvate
TCA cycle
(S)-Malate

Fig. 6

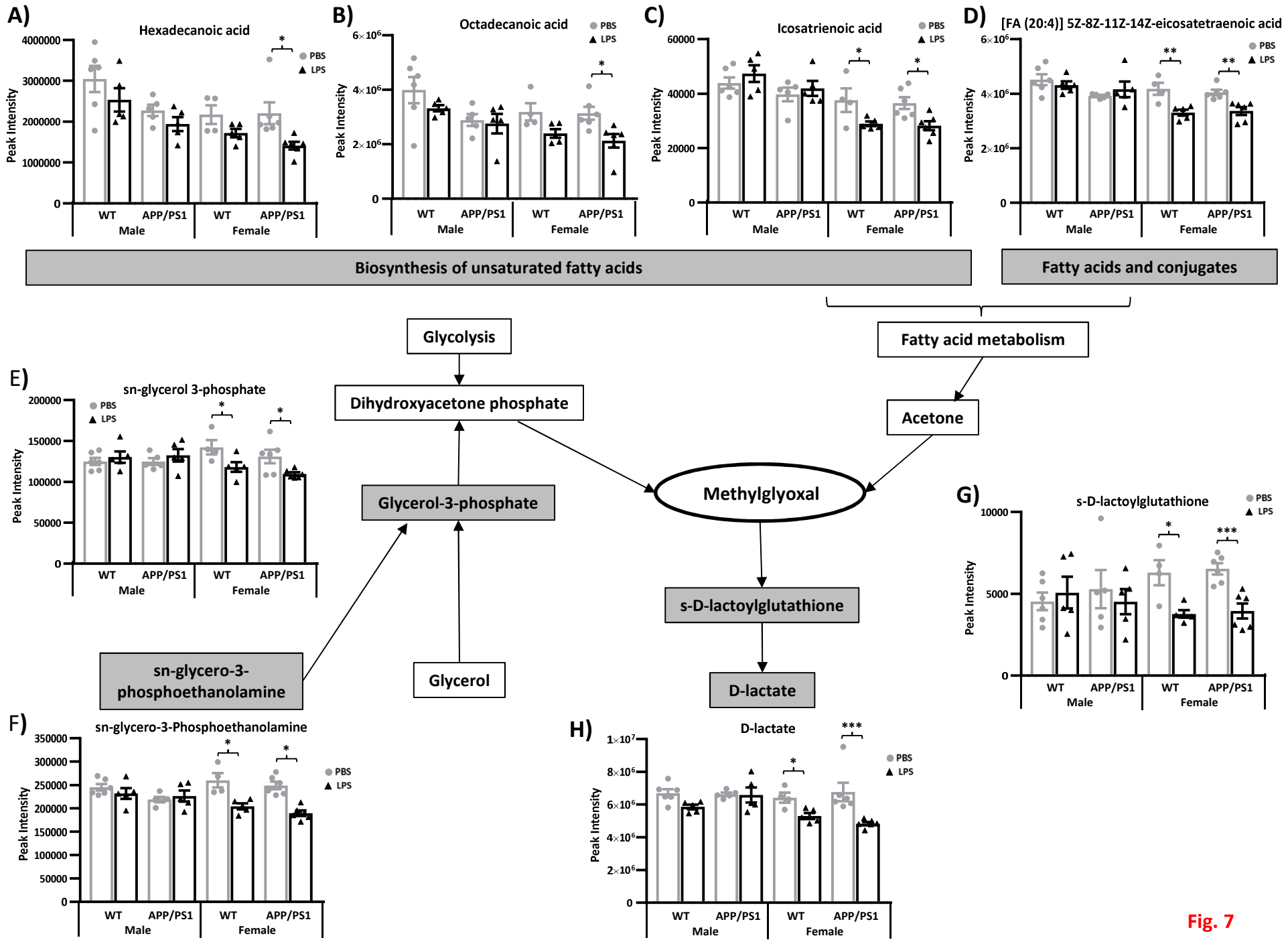
A)
Hexadecanoic acid
B)
Octadecanoic acid
C)
Icosatrienoic acid
D)
[FA (20:4)] 5Z-8Z-11Z-14Z-eicosatetraenoic acid
Peak Intensity
PBS
LPS
WT
APP/PS1
Male
Female
Biosynthesis of unsaturated fatty acids
Fatty acids and conjugates
Glycolysis
Fatty acid metabolism
Dihydroxyacetone phosphate
Acetone
E)
sn-glycerol 3-phosphate
Glycerol-3-phosphate
Methylglyoxal
s-D-lactoylglutathione
G)
s-D-lactoylglutathione
sn-glycero-3-phosphoethanolamine
Glycerol
D-lactate
F)
sn-glycero-3-Phosphoethanolamine
H)
D-lactate

Fig. 7

Fig. 8

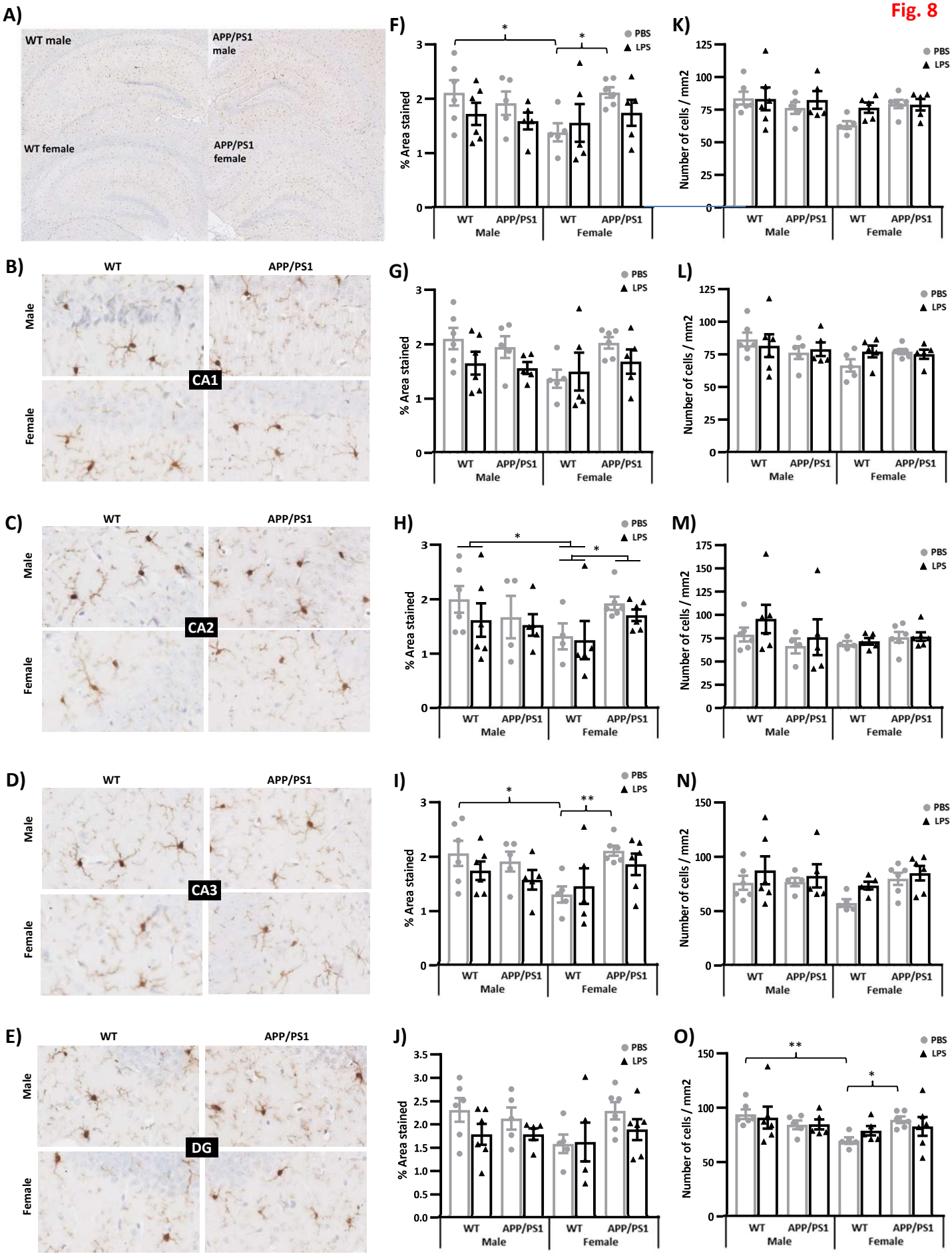
A)
WT male
APP/PS1 male
WT female
APP/PS1 female
B)
WT
APP/PS1
Male
Female
CA1
C)
CA2
D)
CA3
E)
DG
F)
K)
G)
L)
H)
M)
I)
N)
J)
O)
PBS
LPS
% Area stained
Number of cells / mm2
WT
APP/PS1
Male
Female

Table 1. Metabolites differently expressed between males and females and in response to LPS. Statistical significance from 3-way ANOVAs followed by pairwise comparisons testing the effect of LPS within each sex, when appropriate. When significant Genotype, Sex and or their interaction with treatment were observed, metabolites with VIP values below 1.5 were considered discriminant if pairwise comparisons confirmed genotype or sex differences in PBS-treated mice and/or a sexually dimorphic LPS response.

				Genotype effect (PBS-treated)			Sex effect (PBS-treated)			Overall LPS effect			LPS effect in males			LPS effect in females		
Exact mass	**RT (min)**	**Putative metabolite Formula**	**Pathway**	**VIP**	***p***	***vs.* WT**	**VIP**	***p***	***vs.* males**	**VIP**	***p***	***vs.* PBS**	**VIP**	***p***	***vs.* PBS**	**VIP**	***p***	***vs.* PBS**
Amino acid metabolism																		
131.09	11.79	(3R)-beta-Leucine C6H13NO2	Valine, leucine and isoleucine degradation	1.37			2.04	<0.0001	↘	0.75			0.39			0.64		
103.10	15.33	Choline C5H13NO	Glycine, serine and threonine metabolism	0.83			0.71			1.45			2.00	<0.0001	↗	0.69		
222.07	11.11	L-cystathionine C7H14N2O4S	Glycine, serine and threonine metabolism Methionine metabolism	1.35			1.39	0.01	↘	0.89			0.65			0.88		
149.05	8.79	L-methionine C5H11NO2S	Methionine metabolism	0.69			0.57			2.92	<0.0001	↘	2.14	<0.0001	↘	1.88	<0.0001	↘
165.05	9.32	L-methionine S-oxide C5H11NO3S	Methionine metabolism	0.69			0.83			2.52	<0.0001	↘	1.84	<0.0001	↘	1.77	<0.0001	↘
384.12	9.50	S-adenosyl-L-homocysteine C14H20N6O5S	Methionine metabolism	0.92			1.18			0.91			1.70	0.0001	↗	1.10	0.036	↘
219.07	9.59	O-succinyl-L-homoserine C14H20N6O5S	Methionine metabolism	0.72			1.18			2.04	<0.0001	↘	1.31	0.03	↘	1.50	<0.0001	↘
398.14	11.02	S-adenosyl-L-methionine C15H22N6O5S	Methionine metabolism Arginine and proline metabolism	1.13			0.70			1.82	0.0002	↘	1.30			1.37	0.0002	↘
297.09	6.79	5'-methylthioadenosine C11H15N5O3S	Methionine metabolism Arginine and proline metabolism	1.31			1.57	0.0001	↘	2.44	<0.0001	↘	2.00	<0.0001	↘	1.70	<0.0001	↘
132.05	8.62	N-carbamoylsarcosine C4H8N2O3	Arginine and proline metabolism	0.92			1.07			1.84	0.0002	↗	1.37	0.004	↗	1.21	0.005	↗
231.07	8.97	N-succinyl-L-glutamate 5-semialdehyde C9H13NO6	Arginine and proline metabolism	1.25			1.75	0.0005	↗	0.72			1.34	0.009	↗	1.37	0.005	↘
104.02	9.07	Urea-1-carboxylate C2H4N2O3	Arginine and proline metabolism	1.20			0.60			1.87	<0.0001	↗	1.80	<0.0001	↗	1.07	0.03	↗ in WT

188.13	16.71	Homoarginine C7H16N4O2	Arginine and proline metabolism	1.17			1.88	<0.0001	↗	1.06			0.63			1.38		
133.04	10.25	L-aspartate C4H7NO4	Arginine and proline metabolism Lysine biosynthesis	1.00			1.39			1.02			1.78	0.004	↗	0.97		
276.13	10.24	N6-(L-1,3-Dicarboxypropyl)-L-lysine C11H20N2O6	Lysine biosynthesis	1.16			1.52	0.002	↗	0.72			0.32			0.93		
203.08	9.24	N2-acetyl-L-aminoadipate C8H13NO5	Lysine biosynthesis	1.31			1.75	0.001	↗	0.90			0.75			1.14		
161.07	10.10	L-2-aminoadipate C6H11NO4	Lysine biosynthesis	1.44			1.69	0.008	↗	0.80			1.06			0.78		
129.08	9.34	L-pipecolate C6H11NO2	Lysine degradation Alkaloid biosynthesis I	1.38			1.65	<0.0001	↘	0.91			0.86			0.79		
151.06	5.15	(Z)-4-hydroxyphenylacetaldehyde-oxime C8H9NO2	Tyrosine metabolism	1.28			1.85	<0.0001	↘	0.82			0.97			0.57		
190.05	8.17	[FA hydroxy,oxo(7:0/2:0)] 4-hydroxy-2-oxo-Heptanedioic acid C7H10O6	Tyrosine metabolism	1.12			1.59	0.003	↗	0.91			1.30	0.03	↗	1.51	0.0002	↘
165.08	8.00	L-phenylalanine C9H11NO2	Phenylalanine, tyrosine and tryptophan biosynthesis	0.83			0.78			2.19	<0.0001	↗	1.87	<0.0001	↗	1.44	0.003	↗in WT
204.09	9.16	L-tryptophan C11H12N2O2	Phenylalanine, tyrosine and tryptophan biosynthesis Tryptophan metabolism	1.47			1.64	0.09		2.55	<0.0001	↗	1.94	<0.0001	↗	1.67	<0.0001	↗
191.06	9.66	5-hydroxyindoleacetate C10H9NO3	Tryptophan metabolism	1.07			0.84			2.32	<0.0001	↗	2.04	<0.0001	↗	1.31	0.0012	↗
219.11	6.80	Pantothenate C9H17NO5	beta-Alanine metabolism Pantothenate and CoA biosynthesis	1.27			2.06	0.0001	↗	0.75			0.93			1.16		
160.08	6.83	D-alanyl-D-alanine C6H12N2O3	D-Alanine metabolism Peptidoglycan biosynthesis	1.35	0.03	↘	2.08	<0.0001	↘	0.99			0.98			0.72		
612.15	11.03	Glutathione disulfide C20H32N6O12S2	Glutamate metabolism Glutathione metabolism	0.82			1.37			0.77			1.51	0.001	↗	1.10		
140.06	7.25	Methylimidazoleacetic acid C6H8N2O2	Histidine metabolism	0.97			1.40			0.88			1.51	0.002	↗	1.01		
169.08	9.39	N(pi)-methyl-L-histidine	Histidine metabolism	1.32			2.00	<0.0001	↘	1.62	<0.0001	↗	1.70	<0.0001	↗	1.59	0.0005	↗

		C7H11N3O2													
109.02	10.64	Hypotaurine C2H7NO2S	Taurine and hypotaurine metabolism	1.43	2.07	<0.0001	↘	0.95			0.87			0.95		
Carbohydrate metabolism															
118.03	10.42	Succinate C4H6O4	Citrate cycle (TCA cycle) Glyoxylate and dicarboxylate metabolism	1.14	0.65			1.69	0.0003	↘	1.40	0.005	↘	1.18	0.01	↘
192.03	8.66	Isocitrate C6H8O7	Citrate cycle (TCA cycle) Glyoxylate and dicarboxylate metabolism	1.34	1.91	<0.0001	↘	0.96			1.02			0.82		
134.02	10.92	(S)-malate C4H6O5	Citrate cycle (TCA cycle) Pyruvate metabolism Glyoxylate and dicarboxylate metabolism	0.97	0.82			1.46			0.79			1.53	0.0001	↘
90.03	7.25	(D)-lactate C3H6O3	Pyruvate metabolism	0.90	0.95			1.88			1.08			1.55	<0.0001	↘
379.10	9.05	(D)-S-lactoylglutathione C13H21N3O8S	Pyruvate metabolism	0.90	0.93			1.26			0.53			1.63	0.0008	↘
167.98	11.75	Phosphoenolpyruvate C3H5O6P	Citrate cycle (TCA cycle) Pyruvate metabolism Glycolysis / Gluconeogenesis	1.08	1.48	<0.0001	↗	1.23			1.79	0.01	↘	0.78		
88.01	6.81	Pyruvate C3H4O3	Citrate cycle (TCA cycle) Glycolysis / Gluconeogenesis	0.73	0.16			0.70			1.66	0.03	↘	0.53		
170.00	10.31	D-glyceraldehyde 3-phosphate C3H7O6P	Glycolysis / Gluconeogenesis	0.87	0.33			1.70	0.0007	↘	1.10	0.04	↘ in APP/PS1	1.28	0.003	↘ in APP/PS1
185.99	11.39	3-phospho-D-glycerate C3H7O7P	Glycolysis /Gluconeogenesis Glyoxylate and dicarboxylate metabolism	0.99	1.35	<0.0001	↗	1.10			1.69	0.007	↘	0.67		
155.98	11.41	2-phosphoglycolate C2H5O6P	Glyoxolate and dicatboxylate metabolism	1.28	2.11	<0.0001	↘	1.08			1.54	0.0007	↘	0.71		
206.01	11.83	3-oxalomalate C6H6O8	Glyoxolate and dicatboxylate metabolism	1.28	2.00	<0.0001	↘	0.85			0.91			0.61		
164.07	9.24	L-rhamnose C6H12O5	Fructose and mannose metabolism	0.99	0.78			1.16			1.51	0.002	↗	0.85		
182.08	10.09	D-sorbitol C6H14O6	Fructose and mannose metabolism	1.07	0.96			2.06	<0.0001	↘	1.40	0.002	↘ in WT	1.65	<0.0001	↘

276.02	11.62	6-phospho-D-gluconate C6H13O10P	Pentose phosphate pathway	0.79		0.86			1.70	0.0006	↘	1.07	0.08		1.33	0.001	↘
154.00	8.48	Propanoyl phosphate C6H13O10P	Propanoate metabolism C5-Branched dibasic acid metabolism	1.05		0.85			0.98			1.53	0.0009	↗	0.64		
130.03	8.65	Itaconate C5H6O4	C5-Branched dibasic acid metabolism Citrate cycle (TCA cycle)	1.34		1.91	<0.0001	↘	0.94			1.10			0.74		
146.02	9.93	Methyloxaloacetate C5H6O5	C5-Branched dibasic acid metabolism	1.20		1.53	0.006	↘	0.95			0.88			0.94		
Nucleotide metabolism																	
136.04	8.58	Hypoxanthine C5H4N4O	Purine metabolism	0.77		0.78			1.00			1.66	0.03	↗	0.94		
168.03	9.07	Urate C5H4N4O3	Purine metabolism	0.22		0.59			2.17	<0.0001	↗	1.77	<0.0001	↗	1.34	0.006	↗
463.07	11.88	N6-(1,2-Dicarboxyethyl)-AMP C14H18N5O11P	Purine metabolism	0.85		0.71			1.52			0.69			1.52	<0.0001	↘
156.02	7.91	Orotate C5H4N2O4	Pyrimidine metabolism	1.21		1.58	0.005	↗	0.83			1.08			1.18	0.01	↘
242.09	6.82	Thymidine C10H14N2O5	Pyrimidine metabolism	0.57		0.26			2.05	<0.0001	↗	1.88	0.002	↗	1.18	0.0007	↗
126.04	6.82	Thymine C5H6N2O2	Pyrimidine metabolism	0.74		0.98			1.87	<0.0001	↗	1.77	0.002	↗	1.03	0.005	↗
114.04	7.17	5,6-dihydrouracil C4H6N2O2	Pyrimidine metabolism Beta-Alanine metabolism Pantothenate and CoA biosynthesis	0.70		0.88			0.77			1.52	0.0007	↗	0.93		
Lipid metabolism and Fatty acyls																	
284.27	3.88	Octadecanoic acid C18H36O2	Fatty acids biosynthesis Biosynthesis of unsaturated fatty acids	1.13		0.99			1.50	0.004	↘ in WT	0.89			1.46	0.005	↘
256.24	3.91	Hexadecanoic acid C16H32O2	Biosynthesis of unsaturated fatty acids	1.21		1.18			1.52	0.002	↘	0.92			1.35	0.01	↘
306.25	3.88	Icosatrienoic acid C20H34O2	Biosynthesis of unsaturated fatty acids	0.70		094			0.88			0.57			1.41	0.001	↘
304.24	3.88	[FA (20:4)] 5Z,8Z,11Z,14Z-eicosatetraenoic acid C20H32O2	Fatty Acids and Conjugates	0.96		0.85			1.32			0.42			1.62	<0.0001	↘

118.06	5.16	Formyl 3-hydroxy-butanoate C5H10O3	Fatty esters	1.44			2.17	<0.0001	↘	0.97			1.16			0.88		
172.01	10.13	sn-glycerol 3-phosphate C3H9O6P	Glycerolipid metabolism Glycerophospholipid metabolism	0.99			1.34			0.98			0.76			1.33	0.0009	↘
306.26	3.88	sn-glycero-3-Phosphoethanolamine C5H14NO6P	Glycerophospholipid metabolism Ether lipid metabolism	1.26			1.37			1.79			0.47			1.69	<0.0001	↘
393.29	4.82	PGH2-EA C23H39NO4	Eicosanoids	1.11			1.05			1.73	0.0003	↗	1.40	0.01	↗	1.18	0.005	↗
Energy Metabolism																		
506.99	10.98	ATP C10H16N5O13P3	Oxidative phosphorylation Purine metabolism	1.04			0.80			1.97	<0.0001	↘	1.47	0.002	↘	1.28	0.0004	↘
340.00	11.91	D-fructose 1,6-bisphosphate C6H14O12P2	Carbon fixation	1.04			1.54	0.002	↗	1.44	0.0005	↘	1.15	0.05	↘	1.21	0.003	↘
370.01	12.01	D-sedoheptulose 1,7-bisphosphate C7H16O13P2	Carbon fixation	1.23			1.22			1.32			0.81			1.52	<0.0001	↘
Metabolism of Cofactors and Vitamins																		
73.02	10.25	Iminoglycine C2H3NO2	Thiamine metabolism	0.71			0.98			1.00			1.56	0.001	↗	0.91		
152.06	6.87	N1-methyl-2-pyridone-5-carboxamide C7H8N2O2	Nicotinate and nicotinamide metabolism	0.81			0.61			2.73	<0.0001	↗	2.25	<0.0001	↗	1.62	<0.0001	↗
Peptides																		
276.10	11.03	Gamma glutamylglutamic acid C10H16N2O7	Peptide	0.95			0.94			0.89			1.59	0.005	↗	0.90		
262.08	9.71	L-beta-aspartyl-L-glutamicacid C9H14N2O7	Peptide	1.52	0.03	↘ in ♀	0.82			0.65			0.56			0.58		
357.13	7.80	Asp-Ser-His C13H19N5O7	Basic peptide	0.71			0.74			1.54	0.005	↘	0.82			1.36	0.002	↘
508.18	6.81	Asn-Met-Met-Asn C18H32N6O7S2	Hydrophobic peptide	0.52			1.01			1.60			1.57	0.003	↘	0.95		
482.20	8.23	Asp-Phe-Thr-Thr C21H30N4O9	Hydrophobic peptide	1.34	0.03	↗ in ♂	1.59	0.003	↗	0.86			0.69			0.64		
360.14	8.79	Asn-Asn-Asn	Polar peptide	0.72			0.15			2.87	<0.0001	↘	2.10	<0.0001	↘	1.85	<0.0001	↘

		C12H20N6O7																
Biosynthesis of Polyketides and nonribosomal Peptides																		
509.33	4.64	Narbomycin C28H47NO7	Biosynthesis of 12-, 14- and 16-membered macrolides	0.61			0.29			2.14	<0.0001	↗	1.44	0.003	↗	1.50	<0.0001	↗
515.18	11.20	13-dihydrocarminomycin C26H29NO10	Biosynthesis of type II polyketide products	1.21			1.71	0.004	↗	0.84			0.86			0.69		
Biosynthesis of Secondary metabolites																		
200.08	7.89	Dihydroclavaminic acid C8H12N2O4	Clavulanic acid biosynthesis	1.27			2.04	<0.0001	↘	0.80			0.79			0.83		
Not known																		
102.08	16.19	γ-aminobutyramide C4H10N2O	Not known	1.23			1.73	0.004	↗	0.77			1.48	0.003	↗	1.37	0.006	↘
274.05	10.27	1-deoxy-D-altro-heptulose 7-phosphate C7H15O9P	Not known	1.13			1.19			1.24			1.65	0.01	↗	0.58		
281.11	10.68	1-methyladenosine C11H15N5O4	Not known	1.54	0.03	↗ in ♀	0.61			0.1			0.79			0.53		
367.27	4.95	3, 5-tetradecadiencarnitine C21H37NO4	Not known	1.06			1.24			1.57	0.002	↗	1.15	0.01	↗	1.44	0.04	↗
181.99	9.73	3-methylphosphoenolpyruvate C4H7O6P	Not known	1.20			1.77	<0.0001	↘	0.88			0.75			0.83		
181.10	8.58	6-methyltetrahydropterin C7H11N5O	Not known	1.00			1.11			0.83			1.79	0.0006	↗	1.05	0.02	↘
430.20	5.36	Athamantin C24H30O7	Not known	1.31			1.79	0.01	↗	0.85			0.78			0.65		
348.11	9.24	Camptothecin C20H16N2O4	Not known	0.97			0.72			1.59	0.02	↘	1.37	0.009	↘ in WT	1.11		
158.06	4.39	Dimethyl citraconate C7H10O4	Not known	0.97			1.72	0.0005	↘	0.53			0.92			1.11		
159.13	9.46	DL-2-sulfoctanoicacid C8H17NO2	Not known	1.09			1.67	0.0002	↗	0.60			0.41			0.88		
425.35	4.65	Elaidiccarnitine C25H47NO4	Not known	1.20			1.44			1.53	0.004	↗	1.19	0.04	↗in APP/ PS1	1.14	0.03	↗in WT
275.14	8.59	Glutarylcarnitine	Not known	1.36			1.89	0.007	↗	0.68			0.70			0.87		

		C12H21NO6															
246.05	8.65	Glycerophosphoglycerol C6H15O8P	Not known	1.28			1.52	0.003	↗	1.29			0.68			1.49	0.0001	↘
423.33	4.68	Linoelaidylcarnitine C25H45NO4	Not known	1.28			1.42			1.52	0.003	↗	1.24	0.02	↗	0.98	0.04	↗
216.12	10.34	N-acetyl-(L)-arginine C8H16N4O3	Not known	1.15	0.03	↘ in ♀	1.53	0.005	↗	0.87			0.76			1.28	0.0008	↘
202.14	14.08	NG,NG-dimethyl-L-arginine C8H18N4O2	Not known	1.22			0.97			1.32			1.60	0.001	↗	0.81		
243.09	8.89	Nocardicin C C23H26N4O8	Not known	0.91			0.71			1.65			0.71			1.53	<0.0001	↘
175.03	5.16	Nonulose 9-phosphate C9H19O12P	Not known	1.15			1.48	0.004	↘	1.81			1.91	<0.0001	↘	0.70		
249.03	12.35	Norepinephrinesulfate C8H11NO6S	Not known	0.97			1.87	0.003	↗	0.75			1.35	0.008	↗	0.72		
288.06	8.85	Orotidine C10H12N2O8	Not known	1.29			1.56	0.0003	↗	0.92			0.59			1.19	0.007	↘
371.30	4.84	Tetradecanoylcarnitine C21H41NO4	Not known	1.22			1.53	0.04	↘	1.00			0.90			0.77		
573.09	8.83	GDP-3,6-dideoxy-D-galactose C16H25N5O14P2	Not known	1.17			0.81			1.10			1.79	0.002	↗	0.63		
133.07	6.76	N-hydroxyvaline C5H11NO3	Linamarin biosynthesis	1.29			1.70	<0.0001	↘	2.45	<0.0001	↘	2.14	<0.0001	↘	1.61	<0.0001	↘

PBS: Phosphate-buffered saline; WT: wild-type; ♀: female; ♂: male.

Supplementary information

Sex-specific hippocampal metabolic signatures at the onset of systemic inflammation with lipopolysaccharide in the APPswe/PS1dE9 mouse model of Alzheimer's disease

Alessandra Agostini, Ding Yuchun, Bai Li, David A. Kendall and Marie-Christine Pardon

Supplementary Figure 1. Body weight, baseline and post-injection performance in the spontaneous alternation task

Supplementary Table 1. Results of the ANOVAs for behavioural and physiological variables.

Supplementary Table 2. Results of the ANOVAs for plasma cytokine levels

Supplementary metabolomics results

Supplementary Table 3. Potential function of discriminant metabolites in the brain and implication in sex differences in brain function, AD progression and immune status

References for supplementary metabolomics results

Supplementary Figure 2. Discriminant metabolites for genotype differences

Supplementary Figure 3. Discriminant metabolites for sex differences

Supplementary Figure 4. Discriminant metabolites for LPS effects

Supplementary Table 4. Results of the ANOVAs for glial measures

Supplementary Figure 5. Microglial soma size

Supplementary Figure 6. GFAP immunostaining results

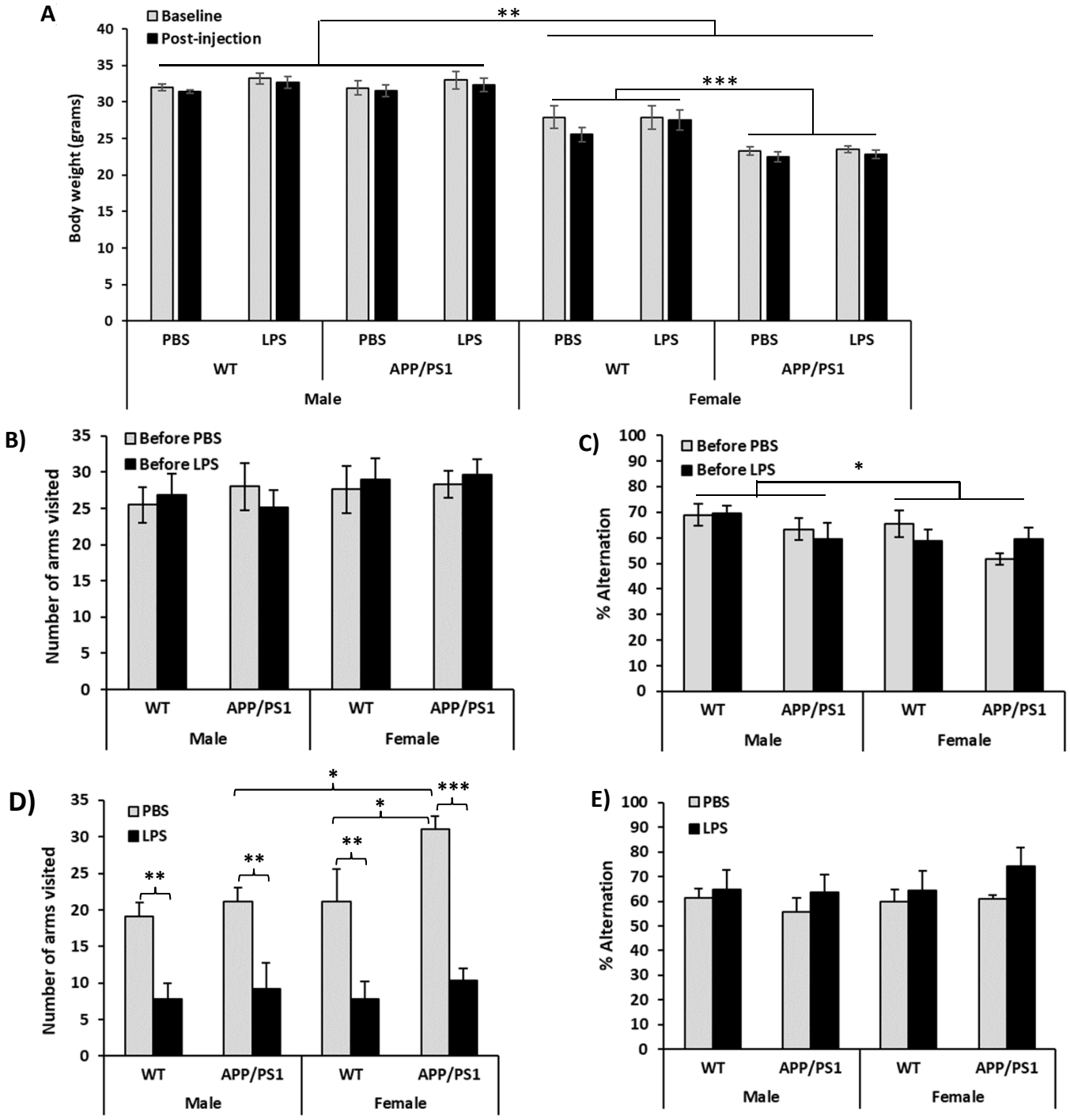

Supplementary Figure 1. Body mass (A) was recorded prior to and 4 hours after the PBS or LPS challenge. The two-way ANOVA with repeated measures revealed a significant Genotype x Sex interaction effect ($F_{(1,36)}$ = 12.22, p=0.0013). Females were overall lighter than males regardless of genotype ($F_{(1,36)}$ = 152.67, p<0.0001) but within females, the APP/PS1 mice were also lighter than their WT littermates (p<0.0001). None of the experimental groups showed significant weight loss at 4 hours following the LPS or PBS challenge. Before injection with PBS or LPS, none of the groups differed for the number of arm visits in the Y-maze (B), but females showed an overall reduction in spatial alternation performance (B; Sex effect: $F_{(1,35)}$ = 4.65, p=0.04). At 4 hours post injection, LPS-treated mice visited significantly less arms of the Y-maze than PBS-treated mice ($F_{(1,36)}$ = 65.53, p<0.0001) and but PBS-treated APP/PS1 mice were also hyperactive compared to PBS-treated APP/PS1 males and WT females (p=0.009 in both cases, C), but their spontaneous alternation performance (D) did not differ. Data are expressed as Means $\pm$ SEM. *, p<0.05; **, p<0.01; **, p<.0001

Supplementary table 1. Results of the two-way repeated measure ANOVAs on behavioral measures.

	Body weight	Food Burrowing*	Arm entries	Alternation rate
Covariate (arm entries)				$F_{(1,31)}$=0.80 p=0.38
Genotype	$F_{(1,36)}$=14.4 **p=0.0006**	$F_{(1,36)}$=0.03 p=0.86	$F_{(1,36)}$=2.12 p=0.15	$F_{(1,36)}$=0.88 p=0.36
Sex	$F_{(1,36)}$=152.67 **p<0.0001**	$F_{(1,36)}$=2.30 p=0.14	$F_{(1,36)}$=3.17 p=0.08	$F_{(1,36)}$=0.11 p=0.74
Treatment	$F_{(1,36)}$=2.30 p=0.14	$F_{(1,36)}$=22.2 **p<0.0001**	$F_{(1,36)}$=20.66 **p<0.0001**	$F_{(1,36)}$=0.41 p=0.53
Time	$F_{(1,35)}$=9.37 **p=0.004**	$F_{(1,36)}$=15.92 **p=0.003**	$F_{(1,36)}$=145.25 **p<0.0001**	$F_{(1,31)}$=0.18 p=0.68
Genotype X Sex	$F_{(1,36)}$=12.22 **p=0.0013**	$F_{(1,36)}$=1.22 p=0.28	$F_{(1,36)}$=0.59 p=0.45	$F_{(1,36)}$=1.09 p=0.30
Genotype X Treatment	$F_{(1,36)}$=0.19 p=0.67	$F_{(1,36)}$=0.20 p=0.66	$F_{(1,36)}$=0.97 p=0.33	$F_{(1,36)}$=0.85 p=0.36
Genotype X Time	$F_{(1,35)}$=0.35 p=0.56	$F_{(1,36)}$=1.62 p=0.21	$F_{(1,36)}$=3.09 p=0.09	$F_{(1,31)}$=2.98 p=0.09
Sex X Treatment	$F_{(1,36)}$=0.17 p=0.68	$F_{(1,36)}$=0.37 p=0.55	$F_{(1,36)}$=0.28 p=0.60	$F_{(1,36)}$=0.18 p=0.67
Sex X Time	$F_{(1,35)}$=1.06 p=0.31	$F_{(1,36)}$=0.06 p=0.81	$F_{(1,36)}$=0.25 p=0.62	$F_{(1,31)}$=4.25 **p=0.048**
Treatment X Time	$F_{(1,35)}$=1.02 p=0.32	$F_{(1,36)}$=9.47 **p=0.004**	$F_{(1,36)}$=58.55 **p<0.0001**	$F_{(1,31)}$=0.65 p=0.43
Genotype X Sex X Treatment	$F_{(1,36)}$=0.04 p=0.84	$F_{(1,36)}$=3.13 p=0.08	$F_{(1,36)}$=0.04 p=0.84	$F_{(1,36)}$=0.97 p=0.33
Genotype X Sex X Time	$F_{(1,35)}$=0.32 p=0.57	$F_{(1,36)}$=0.46 p=0.50	$F_{(1,36)}$=1.20 p=0.28	$F_{(1,30)}$=0.73 p=0.40
Genotype X Treatment X Time	$F_{(1,35)}$=1.05 p=0.31	$F_{(1,36)}$=0.12 p=0.73	$F_{(1,36)}$=0.24 p=0.63	$F_{(1,30)}$=0.01 p=0.91
Sex X Treatment X Time	$F_{(1,35)}$=1.29 p=0.27	$F_{(1,36)}$=0.30 p=0.59	$F_{(1,36)}$=3.79 p=0.06	$F_{(1,30)}$=0.00 p=0.95
Genotype X Sex X Treatment X Time	$F_{(1,35)}$=0.59 p=0.45	$F_{(1,36)}$=0.09 p=0.77	$F_{(1,36)}$=1.94 p=0.17	$F_{(1,30)}$=0.78 p=0.38

*: Food burrowing data were rank-transformed prior to statistical analyses.

Supplementary table 2. Results of the two-way repeated measure ANOVAs on plasma cytokine levels. Data were rank-transformed prior to statistical analyses.

	IL-6	TNF-α	INF-γ	IL-1β	IL-10
Genotype	$F_{(1,30)}$=0.43 p=0.51	$F_{(1,30)}$=0.21 p=0.65	$F_{(1,30)}$=0.59 p=0.45	$F_{(1,30)}$=0.05 p=0.83	$F_{(1,30)}$=0.88 p=0.35
Sex	$F_{(1,30)}$=0.76 p=0.39	$F_{(1,30)}$=1.04 p=0.31	$F_{(1,30)}$=0.41 p=0.52	$F_{(1,30)}$=0.93 p=0.34	$F_{(1,30)}$=5.07 **p=0.03**
Treatment	$F_{(1,30)}$=116.02 **p<0.0001**	$F_{(1,30)}$=7.82 **p=0.0089**	$F_{(1,30)}$=2.7 p=0.11	$F_{(1,30)}$=0.17 p=0.68	$F_{(1,30)}$=23.49 **p<0.0001**
Genotype X Sex	$F_{(1,30)}$=0.03 p=0.87	$F_{(1,30)}$=0.09 p=0.77	$F_{(1,30)}$=0.37 p=0.55	$F_{(1,30)}$=0.90 p=0.35	$F_{(1,30)}$=0.00 p=0.95
Genotype X Treatment	$F_{(1,30)}$=4.01 p=0.054	$F_{(1,30)}$=0.48 p=0.49	$F_{(1,30)}$=1.12 p=0.30	$F_{(1,30)}$=0.40 p=0.53	$F_{(1,30)}$=0.18 p=0.67
Sex X Treatment	$F_{(1,30)}$=3.13 p=0.09	$F_{(1,30)}$=2.15 p=0.15	$F_{(1,30)}$=0.98 p=0.33	$F_{(1,30)}$=0.77 p=0.38	$F_{(1,30)}$=4.54 **p=0.04**
Genotype X Sex X Treatment	$F_{(1,30)}$=3.00 p=0.09	$F_{(1,30)}$=2.69 p=0.11	$F_{(1,30)}$=0.90 p=0.35	$F_{(1,30)}$=2.26 p=0.14	$F_{(1,30)}$=1.68 p=0.20

Supplementary metabolomics results

Lack of major metabolic perturbations in the hippocampus of 4.5-month-old APP/PS1 mice

5 of the 98 selected metabolites were found to significantly discriminate between PBS-treated WT and APP/PS1 mice (Table1), albeit predominantly in females. Levels of L-beta-aspartyl-L-glutamic acid, which belongs to the family of N-acyl-alpha amino acids and derivatives which are known for their anti-inflammatory action (1), were particularly reduced in female APP/PS1 mice (Suppl. Fig. 2A), but its function and implication in AD pathology is, to the best of our knowledge, unknown. 1-Methyladenosine, an oxidized nucleoside known to be immunosuppressive on macrophage function (2) and found in elevated levels in the urine of patients with mild-to-moderate AD (3), was more abundant in the hippocampus of female APP/PS1 mice compared to their WT female littermates (Suppl. Fig. 2B).

Significant Genotype X Treatment interactions were also found for N-acetyl-(L)-arginine ($F_{(1,34)}$=12.07, p=0.001), whose levels were significantly lower in PBS-treated APP/PS1 females compared to PBS-treated WT females (Suppl. Fig. 2C), and for the hydrophobic tetrapeptide Asp-Phe-Thr-Thr ($F_{(1,34)}$=5.40, p=0.03), whose levels were significantly increased in PBS-treated APP/PS1 males compared to their PBS-treated counterparts (Suppl. Fig. 2D). Their function and potential roles in AD pathology are also, to the best of our knowledge, unknown.

Sex differences in the hippocampal metabolic profile are independent of the APP/PS1 genotype.

Forty-one metabolites with sex differences were identified revealing major changes in amino acids, carbohydrate metabolism and fatty acyls (Table 1). A few metabolites from other chemical classes and many unknown metabolites were also found in different levels between PBS-treated males and females (Table 1). Metabolic differences in the methionine and pyruvate metabolic pathways are described in the main manuscript and illustrated Fig. 5 and 6, respectively. Changes in other metabolites with previously associated with differences immune function are described below. Their potential role in brain function or implication in AD progression is presented in Suppl. Table 3.

These included reduced levels of (3R)-beta leucine (Suppl. Fig. 3), a degradation product of the anti-inflammatory amino acid L-Leucine (4), D-alanyl-D-alanine (Suppl. Fig. 3B), an anti-inflammatory antibiotic-binding protein (5), and N(pi)-methyl-L-histidine (Suppl. Fig. 3C), a metabolic product of the amino acid histidine known to be negatively associated with inflammation in obese women (6). Females also presented with an increased abundance of N-Succinyl-L-glutamate 5-semialdehyde (Suppl. Fig. 3D), a metabolite found to be elevated in the plasma of lung cancer patients harbouring a mutation in the epidermal growth factor receptor (7) that also exacerbate their pro-inflammatory status (8).

Lysine, whose dietary restriction was found to trigger pro-inflammatory changes (9), indicated the major anti-inflammatory pathway upregulated in females as seen by elevated levels in three metabolites involved in lysine biosynthesis :N6-(L-1,3-Dicarboxypropyl)-L-lysine, N2-Acetyl-L-aminoadipate and L-2-Aminoadipate (Suppl. Fig. 3E-G), and reduced levels of L-pipecolate (Suppl. Fig. 3H), a degradation product of L-lysine whose urine levels are positively associated with low grade inflammation (10). Differences in amino acid metabolism also indicative of anti-inflammatory effects in females included increased abundance of pantothenate (vitamin B5; Suppl. Fig. 3I), whose dietary intake was found to alleviate chronic low grade inflammation (11) and norepinephrinesulfate (Suppl. Fig. 3O), a metabolite of the anti-inflammatory neurotransmitter norepinephrine (12), as well as reduced levels of (Z)-4-

Hydroxyphenylacetaldehyde-oxime (Suppl. Fig. 3J), an enzyme involved in tyrosine metabolism found in increased levels in inflammatory bowel disease (13), and homoarginine (Suppl. Fig. 3K), known to be negatively associated with pro-inflammatory changes (14).

Changes in carbohydrate metabolism and fatty acyls seen in females were indicative of a pro-inflammatory status. Furthermore, isocitrate, a substrate of the tricarboxylic acid (TCA) cycle found to exert anti-inflammatory effects in a rat model of mild anemia of inflammation (15) and itaconate, a potent anti-inflammatory TCA derivative found in immune cells (16), were also less abundant in the female hippocampus (Suppl. Fig. 3M&N, respectively). Hippocampal concentrations of formyl 3-hydroxy-butanoate, a fatty ester, were also significantly lower in females (Suppl. Fig. 3L) and fatty esters are thought to be anti-inflammatory (17).

Metabolites differentially expressed in PBS- and LPS-treated mice regardless of sex and genotype.

Thirty six metabolites were altered to similar extents by LPS in all experimental groups (Table 1). The most significant changes were those affecting tryptophan and methionine metabolism, as described in the main manuscript and represented Figs. 4&5, respectively. Changes to other metabolites associated with immune status are described below and represented Suppl. Fig. 4, and the potential association of these metabolites in brain function, sex differences and/or AD progression is described in Suppl. Table 3.

These metabolic differences included increased levels of thymidine and thymine (Suppl. Fig. 4A&B), two derivatives of the anti-inflammatory nucleotide pyrimidine (18) as well as reduced levels of the inflammation signalling molecule adenosine triphosphate (ATP) (19), particularly in WT mice (Suppl. Fig. 4C) and of succinate (Suppl. Fig. 4D), a pro-inflammatory intermediate of the TCA cycle which plays a crucial role in ATP generation (20).

Pro-inflammatory metabolic changes included increased levels of N(pi)-methyl-L-histidine (Suppl. Fig. 4C), an histidine derivative positively associated with levels of pro-inflammatory markers (21), urate (Suppl. Fig. 4E) known to cause cognitive deficits through enhancing hippocampal inflammation (22), and of its downstream metabolite urea-1-carboxylate (Suppl. Fig. 4F). LPS-treated mice also had elevated hippocampal levels of L-phenylalanine (Suppl. Fig. 4G), whose circulating levels are increased in elderly people with chronic low grade inflammation (23) and prostaglandin-H2-ethanolamide (PGH2-EA) (Suppl. Fig. 4H), a precursor of prostaglandin E2 (PGE_2), which plays a major role in acute inflammation and transition to chronic inflammation (24), and is a key mediator of LPS-induced sickness (25).

Metabolites sex-dependently affected by LPS

Forty-six metabolites showed sex-dependent effects of LPS, of which twenty-one were selectively altered in males, twenty were selectively altered in females, and five showed opposite effects in the two sexes (Table 1). These changes particularly affected two metabolic pathways: pyruvate (Fig. 6) and methylglyoxal (Fig. 8). Changes in other metabolites known to be associated with immunomodulation are reported below and illustrated Suppl. Fig. 4.

Metabolic effects of LPS in males

Levels of methylimidazoleacetic acid (Sex X Treatment: $F_{(1,34)}=13.22$, $p=0.0009$, Suppl. Fig. 4J), a metabolite of the pro-inflammatory mediator histamine (26) were increased by LPS in APP/PS1 males.

Other metabolic changes found in LPS-treated males include increased levels of norepinephrinesulfate (Sex X Treatment: $F_{(1,34)}$=6.64, p=0.01, Suppl. Fig. 3O), a metabolite of the anti-inflammatory neurotransmitter norepinephrine (12), choline (Sex X Treatment: $F_{(1,34)}$=19.89, p<0.0001, Suppl. Fig. 4K), a precursor of acetylcholine and agonist of α7 nicotinic receptors expressed in neurons and macrophages with established anti-inflammatory effects (27, 28), found to dose-dependently inhibit LPS-induced TNFa production by macrophages (29), L-rhamnose (Sex X Treatment: $F_{(1,34)}$=7.25, p=0.01, Suppl. Fig. 4L), previously shown able to inhibit pro-inflammatory cytokines production (30), and hypoxantine (Sex X Treatment: $F_{(1,34)}$=10.06, p=0.003, Suppl. Fig. 4M), whose levels are negatively correlated with the severity of mucosal inflammation (31).

Metabolic effects of LPS in females

6-Phospho-D-gluconate (Suppl. Fig. 4N), an intermediate of the pentose phosphate pathway known to trigger pro-inflammatory cytokines secretion in LPS-activated macrophages (32), was less abundant in LPS-treated females

Pro-inflammatory metabolic changes found in LPS-treated females include reduced levels of N2-Succinyl-L-ornithine (Sex X Treatment: $F_{(1,34)}$=6.25, p=0.02, Suppl. Fig. 4N), a degradation product of the anti-inflammatory amino acid arginine (33), and, in WT LPS-treated females, and homoarginine (Suppl. Fig. 3K), known to be negatively associated with pro-inflammatory changes (14).

Metabolites showing opposite pattern in LPS-treated males and females

Two of the five metabolites that showed opposite effects of LPS in males and females, S-Adenosy-L-homocysteine Fig. 4E) and N-Succinyl-L-glutamate 5-semialdehyde (Suppl. Fig. 3D), have been reported to be associated with increased inflammation. They both were found more abundant in male hippocampi but less abundant in female hippocampi 4 hours after LPS administration.

Suppl. Table 3. Physiological role of metabolites from known metabolic pathways differently expressed between PBS-treated WT and APP/PS1 mice, PBS-treated males and females and in response to LPS.

Putative metabolite	Metabolic Pathway	Physiological role in the brain	Implication in sex differences in brain function	Implication in Alzheimer's disease (AD)	Implication in immune status
Amino acid metabolism					
(3R)-beta-Leucine	Valine, leucine and isoleucine degradation	Degradation product of L-Leucine which is produced by muscle protein catabolism and serves as a donor for brain glutamate synthesis by astrocytes and cerebral protein synthesis (34).	Not known	Increased serum levels of l-leucine in AD patients and in the 3xTg mouse model of AD (35). L-leucine up-regulates tau phosphorylation in 3xTg mice (35).	L- leucine reduces inflammation and increases repair after muscle injury in rats (4).
Choline	Glycine, serine and threonine metabolism	Precursor for the cerebral synthesis of acetylcholine, a neurotransmitter essential for cognitive function, and phospholipid phosphatidylcholine, a major constituent of biological membranes in neurons and glial cells (36, 37).	Higher choline concentrations in the hippocampus of cognitively intact elderly females (38).	Loss of cholinergic function in AD is associated with memory decline (39). Dietary intake of choline improves cognitive function in AD patients and mouse models (37).	Agonist of α7 nicotinic receptors expressed on macrophages, supresses LPS-induced TNFa production by macrophages (29).
L-cystathionine	Glycine, serine and threonine metabolism Methionine metabolism	Intermediate in the transsulfuration pathway which decreases neurotoxic homocysteine concentrations (40) Mediates the conversion of homocysteine into cysteine (Fig. 5).	Not known	Increased levels in the temporal cortex of post-mortem AD brains (41).	Inhibits the expression of the pro-inflammatory cytokine MCP-1 in macrophages *in vitro* (42).
L-methionine	Methionine metabolism	Key role in epigenetic regulation in the brain through conversion into homocysteine via S-adenosyl-L-methionine (43).	No differences in mouse brain concentrations (44).	Decreased levels in the temporal cortex of post-mortem AD brains (41). Elevated CSF levels in MCI and AD (45). Excess dietary methionine induces cognitive and neurological hallmarks of AD in mice (46).	Excess dietary methionine induces astrocyte and microglia activation in the hippocampus (46). Induces pro-inflammatory activation in macrophages in vitro (47).
L-methionine S-oxide	Methionine metabolism	Toxic oxidation product of methionine (48).	Not known	Increased production triggers Aβ aggregation (49).	Inhibition reduces TNFa and IL1β secretion in LPS-stimulated microglia (50).
S-adenosyl-L-homocysteine	Methionine metabolism	Biosynthetic precursor of homocysteine (Fig. 5) which is neurotoxic and pro-inflammatory in microglia (51). Formed by demethylation of S-adenosyl-L-methionine.	No differences in mouse brain concentrations (44).	Increased levels in the post-mortem AD brain are associated with cognitive dysfunction and neurological hallmarks of AD (52). Increase Aβ formation in BV-2 microglial cells (53).	Induces pro-inflammatory activation in endothelial cells in vitro (54).
O-succinyl-L-homoserine	Methionine metabolism	Mediates the conversion of homocysteine into cystathionine (Fig. 5).	Not known	Not known	Not known

S-adenosyl-L-methionine	Methionine metabolism Arginine and proline metabolism	Main donor of methyl groups for DNA methylation in the brain (43). Dietary supplementation improves cognitive abilities in mice (55).	No differences in mouse brain concentrations (44).	Decreased levels in the post-mortem AD brain (56) and CSF of AD patients (57).	Inhibits TNFa production and enhances IL-6 and IL-10 secretion in LPS-stimulated human macrophages and/or murine monocytes (58, 59).
5'-methylthioadenosine	Methionine metabolism Arginine and proline metabolism	Neuro-protective and anti-inflammatory derivative of methionine.	Not known	Increased CSF levels in MCI impaired patients (60).	Reduces brain damage; inhibits INFg and TNFa production and enhances IL-10 production in animal models of neuroinflammation (61).
N-carbamoylsarcosine	Arginine and proline metabolism	Not known	Not known	Not known	Not known
N-succinyl-L-glutamate 5-semialdehyde	Arginine and proline metabolism	Not known	Not known	Not known	Elevated in plasma from lung cancer patients harbouring a genetic mutation (7) which increases their susceptibility to inflammation (8).
Urea-1-carboxylate	Arginine and proline metabolism	Not known	Not known	Not known	Not known
Homoarginine	Arginine and proline metabolism	Precursor of the free radical nitric oxide. Unclear role in healthy brain function (62).	Not known	Not known	Reduced plasma levels associated with increased C-reactive protein levels in chronic kidney disease patients (14).
L-aspartate	Arginine and proline metabolism Lysine biosynthesis	Excitatory amino acid and selective glutamatergic NMDA receptor agonist (63).	Not known	Not known	No known
N6-(L-1,3-Dicarboxypropyl)-L-lysine	Lysine biosynthesis	Not known	Not known	Not known	Not known
N2-acetyl-L-aminoadipate	Lysine biosynthesis	Not known	Not known	Not known	Not known
L-2-aminoadipate	Lysine degradation	Intermediate in lysine degradation. Antagonises excitatory NMDA receptors and reduces kynurenine levels in the hippocampus (64).	Not known	Increased plasma levels in MCI and AD patients (65).	Produced by peritoneal cells in response to acute inflammation (66). Inhibits kynurenine production by astrocytes (64).
L-pipecolate	Lysine degradation Alkaloid biosynthesis I	Major degradation product of lysine in the murine brain (67).	Not known	Reduced CSF levels in MCI, but not AD, patients (60).	Urine levels are positively associated with low grade inflammation in healthy individuals (10).
(Z)-4-hydroxyphenylacetaldehyde-oxime	Tyrosine metabolism	Not known	Not known	Not known	Increased gut levels in inflammatory bowel disease (13).
[FA hydroxy,oxo(7:0/2:0)]	Tyrosine metabolism	Not known	Not known	Not known	Not known

4-hydroxy-2-oxo-Heptanedioic acid					
L-phenylalanine	Phenylalanine, tyrosine and tryptophan biosynthesis	Dietary precursor of catecholamines. Accumulation in the brain due to impaired degradation causes brain damage and mental retardation (68).	Not known	Increased circulating levels correlate with inflammation in a subgroup of AD patients (69).	Increased circulating levels in elderly people with chronic low grade inflammation (23).
L-tryptophan	Phenylalanine, tyrosine and tryptophan biosynthesis Tryptophan metabolism	Dietary precursor of serotonin and vitamin B3 (nicotinic acid). Improves mood and cognition by enhancing serotoninergic neurotransmission (70) and nicotinamide pathway (71)	Women are more susceptible to episodic memory impairment caused by acute tryptophan depletion (72). Lower plasma tryptophan levels in females associated with reduced serotonin synthesis rate throughout the brain (73).	Reduced CSF levels in MCI, but not AD, patients (60). Reduced serotoninergic neurotransmission associated with the development of cognitive symptoms in AD (74). Upregulation of kynurenine pathway associated with neurological hallmarks of AD (75).	Increases inflammation via stimulation of the kynurenine pathway (76). Serotoninergic neurotransmission thought to protect against neuroinflammation (77).
5-hydroxyindoleacetate	Tryptophan metabolism	End metabolite of the serotonin pathway of tryptophan metabolism (Fig. 6).	See L-tryptophan	Elevated CSF levels in MCI and AD (45).	See L-tryptophan
Pantothenate	beta-Alanine metabolism Pantothenate and CoA biosynthesis	Vitamin B5. Substrate for the biosynthesis of coenzyme A which contributes to the structure and function of brain cells *via* its role in the synthesis and oxidation of fatty acids (71).	Not known	Dietary intake positively associated with cerebral Aβ burden in MCI patients (78).	Dietary intake lower systemic inflammation (C-reactive protein levels) in healthy adults over 40 (11).
D-alanyl-D-alanine	D-Alanine metabolism Peptidoglycan biosynthesis	Not known	Not known	Not known	Anti-inflammatory antibiotic-binding protein (5).
Glutathione disulphide (GSSG)	Glutamate metabolism Glutathione metabolism	Toxic oxidation product of the anti-oxidant glutathione produced and exported by astrocytes in the brain (79).	No sex differences in brain tissue content with aging in mice despite the most pronounced decline in glutathione concentrations seen in males (80).	Higher activity of glutathione reductase activity, which catalyses the reduction of GSSG disulphide in glutathione, in the temporal cortex of AD patients (81), but unaltered GSSG contents (82).	Increased circulating levels during acute systemic inflammation in the rats (83).
Methylimidazoleacetic acid	Histidine metabolism	Main metabolite of histamine, a neuromodulator, also involved in cognition, wakefulness and anxiety and motivated behaviours (84, 85).	Not known	Degeneration of histaminergic nerve fibres in AD (86).	Histamine is produced by immune cells in the brain, induces pro-inflammatory microglial activation but inhibits LPS-induced microglial activation (87).
N(pi)-methyl-L-histidine	Histidine metabolism	Derivative of histidine, a precursor of brain histamine (85).	Not known	Not known	Serum histidine levels are negatively associated with systemic inflammation (C-reactive protein levels) in obese women (6).
Hypotaurine	Taurine and	Intermediate in the synthesis of	Not known	Not known	Suppresses inflammatory and

	hypotaurine metabolism	taurine from the methionine derivative cysteine (Fig. 5) in neurons, astrocytes and microglia (88, 89).			neuropathic pain (90).
Carbohydrate metabolism					
Succinate	Citrate cycle (TCA cycle) Glyoxylate and dicarboxylate metabolism	Support brain energy metabolism by promoting ATP generation in mitochondria (91). Ameliorates metabolic deficits of glial cells with mitochondrial dysfunction (92).	Not known	Reduced whole brain content from 9 months of age in an APP/PS1 mouse model (93).	Pro-inflammatory mediator in macrophages mediating LPS-induced IL-1β production (20, 94).
Isocitrate	Citrate cycle (TCA cycle) Glyoxylate and dicarboxylate metabolism	Not known	Not known	Increased CSF levels in a transgenic rat model of tauopathy (95).	Anti-inflammatory in rat model of anaemia of inflammation (15). Microglial deficiency in isocitrate dehydrogenase, the enzyme that catalyses oxidative decarboxylation of isocitrate, suppresses LP-induced pro-inflammatory cytokine production (TNFa, IL-6, IL-1β) (96).
(S)-malate	Citrate cycle (TCA cycle) Pyruvate metabolism Glyoxylate and dicarboxylate metabolism	Metabolite of the KREBS cycle which promotes mitochondrial ATP generation and can be recycled into pyruvate (97).	Not known	Not known	Produced by pro-inflammatory activation of macrophages (98).
(D)-lactate	Pyruvate metabolism	Produced by methylglyoxal metabolism. Excess levels can cause encephalopathy (99).	Sex differences in D-lactate metabolism may contribute to reduced association between microbiota and neurological symptoms in females (100).	Methylglyoxal can cause Aβ aggregation (101) and its neurotoxicity is associated with AD (102).	Methylglyoxal is pro-inflammatory and activates glial cells in the brain (103).
(D)-S-lactoylglutathione	Pyruvate metabolism	Intermediate in the formation of D-lactate from methylglyoxal.	Not known	Not known	Not known
Phosphoenolpyruvate	Citrate cycle (TCA cycle) Pyruvate metabolism Glycolysis / Gluconeogenesis	Intermediate in glycolysis and gluconeogenesis.	Not known	Not known	Systemic LPS increases brain levels of phosphoenolpyruvate carboxykinase (104), which catalyses the conversion of oxaloacetate to phosphoenolpyruvate in gluconeogenesis and has anti-inflammatory effects on LPS-induced circulating pro-inflammatory cytokines levels (104) and macrophages phenotype

					(105).
Pyruvate	Citrate cycle (TCA cycle) Glycolysis / Gluconeogenesis	Intermediate metabolite of glucose with potent antioxidant and anti-inflammatory properties (106).	Sex differences in pyruvate metabolism associated with reduced oxidative stress and damage in females (107, 108).	Improves cognitive performance in mouse models of AD without affecting tau or Aβ pathology (109, 110).	Ethyl derivatives of pyruvate alleviate pro-inflammatory changes in the brain (111, 112).
D-glyceraldehyde 3-phosphate	Glycolysis / Gluconeogenesis	Intermediate in glycolysis and gluconeogenesis.	Not known	Not known	Not known
3-phospho-D-glycerate	Glycolysis /Gluconeogenesis Glyoxylate and dicarboxylate metabolism	Conversion of 3-phospho-D-glycerate to phosphohydroxypyruvate by the enzyme 3-phosphoglycerate dehydrogenase (3PGDH) is the first step in serine production. Deficiency in 3PGDH causes brain atrophy, seizures and psychomotor retardation (113).	Not known	Not known	3PGDH is an astrocytic enzyme that catalases the production of serine by neurons and glia (114) and is anti-inflammatory in fibroblasts (115).
2-phosphoglycolate	Glyoxolate and dicatboxylate metabolism	Possible indicator of damage and repair of DNA ends (116).	Not known	Decreased expression and activity in AD brain of phosphoglucomutase 1 (PGM1) the glycolytic enzyme that catalyses the conversion of 3-phosphoglycerate to 2-phosphoglycerate (117).	Not known
3-oxalomalate	Glyoxolate and dicatboxylate metabolism	Not known	Not known	Not known	Antioxidant in LPS-activated macrophages (118).
L-rhamnose	Fructose and mannose metabolism	Not known	Not known	Not known	Inhibits pro-inflammatory cytokines production in macrophages (119).
D-sorbitol	Fructose and mannose metabolism	Intermediate in the production of fructose from glucose in the brain (120).	Not known	Elevated levels in the post-mortem AD brain (121).	Anti-inflammatory properties in resident cells from articular cartilage (122).
6-phospho-D-gluconate	Pentose phosphate pathway	Regulatory control of brain metabolism (123).	Not known	Increased activity of the pentose phosphate pathway associated with increased pro-oxidant activity in the post mortem AD brain (124)	Triggers pro-inflammatory cytokines secretion in LPS-activated macrophages (32).
Propanoyl phosphate	Propanoate metabolism C5-Branched dibasic acid metabolism	Not known	Not known	Not known	Not known
Itaconate	C5-Branched dibasic acid metabolism Citrate cycle (TCA cycle)	Endogenous antibiotic in the brain (125).	Not known	Not known	Anti-inflammatory metabolite found in macrophages (16) and produced by microglia (125).

Methyloxaloacetate	C5-Branched dibasic acid metabolism	Not known	Not known	Not known	Not known
Nucleotide metabolism					
Hypoxanthine	Purine metabolism	Endogenous ligand of benzodiazepine-binding sites in the brain (126).	Not known	Increased brain concentration in a transgenic rat model of tauopathy (95). Elevated CSF levels in MCI patients (45).	Hypoxanthine is anti-inflammatory and depleted in LPS-stimulated macrophages (127).
Urate	Purine metabolism	Neuroprotective and antioxidant at physiological levels (128).	Reduced brain tissue contents in women (129).	Increased CSF contents in AD (130). Trends towards reduced levels in the post-mortem AD brain (129).	High uric acid diet causes cognitive deficits by inducing hippocampal neuroinflammation (22). Suppresses LPS-induced pro-inflammatory microglial activation in vitro (131).
N6-(1,2-Dicarboxyethyl)-AMP	Purine metabolism	Not known	Not known	Not known	Not known
Orotate	Pyrimidine metabolism	Not known	Not known	Not known	Not known
Thymidine	Pyrimidine metabolism	Not known	Not known	Not known	Not known
Thymine	Pyrimidine metabolism	Not known	Not known	Not known	Not known
5,6-dihydrouracil	Pyrimidine metabolism Beta-Alanine metabolism Pantothenate and CoA biosynthesis	Not known	Not known	Not known	Not known
Lipid metabolism and Fatty acyls					
Octadecanoic acid (18:0 stearic acid)	Fatty acids biosynthesis Biosynthesis of unsaturated fatty acids	Needed for the synthesis of membranes of neurons and astrocytes during brain development (132).	No sex differences in mouse brain content with normal diet (133).	Induces tau phosphorylation in cultured neurons and astrocytes (134). Triggers secretion of Aβ peptide (135). Reduced levels in the post-mortem AD brain (136).	Accumulates primarily in astrocytes (137) where it triggers the release of TNFα and IL-6 (138).
Hexadecanoic acid (16:0 palmitic acid)	Biosynthesis of unsaturated fatty acids	Dietary administration, which enters the brain, improves cognitive and motor function (139).	No sex differences in mouse brain content with normal diet (133).	Induces tau phosphorylation and amyloid processing in cultured neurons and astrocytes (134, 135, 140). Increased levels in the post-mortem AD brain (136).	Triggers astrocytic release of TNFα and IL-6 in vitro (138). Impairs the protective migratory and phagocytic activities of microglia in both males and females (141).

Icosatrienoic acid 20:3	Biosynthesis of unsaturated fatty acids	Increased brain levels associated with reduced brain growth in developing rats fed with an essential fatty acid deficient diet (142). Intermediate in the synthesis of Arachidonic acid.	Not known	Not known	Not known
[FA (20:4)] 5Z,8Z,11Z,14Z-eicosatetraenoic acid (20:4 Arachidonic acid)	Fatty Acids and Conjugates	Contributes in brain growth and function in combination with other fatty acids (143).	No sex differences in mouse brain content with normal diet (133).	Triggers secretion of Aβ peptide (135). Reduced levels in the post-mortem AD brain (136, 144).	Precursor of potent pro-inflammatory eicosanoids (e.g. prostaglandins) in astrocytes (145). Does not trigger pro-inflammatory cytokine release in astrocytes (138).
PGH2-EA	Eicosanoids	Metabolite of the endocannabinoid anandamide known to modulate the brain reward system (146)	Not known	Increases the neurotoxicity of Aβ peptide (147).	Precursor of prostaglandin E2 which mediates LPS-induced sickness (148).
Formyl 3-hydroxy-butanoate	Fatty esters	Not known	Not known	Not known	Not known
sn-glycerol 3-phosphate	Glycerolipid metabolism Glycerophospholipid metabolism	Intermediate in the glycolysis metabolic pathway. Increased biosynthesis in the hippocampus during long-term potentiation (149).	Not known	Not known	Not known
sn-glycero-3-Phosphoethanolamine	Glycerophospholipid metabolism Ether lipid metabolism	Not known.	Not known	Not known	Not known
Energy Metabolism					
ATP	Oxidative phosphorylation Purine metabolism	Main cellular source of energy in the brain, which can improve cognitive function (150).	Greater ATP production in female mitochondria in the rodent brain (107)	Decreased brain contents in a transgenic rat model of tauopathy (95) and mouse model of amyloidosis (151).	Pro-inflammatory signalling molecule in the brain via increased synthesis of prostaglandin E2 (19). Produced by microglia and astrocytes, leading to microglial activation and chemotactic factor for microglia towards tissue injury (152, 153)
D-fructose 1,6-bisphosphate	Carbon fixation	Neuroprotective high energy glycolytic intermediate (154).	Not known	Not known	Anti-inflammatory in pain models (155)
D-sedoheptulose 1,7-bisphosphate	Carbon fixation	Not known	Not known	Not known	Not known
Metabolism of Cofactors and Vitamins					
Iminoglycine	Thiamine metabolism	Not known	Not known	Not known	Not known

N1-methyl-2-pyridone-5-carboxamide	Nicotinate and nicotinamide metabolism	Toxic end metabolite of the tryptophan-nicotinamide pathway (156)	Not known	Not known	Elevated circulating levels associated with systemic inflammation (157).
Peptides					
Gamma glutamylglutamic acid	Peptide	Not known	Not known	Not known	Not known
L-beta-aspartyl-L-glutamicacid	Peptide	Not known	Not known	Not known	Belongs to the family of N-acyl-alpha amino acids and derivatives which are known for their anti-inflammatory action (1)
Asp-Ser-His	Basic peptide	Not known	Not known	Not known	Not known
Asn-Met-Met-Asn	Hydrophobic peptide	Not known	Not known	Not known	Not known
Asp-Phe-Thr-Thr	Hydrophobic peptide	Not known	Not known	Not known	Not known
Asn-Asn-Asn	Polar peptide	Not known	Not known	Not known	Not known
Biosynthesis of Polyketides and nonribosomal Peptides					
Narbomycin	Biosynthesis of 12-, 14- and 16-membered macrolides	Not known	Not known	Not known	Not known
13-dihydrocarminomycin	Biosynthesis of type II polyketide products	Not known	Not known	Not known	Not known
Biosynthesis of Secondary metabolites					
Dihydroclavaminic acid C8H12N2O4	Clavulanic acid biosynthesis	Not known	Not known	Not known	Not known
Not known					
γ-aminobutyramide C4H10N2O	Not known	Not known	Not known	Not known	Not known
1-deoxy-D-altro-heptulose 7-phosphate	Not known	Not known	Not known	Not known	Not known
1-methyladenosine	Not known			Increased urinary levels in patients with mild-to-moderate Alzheimer's disease (3).	Immunosuppressive on macrophage function (2).
3, 5-tetradecadiencarnitine	Not known	Not known	Not known	Not known	Not known
3-methylphosphoenol-pyruvate	Not known	Not known	Not known	Not known	Not known
6-methyltetrahydropterin	Not known	Not known	Not known	Not known	Not known

Athamantin	Not known	Not known	Not known	Not known	Not known
Camptothecin	Not known	Not known	Not known	Not known	Not known
Dimethyl citraconate	Not known	Not known	Not known	Not known	Not known
DL-2-sulfoctanoicacid	Not known	Not known	Not known	Not known	Not known
Elaidiccarnitine	Not known	Not known	Not known	Not known	Not known
Glutarylcarnitine	Not known	Not known	Not known	Not known	Not known
Glycerophosphoglycerol	Not known	Not known	Not known	Not known	Not known
Linoelaidylcarnitine	Not known	Not known	Not known	Not known	Not known
N-acetyl-(L)-arginine	Not known	Not known	Not known	Not known	Not known
NG,NG-dimethyl-L-arginine	Not known	Not known	Not known	Not known	Not known
Nocardicin C	Not known	Not known	Not known	Not known	Not known
Nonulose 9-phosphate	Not known	Not known	Not known	Not known	Not known
Norepinephrinesulfate	Not known	Not known	Not known	Not known	Not known
Orotidine	Not known	Not known	Not known	Not known	Not known
Tetradecanoylcarnitine	Not known	Not known	Not known	Not known	Not known
GDP-3,6-dideoxy-D-galactose	Not known	Not known	Not known	Not known	Not known
N-hydroxyvaline	Linamarin biosynthesis	Not known	Not known	Not known	Not known

References

1. Burstein SH. N-Acyl Amino Acids (Elmiric Acids): Endogenous Signaling Molecules with Therapeutic Potential. Mol Pharmacol. 2018;93(3):228-38.
2. Itoh K, Majima T, Edo K, Mizugaki M, Ishida N. Suppressive effect of 1-methyladenosine on the generation of chemiluminescence by mouse peritoneal macrophages stimulated with opsonized zymosan. Tohoku J Exp Med. 1989;157(3):205-14.
3. Lee SH, Kim I, Chung BC. Increased urinary level of oxidized nucleosides in patients with mild-to-moderate Alzheimer's disease. Clin Biochem. 2007;40(13-14):936-8.
4. Kato H, Miura K, Nakano S, Suzuki K, Bannai M, Inoue Y. Leucine-enriched essential amino acids attenuate inflammation in rat muscle and enhance muscle repair after eccentric contraction. Amino Acids. 2016;48(9):2145-55.
5. van der Aart LT, Lemmens N, van Wamel WJ, van Wezel GP. Substrate Inhibition of VanA by d-Alanine Reduces Vancomycin Resistance in a VanX-Dependent Manner. Antimicrob Agents Chemother. 2016;60(8):4930-9.
6. Niu YC, Feng RN, Hou Y, Li K, Kang Z, Wang J, et al. Histidine and arginine are associated with inflammation and oxidative stress in obese women. Br J Nutr. 2012;108(1):57-61.
7. Pamungkas AD, Medriano CA, Sim E, Lee S, Park YH. A pilot study identifying a potential plasma biomarker for determining EGFR mutations in exons 19 or 21 in lung cancer patients. Mol Med Rep. 2017;15(6):4155-61.
8. Jacobs JM, Traeger L, Eusebio J, Simon NM, Sequist LV, Greer JA, et al. Depression, inflammation, and epidermal growth factor receptor (EGFR) status in metastatic non-small cell lung cancer: A pilot study. J Psychosom Res. 2017;99:28-33.
9. Han H, Yin J, Wang B, Huang XG, Yao JM, Zheng J, et al. Effects of dietary lysine restriction on inflammatory responses in piglets. Sci Rep-Uk. 2018;8.
10. Pietzner M, Kaul A, Henning AK, Kastenmuller G, Artati A, Lerch MM, et al. Comprehensive metabolic profiling of chronic low-grade inflammation among generally healthy individuals. BMC Med. 2017;15(1):210.
11. Jung S, Kim MK, Choi BY. The long-term relationship between dietary pantothenic acid (vitamin B-5) intake and C-reactive protein concentration in adults aged 40 years and older. Nutr Metab Cardiovas. 2017;27(9):806-16.
12. Pongratz G, Straub RH. The sympathetic nervous response in inflammation. Arthritis Res Ther. 2014;16(6):504.
13. Jansson J, Willing B, Lucio M, Fekete A, Dicksved J, Halfvarson J, et al. Metabolomics reveals metabolic biomarkers of Crohn's disease. PLoS One. 2009;4(7):e6386.
14. Ravani P, Maas R, Malberti F, Pecchini P, Mieth M, Quinn R, et al. Homoarginine and mortality in pre-dialysis chronic kidney disease (CKD) patients. PLoS One. 2013;8(9):e72694.
15. Richardson CL, Delehanty LL, Bullock GC, Rival CM, Tung KS, Kimpel DL, et al. Isocitrate ameliorates anemia by suppressing the erythroid iron restriction response. J Clin Invest. 2013;123(8):3614-23.
16. Mills EL, Ryan DG, Prag HA, Dikovskaya D, Menon D, Zaslona Z, et al. Itaconate is an anti-inflammatory metabolite that activates Nrf2 via alkylation of KEAP1. Nature. 2018;556(7699):113-+.
17. Kuda O, Brezinova M, Rombaldova M, Slavikova B, Posta M, Beier P, et al. Docosahexaenoic Acid-Derived Fatty Acid Esters of Hydroxy Fatty Acids (FAHFAs) With Anti-inflammatory Properties. Diabetes. 2016;65(9):2580-90.
18. Nofal ZM, Fahmy HH, Zarea ES, El-Eraky W. Synthesis of New Pyrimidine Derivatives with Evaluation of Their Anti-Inflammatory and Analgesic Activities. Acta Pol Pharm. 2011;68(4):507-17.
19. Fiebich BL, Akter S, Akundi RS. The two-hit hypothesis for neuroinflammation: role of exogenous ATP in modulating inflammation in the brain. Front Cell Neurosci. 2014;8:260.
20. Mills E, O'Neill LA. Succinate: a metabolic signal in inflammation. Trends Cell Biol. 2014;24(5):313-20.
21. McKay TB, Hjortdal J, Sejersen H, Asara JM, Wu J, Karamichos D. Endocrine and Metabolic Pathways Linked to Keratoconus: Implications for the Role of Hormones in the Stromal Microenvironment. Sci Rep. 2016;6:25534.
22. Shao XN, Lu WJ, Gao FB, Li DD, Hu J, Li Y, et al. Uric Acid Induces Cognitive Dysfunction through Hippocampal Inflammation in Rodents and Humans. J Neurosci. 2016;36(43):10990-1005.
23. Capuron L, Schroecksnadel S, Feart C, Aubert A, Higueret D, Barberger-Gateau P, et al. Chronic Low-Grade Inflammation in Elderly Persons Is Associated with Altered Tryptophan and Tyrosine Metabolism: Role in Neuropsychiatric Symptoms. Biol Psychiat. 2011;70(2):175-82.
24. Aoki T, Narumiya S. Prostaglandins and chronic inflammation. Trends Pharmacol Sci. 2012;33(6):304-11.
25. Saper CB, Romanovsky AA, Scammell TE. Neural circuitry engaged by prostaglandins during the sickness syndrome. Nat Neurosci. 2012;15(8):1088-95.

26. Branco ACCC, Yoshikawa FSY, Pietrobon AJ, Sato MN. Role of Histamine in Modulating the Immune Response and Inflammation. Mediat Inflamm. 2018.
27. Wang H, Yu M, Ochani M, Amella CA, Tanovic M, Susarla S, et al. Nicotinic acetylcholine receptor alpha 7 subunit is an essential regulator of inflammation. Nature. 2003;421(6921):384-8.
28. Rowley TJ, McKinstry A, Greenidge E, Smith W, Flood P. Antinociceptive and anti-inflammatory effects of choline in a mouse model of postoperative pain. Brit J Anaesth. 2010;105(2):201-7.
29. Parrish WR, Puerta MG, Ochani M, Ochani K, Moskovic D, Lin X, et al. Choline suppresses inflammatory responses. Shock. 2006;25:45-.
30. Watanabe Y, Tateno H, Nakamura-Tsuruta S, Kominami J, Hirabayashi J, Nakamura O, et al. The function of rhamnose-binding lectin in innate immunity by restricted binding to Gb3. Dev Comp Immunol. 2009;33(2):187-97.
31. Lee JS, Wang RX, Alexeev EE, Lanis JM, Battista KD, Glover LE, et al. Hypoxanthine is a checkpoint stress metabolite in colonic epithelial energy modulation and barrier function. J Biol Chem. 2018;293(16):6039-51.
32. Baardman J, Verberk SGS, Prange KHM, van Weeghel M, van der Velden S, Ryan DG, et al. A Defective Pentose Phosphate Pathway Reduces Inflammatory Macrophage Responses during Hypercholesterolemia. Cell Rep. 2018;25(8):2044-52 e5.
33. Wu T, Wang C, Ding L, Shen Y, Cui H, Wang M, et al. Arginine Relieves the Inflammatory Response and Enhances the Casein Expression in Bovine Mammary Epithelial Cells Induced by Lipopolysaccharide. Mediators Inflamm. 2016;2016:9618795.
34. Yudkoff M, Daikhin Y, Nissim I, Horyn O, Luhovyy B, Luhovyy B, et al. Brain amino acid requirements and toxicity: the example of leucine. J Nutr. 2005;135(6 Suppl):1531S-8S.
35. Li HJ, Ye D, Xie W, Hua F, Yang YL, Wu J, et al. Defect of branched-chain amino acid metabolism promotes the development of Alzheimer's disease by targeting the mTOR signaling. Bioscience Rep. 2018;38.
36. Loffelholz K, Klein J, Koppen A. Choline, a Precursor of Acetylcholine and Phospholipids in the Brain. Progress in Brain Research. 1993;98:197-200.
37. Blusztajn JK, Slack BE, Mellott TJ. Neuroprotective Actions of Dietary Choline. Nutrients. 2017;9(8).
38. Chen CS, Kuo YT, Tsai HY, Li CW, Lee CC, Yen CF, et al. Brain Biochemical Correlates of the Plasma Homocysteine Level: A Proton Magnetic Resonance Spectroscopy Study in the Elderly Subjects. Am J Geriat Psychiat. 2011;19(7):618-26.
39. Francis PT, Palmer AM, Snape M, Wilcock GK. The cholinergic hypothesis of Alzheimer's disease: a review of progress. J Neurol Neurosur Ps. 1999;66(2):137-47.
40. Hensley K, Denton TT. Alternative functions of the brain transsulfuration pathway represent an underappreciated aspect of brain redox biochemistry with significant potential for therapeutic engagement. Free Radical Bio Med. 2015;78:123-34.
41. Gueli MC, Taibi G. Alzheimer's disease: amino acid levels and brain metabolic status. Neurol Sci. 2013;34(9):1575-9.
42. Zhu MZ, Du JB, Liu AD, Holmberg L, Chen SY, Bu DF, et al. L-cystathionine inhibits oxidized low density lipoprotein-induced THP-1-derived macrophage inflammatory cytokine monocyte chemoattractant protein-1 generation via the NF-kappa B pathway. Sci Rep-Uk. 2015;5.
43. McGowan PO, Meaney MJ, Szyf M. Diet and the epigenetic (re)programming of phenotypic differences in behavior. Brain Res. 2008;1237:12-24.
44. Witham KL, Butcher NJ, Sugamori KS, Brenneman D, Grant DM, Minchin RF. 5-methyl-tetrahydrofolate and the S-adenosylmethionine cycle in C57BL/6J mouse tissues: gender differences and effects of arylamine N-acetyltransferase-1 deletion. PLoS One. 2013;8(10):e77923.
45. Kaddurah-Daouk R, Zhu H, Sharma S, Bogdanov M, Rozen SG, Matson W, et al. Alterations in metabolic pathways and networks in Alzheimer's disease. Transl Psychiat. 2013;3.
46. Tapia-Rojas C, Lindsay CB, Montecinos-Oliva C, Arrazola MS, Retamales RM, Bunout D, et al. Is L-methionine a trigger factor for Alzheimer's-like neurodegeneration?: Changes in Abeta oligomers, tau phosphorylation, synaptic proteins, Wnt signaling and behavioral impairment in wild-type mice. Mol Neurodegener. 2015;10:62.
47. Dos Santos LM, da Silva TM, Azambuja JH, Ramos PT, Oliveira PS, da Silveira EF, et al. Methionine and methionine sulfoxide treatment induces M1/classical macrophage polarization and modulates oxidative stress and purinergic signaling parameters. Mol Cell Biochem. 2017;424(1-2):69-78.
48. Stadtman ER, Van Remmen H, Richardson A, Wehr NB, Levine RL. Methionine oxidation and aging. Biochim Biophys Acta. 2005;1703(2):135-40.
49. Moskovitz J, Du F, Bowman CF, Yan SS. Methionine sulfoxide reductase A affects beta-amyloid solubility and mitochondrial function in a mouse model of Alzheimer's disease. Am J Physiol Endocrinol Metab. 2016;310(6):E388-93.

50. Fan H, Wu PF, Zhang L, Hu ZL, Wang W, Guan XL, et al. Methionine Sulfoxide Reductase A Negatively Controls Microglia-Mediated Neuroinflammation via Inhibiting ROS/MAPKs/NF-kappa B Signaling Pathways Through a Catalytic Antioxidant Function. Antioxid Redox Sign. 2015;22(10):832-47.
51. Chen S, Dong ZP, Cheng M, Zhao YQ, Wang MY, Sai N, et al. Homocysteine exaggerates microglia activation and neuroinflammation through microglia localized STAT3 overactivation following ischemic stroke. J Neuroinflamm. 2017;14.
52. Kennedy BP, Bottiglieri T, Arning E, Ziegler MG, Hansen LA, Masliah E. Elevated S-adenosylhomocysteine in Alzheimer brain: influence on methyltransferases and cognitive function. J Neural Transm (Vienna). 2004;111(4):547-67.
53. Lin HC, Hsieh HM, Chen YH, Hu ML. S-Adenosylhomocysteine increases beta-amyloid formation in BV-2 microglial cells by increased expressions of beta-amyloid precursor protein and presenilin 1 and by hypomethylation of these gene promoters. Neurotoxicology. 2009;30(4):622-7.
54. Barroso M, Kao D, Blom HJ, de Almeida IT, Castro R, Loscalzo J, et al. S-adenosylhomocysteine induces inflammation through NFkB: A possible role for EZH2 in endothelial cell activation. Bba-Mol Basis Dis. 2016;1862(1):82-92.
55. Montgomery SE, Sepehry AA, Wangsgaard JD, Koenig JE. The Effect of S-Adenosylmethionine on Cognitive Performance in Mice: An Animal Model Meta-Analysis. Plos One. 2014;9(10).
56. Morrison LD, Smith DD, Kish SJ. Brain S-adenosylmethionine levels are severely decreased in Alzheimer's disease. J Neurochem. 1996;67(3):1328-31.
57. Linnebank M, Popp J, Smulders Y, Smith D, Semmler A, Farkas M, et al. S-Adenosylmethionine Is Decreased in the Cerebrospinal Fluid of Patients with Alzheimer's Disease. Neurodegener Dis. 2010;7(6):373-8.
58. Pfalzer AC, Choi SW, Tammen SA, Park LK, Bottiglieri T, Parnell LD, et al. S-adenosylmethionine mediates inhibition of inflammatory response and changes in DNA methylation in human macrophages. Physiol Genomics. 2014;46(17):617-23.
59. Song ZY, Chen T, Uriarte S, Hill D, Barve S, McClain C. S-Adenosylmethionine (SAMe) modulates interleukin-10 and interleukin-6, but not TNF, production by adenosine (A2) receptor. Gastroenterology. 2004;126(4):A684-A.
60. Ibanez C, Simo C, Barupal DK, Fiehn O, Kivipelto M, Cedazo-Minguez A, et al. A new metabolomic workflow for early detection of Alzheimer's disease. J Chromatogr A. 2013;1302:65-71.
61. Moreno B, Hevia H, Santamaria M, Sepulcre J, Munoz J, Garcia-Trevijano ER, et al. Methylthioadenosine reverses brain autoimmune disease. Ann Neurol. 2006;60(3):323-34.
62. Bernstein HG, Jager K, Dobrowolny H, Steiner J, Keilhoff G, Bogerts B, et al. Possible sources and functions of L-homoarginine in the brain: review of the literature and own findings. Amino Acids. 2015;47(9):1729-40.
63. Herring BE, Silm K, Edwards RH, Nicoll RA. Is Aspartate an Excitatory Neurotransmitter? J Neurosci. 2015;35(28):10168-71.
64. Wu HQ, Ungerstedt U, Schwarcz R. L-Alpha-Aminoadipic Acid as a Regulator of Kynurenic Acid Production in the Hippocampus - a Microdialysis Study in Freely Moving Rats. Eur J Pharmacol. 1995;281(1):55-61.
65. Wang G, Zhou Y, Huang FJ, Tang HD, Xu XH, Liu JJ, et al. Plasma Metabolite Profiles of Alzheimer's Disease and Mild Cognitive Impairment. J Proteome Res. 2014;13(5):2649-58.
66. Lin H, Levison BS, Buffa JA, Huang Y, Fu X, Wang Z, et al. Myeloperoxidase-mediated protein lysine oxidation generates 2-aminoadipic acid and lysine nitrile in vivo. Free Radical Bio Med. 2017;104:20-31.
67. Posset R, Opp S, Struys EA, Volkl A, Mohr H, Hoffmann GF, et al. Understanding cerebral L-lysine metabolism: the role of L-pipecolate metabolism in Gcdh-deficient mice as a model for glutaric aciduria type I. J Inherit Metab Dis. 2015;38(2):265-72.
68. Williams RA, Mamotte CD, Burnett JR. Phenylketonuria: an inborn error of phenylalanine metabolism. Clin Biochem Rev. 2008;29(1):31-41.
69. Wissmann P, Geisler S, Leblhuber F, Fuchs D. Immune activation in patients with Alzheimer's disease is associated with high serum phenylalanine concentrations. J Neurol Sci. 2013;329(1-2):29-33.
70. Jenkins TA, Nguyen JC, Polglaze KE, Bertrand PP. Influence of Tryptophan and Serotonin on Mood and Cognition with a Possible Role of the Gut-Brain Axis. Nutrients. 2016;8(1).
71. Kennedy DO. B Vitamins and the Brain: Mechanisms, Dose and Efficacy-A Review. Nutrients. 2016;8(2).
72. Sambeth A, Blokland A, Harmer CJ, Kilkens TO, Nathan PJ, Porter RJ, et al. Sex differences in the effect of acute tryptophan depletion on declarative episodic memory: a pooled analysis of nine studies. Neurosci Biobehav Rev. 2007;31(4):516-29.
73. Nishizawa S, Benkelfat C, Young SN, Leyton M, Mzengeza S, DeMontigny C, et al. Differences between males and females in rates of serotonin synthesis in human brain. P Natl Acad Sci USA. 1997;94(10):5308-13.

74. Smith GS, Barrett FS, Joo JH, Nassery N, Savonenko A, Sodums DJ, et al. Molecular imaging of serotonin degeneration in mild cognitive impairment. Neurobiol Dis. 2017;105:33-41.
75. Wu W, Nicolazzo JA, Wen L, Chung R, Stankovic R, Bao SSS, et al. Expression of Tryptophan 2,3-Dioxygenase and Production of Kynurenine Pathway Metabolites in Triple Transgenic Mice and Human Alzheimer's Disease Brain. Plos One. 2013;8(4).
76. Davis I, Liu AM. What is the tryptophan kynurenine pathway and why is it important to neurotherapeutics? Expert Rev Neurother. 2015;15(7):719-21.
77. Wu H, Denna TH, Storkersen JN, Gerriets VA. Beyond a neurotransmitter: The role of serotonin in inflammation and immunity. Pharmacol Res. 2019;140:100-14.
78. Lee JH, Ahn SY, Lee HA, Won KS, Chang HW, Oh JS, et al. Dietary intake of pantothenic acid is associated with cerebral amyloid burden in patients with cognitive impairment. Food Nutr Res. 2018;62.
79. Dringen R, Hirrlinger J. Glutathione pathways in the brain. Biol Chem. 2003;384(4):505-16.
80. Wang H, Liu HL, Liu RM. Gender difference in glutathione metabolism during aging in mice. Exp Gerontol. 2003;38(5):507-17.
81. Schuessel K, Leutner S, Cairns NJ, Muller WE, Eckert A. Impact of gender on upregulation of antioxidant defence mechanisms in Alzheimer's disease brain. J Neural Transm. 2004;111(9):1167-82.
82. Adams JD, Jr., Klaidman LK, Odunze IN, Shen HC, Miller CA. Alzheimer's and Parkinson's disease. Brain levels of glutathione, glutathione disulfide, and vitamin E. Mol Chem Neuropathol. 1991;14(3):213-26.
83. Ikegami K, Lalonde C, Young YK, Picard L, Demling R. Comparison of plasma reduced glutathione and oxidized glutathione with lung and liver tissue oxidant and antioxidant activity during acute inflammation. Shock. 1994;1(4):307-12.
84. Passani MB, Panula P, Lin JS. Histamine in the brain. Front Syst Neurosci. 2014;8:64.
85. Yoshikawa T, Nakamura T, Shibakusa T, Sugita M, Naganuma F, Iida T, et al. Insufficient intake of L-histidine reduces brain histamine and causes anxiety-like behaviors in male mice. J Nutr. 2014;144(10):1637-41.
86. Panula P, Rinne J, Kuokkanen K, Eriksson KS, Sallmen T, Kalimo H, et al. Neuronal histamine deficit in Alzheimer's disease. Neuroscience. 1998;82(4):993-7.
87. Barata-Antunes S, Cristovao AC, Pires J, Rocha SM, Bernardino L. Dual role of histamine on microglia-induced neurodegeneration. Biochim Biophys Acta Mol Basis Dis. 2017;1863(3):764-9.
88. Vitvitsky V, Garg SK, Banerjee R. Taurine biosynthesis by neurons and astrocytes. J Biol Chem. 2011;286(37):32002-10.
89. Brand A, Leibfritz D, Hamprecht B, Dringen R. Metabolism of cysteine in astroglial cells: synthesis of hypotaurine and taurine. J Neurochem. 1998;71(2):827-32.
90. Hara K, Nakamura M, Haranishi Y, Terada T, Kataoka K, Sata T. Antinociceptive effect of intrathecal administration of hypotaurine in rat models of inflammatory and neuropathic pain. Amino Acids. 2012;43(1):397-404.
91. Stovell MG, Mada MO, Helmy A, Carpenter TA, Thelin EP, Yan JL, et al. The effect of succinate on brain NADH/NAD(+) redox state and high energy phosphate metabolism in acute traumatic brain injury. Sci Rep. 2018;8(1):11140.
92. Giorgi-Coll S, Amaral AI, Hutchinson PJA, Kotter MR, Carpenter KLH. Succinate supplementation improves metabolic performance of mixed glial cell cultures with mitochondrial dysfunction. Sci Rep. 2017;7(1):1003.
93. Forster DM, James MF, Williams SR. Effects of Alzheimer's disease transgenes on neurochemical expression in the mouse brain determined by 1H MRS in vitro. Nmr Biomed. 2012;25(1):52-8.
94. Tannahill GM, Curtis AM, Adamik J, Palsson-McDermott EM, McGettrick AF, Goel G, et al. Succinate is an inflammatory signal that induces IL-1 beta through HIF-1 alpha. Nature. 2013;496(7444):238-+.
95. Karlikova R, Micova K, Najdekr L, Gardlo A, Adam T, Majerova P, et al. Metabolic status of CSF distinguishes rats with tauopathy from controls. Alzheimers Res Ther. 2017;9.
96. Chae U, Kim HS, Kim KM, Lee H, Lee HS, Park JW, et al. IDH2 Deficiency in Microglia Decreases the Pro-inflammatory Response via the ERK and NF-kappaB Pathways. Inflammation. 2018;41(5):1965-73.
97. Manjeri GR, Rodenburg RJ, Blanchet L, Roelofs S, Nijtmans LG, Smeitink JA, et al. Increased mitochondrial ATP production capacity in brain of healthy mice and a mouse model of isolated complex I deficiency after isoflurane anesthesia. J Inherit Metab Dis. 2016;39(1):59-65.
98. O'Neill LA. A broken krebs cycle in macrophages. Immunity. 2015;42(3):393-4.
99. Bosoi CR, Rose CF. Elevated cerebral lactate: Implications in the pathogenesis of hepatic encephalopathy. Metab Brain Dis. 2014;29(4):919-25.
100. Wallis A, Butt H, Ball M, Lewis DP, Bruck D. Support for the microgenderome invites enquiry into sex differences. Gut Microbes. 2017;8(1):46-52.

101. Woltjer RL, Maezawa I, Ou JJ, Montine KS, Montine TJ. Advanced glycation endproduct precursor alters intracellular amyloid-beta/A beta PP carboxy-terminal fragment aggregation and cytotoxicity. J Alzheimers Dis. 2003;5(6):467-76.
102. Angeloni C, Zambonin L, Hrelia S. Role of methylglyoxal in Alzheimer's disease. Biomed Res Int. 2014;2014:238485.
103. Allaman I, Belanger M, Magistretti PJ. Methylglyoxal, the dark side of glycolysis. Front Neurosci-Switz. 2015;9.
104. Sadasivam M, Ramatchandirin B, Balakrishnan S, Selvaraj K, Prahalathan C. The role of phosphoenolpyruvate carboxykinase in neuronal steroidogenesis under acute inflammation. Gene. 2014;552(2):249-54.
105. Ko CW, Counihan D, Wu J, Hatzoglou M, Puchowicz MA, Croniger CM. Macrophages with a deletion of the phosphoenolpyruvate carboxykinase 1 (Pck1) gene have a more proinflammatory phenotype. Journal of Biological Chemistry. 2018;293(9):3399-409.
106. Das UN. Pyruvate is an endogenous anti-inflammatory and anti-oxidant molecule. Med Sci Monitor. 2006;12(5):Ra79-Ra84.
107. Gaignard P, Savouroux S, Liere P, Pianos A, Therond P, Schumacher M, et al. Effect of Sex Differences on Brain Mitochondrial Function and Its Suppression by Ovariectomy and in Aged Mice. Endocrinology. 2015;156(8):2893-904.
108. Wagner AK, Bayir H, Ren DX, Puccio A, Zafonte RD, Kochanek PM. Relationships between cerebrospinal fluid markers of excitotoxicity, ischemia, and oxidative damage after severe TBI: The impact of gender, age, and hypothermia. J Neurotraum. 2004;21(2):125-36.
109. Isopi E, Granzotto A, Corona C, Bomba M, Ciavardelli D, Curcio M, et al. Pyruvate prevents the development of age-dependent cognitive deficits in a mouse model of Alzheimer's disease without reducing amyloid and tau pathology. Neurobiology of Disease. 2015;81:214-24.
110. Koivisto H, Leinonen H, Puurula M, Hafez HS, Barrera GA, Stridh MH, et al. Chronic Pyruvate Supplementation Increases Exploratory Activity and Brain Energy Reserves in Young and Middle-Aged Mice. Front Aging Neurosci. 2016;8:41.
111. Lee HK, Kim ID, Kim SW, Lee H, Park JY, Yoon SH, et al. Anti-inflammatory and anti-excitoxic effects of diethyl oxopropanamide, an ethyl pyruvate bioisoster, exert robust neuroprotective effects in the postischemic brain. Sci Rep. 2017;7:42891.
112. Lee HK, Kim SW, Jin Y, Kim ID, Park JY, Yoon SH, et al. Anti-inflammatory effects of OBA-09, a salicylic acid/pyruvate ester, in the postischemic brain. Brain Res. 2013;1528:68-79.
113. Tabatabaie L, Klomp LWJ, Rubio-Gozalbo ME, Spaapen LJM, Haagen AAM, Dorland L, et al. Expanding the clinical spectrum of 3-phosphoglycerate dehydrogenase deficiency. J Inherit Metab Dis. 2011;34(1):181-4.
114. Ehmsen JT, Ma TM, Sason H, Rosenberg D, Ogo T, Furuya S, et al. D-Serine in Glia and Neurons Derives from 3-Phosphoglycerate Dehydrogenase. J Neurosci. 2013;33(30):12464-9.
115. Hamano M, Haraguchi Y, Sayano T, Zyao C, Arimoto Y, Kawano Y, et al. Enhanced vulnerability to oxidative stress and induction of inflammatory gene expression in 3-phosphoglycerate dehydrogenase-deficient fibroblasts. Febs Open Bio. 2018;8(6):914-22.
116. Knight J, Hinsdale M, Holmes R. Glycolate and 2-phosphoglycolate content of tissues measured by ion chromatography coupled to mass spectrometry. Anal Biochem. 2012;421(1):121-4.
117. Newman SF, Sultana R, Perluigi M, Coccia R, Cai J, Pierce WM, et al. An increase in S-glutathionylated proteins in the Alzheimer's disease inferior parietal lobule, a proteomics approach. J Neurosci Res. 2007;85(7):1506-14.
118. Irace C, Esposito G, Maffettone C, Rossi A, Festa M, Iuvone T, et al. Oxalomalate affects the inducible nitric oxide synthase expression and activity. Life Sci. 2007;80(14):1282-91.
119. Watanabe Y, Tateno H, Nakamura-Tsuruta S, Kominami J, Hirabayashi J, Nakamura O, et al. The function of rhamnose-binding lectin in innate immunity by restricted binding to Gb3. Dev Comp Immunol. 2009;33(2):187-97.
120. Hwang JJ, Jiang L, Hamza M, Dai F, Belfort-DeAguiar R, Cline G, et al. The human brain produces fructose from glucose. JCI Insight. 2017;2(4):e90508.
121. Xu JS, Begley P, Church SJ, Patassini S, McHarg S, Kureishy N, et al. Elevation of brain glucose and polyol-pathway intermediates with accompanying brain-copper deficiency in patients with Alzheimer's disease: metabolic basis for dementia. Sci Rep-Uk. 2016;6.
122. Mongkhon JM, Thach M, Shi Q, Fernandes JC, Fahmi H, Benderdour M. Sorbitol-modified hyaluronic acid reduces oxidative stress, apoptosis and mediators of inflammation and catabolism in human osteoarthritic chondrocytes. Inflamm Res. 2014;63(8):691-701.
123. Kauffman FC, Brown JG, Passonneau JV, Lowry OH. Effects of Changes in Brain Metabolism on Levels of Pentose Phosphate Pathway Intermediates. Journal of Biological Chemistry. 1969;244(13):3647-+.
124. Palmer AM. The activity of the pentose phosphate pathway is increased in response to oxidative stress in Alzheimer's disease. J Neural Transm. 1999;106(3-4):317-28.

125. Michelucci A, Cordes T, Ghelfi J, Pailot A, Reiling N, Goldmann O, et al. Immune-responsive gene 1 protein links metabolism to immunity by catalyzing itaconic acid production. P Natl Acad Sci USA. 2013;110(19):7820-5.
126. Asano T, Spector S. Identification of Inosine and Hypoxanthine as Endogenous Ligands for the Brain Benzodiazepine-Binding Sites. P Natl Acad Sci USA. 1979;76(2):977-81.
127. Rattigan KM, Pountain AW, Regnault C, Achcar F, Vincent IM, Goodyear CS, et al. Metabolomic profiling of macrophages determines the discrete metabolomic signature and metabolomic interactome triggered by polarising immune stimuli. Plos One. 2018;13(3).
128. Fang P, Li X, Luo JJ, Wang H, Yang XF. A Double-edged Sword: Uric Acid and Neurological Disorders. Brain Disord Ther. 2013;2(2):109.
129. McFarland NR, Burdett T, Desjardins CA, Frosch MP, Schwarzschild MA. Postmortem brain levels of urate and precursors in Parkinson's disease and related disorders. Neurodegener Dis. 2013;12(4):189-98.
130. Tohgi H, Abe T, Takahashi S, Kikuchi T. The urate and xanthine concentrations in the cerebrospinal fluid in patients with vascular dementia of the Binswanger type, Alzheimer type dementia, and Parkinson's disease. J Neural Transm Park Dis Dement Sect. 1993;6(2):119-26.
131. Bao LH, Zhang YN, Zhang JN, Gu L, Yang HM, Huang YY, et al. Urate inhibits microglia activation to protect neurons in an LPS-induced model of Parkinson's disease. J Neuroinflamm. 2018;15.
132. Bourre JM, Gozlandevillierre N, Morand O, Baumann N. Importance of Exogenous Saturated Fatty-Acids during Brain-Development and Myelination in Mice. Ann Biol Anim Bioch. 1979;19(Nb1):173-80.
133. Rodriguez-Navas C, Morselli E, Clegg DJ. Sexually dimorphic brain fatty acid composition in low and high fat diet-fed mice. Mol Metab. 2016;5(8):680-9.
134. Patil S, Chan C. Palmitic and stearic fatty acids induce Alzheimer-like hyperphosphorylation of tau in primary rat cortical neurons. Neurosci Lett. 2005;384(3):288-93.
135. Amtul Z, Uhrig M, Rozmahel RF, Beyreuther K. Structural Insight into the Differential Effects of Omega-3 and Omega-6 Fatty Acids on the Production of A beta Peptides and Amyloid Plaques. Journal of Biological Chemistry. 2011;286(8):6100-7.
136. Fraser T, Tayler H, Love S. Fatty Acid Composition of Frontal, Temporal and Parietal Neocortex in the Normal Human Brain and in Alzheimer's Disease. Neurochem Res. 2010;35(3):503-13.
137. Bourre JM, Gozlan-Devillierre N, Pollet S, Maurin Y, Baumann N. In vivo incorporation of exogenous stearic acid in synaptosomes: high occurrence of non-esterified fatty acids. Neurosci Lett. 1977;4(6):309-13.
138. Gupta S, Knight AG, Gupta S, Keller JN, Bruce-Keller AJ. Saturated long-chain fatty acids activate inflammatory signaling in astrocytes. J Neurochem. 2012;120(6):1060-71.
139. Moazedi AA, Hossienzadeh Z, Chinpardaz R. The effects of coadministration palmitic acid and oleic acid (omega 9) on spatial learning and motor activity in adult male rat. Pak J Biol Sci. 2007;10(20):3650-5.
140. Patil S, Sheng L, Masserang A, Chan C. Palmitic acid-treated astrocytes induce BACE1 upregulation and accumulation of C-terminal fragment of APP in primary cortical neurons. Neurosci Lett. 2006;406(1-2):55-9.
141. Yanguas-Casas N, Crespo-Castrillo A, de Ceballos ML, Chowen JA, Azcoitia I, Arevalo MA, et al. Sex differences in the phagocytic and migratory activity of microglia and their impairment by palmitic acid. Glia. 2018;66(3):522-37.
142. Odutuga AA. Long-term deficiency of essential fatty acids in rats and its effect on brain recovery. Clin Exp Pharmacol Physiol. 1979;6(4):361-6.
143. Harauma A, Yasuda H, Hatanaka E, Nakamura MT, Salem N, Jr., Moriguchi T. The essentiality of arachidonic acid in addition to docosahexaenoic acid for brain growth and function. Prostaglandins Leukot Essent Fatty Acids. 2017;116:9-18.
144. Snowden SG, Ebshiana AA, Hye A, An Y, Pletnikova O, O'Brien R, et al. Association between fatty acid metabolism in the brain and Alzheimer disease neuropathology and cognitive performance: A nontargeted metabolomic study. Plos Med. 2017;14(3).
145. Hussain G, Schmitt F, Loeffler JP, de Aguilar JLG. Fatting the brain: a brief of recent research. Frontiers in Cellular Neuroscience. 2013;7.
146. Scherma M, Masia P, Satta V, Fratta W, Fadda P, Tanda G. Brain activity of anandamide: a rewarding bliss? Acta Pharmacol Sin. 2019;40(3):309-23.
147. Boutaud O, Montine TJ, Chang L, Klein WL, Oates JA. PGH2-derived levuglandin adducts increase the neurotoxicity of amyloid beta1-42. J Neurochem. 2006;96(4):917-23.
148. Saper CB, Romanovsky AA, Scammell TE. Neural circuitry engaged by prostaglandins during the sickness syndrome. Nat Neurosci. 2012;15(8):1088-95.
149. Martano G, Murru L, Moretto E, Gerosa L, Garrone G, Krogh V, et al. Biosynthesis of glycerol phosphate is associated with long-term potentiation in hippocampal neurons. Metabolomics. 2016;12(8).

150. Owen L, Sunram-Lea SI. Metabolic Agents that Enhance ATP can Improve Cognitive Functioning: A Review of the Evidence for Glucose, Oxygen, Pyruvate, Creatine, and L-Carnitine. Nutrients. 2011;3(8):735-55.
151. Zhang C, Rissman RA, Feng J. Characterization of ATP alternations in an Alzheimer's disease transgenic mouse model. J Alzheimers Dis. 2015;44(2):375-8.
152. Inoue K. Microglial activation by purines and pyrimidines. Glia. 2002;40(2):156-63.
153. Davalos D, Grutzendler J, Yang G, Kim JV, Zuo Y, Jung S, et al. ATP mediates rapid microglial response to local brain injury in vivo. Nat Neurosci. 2005;8(6):752-8.
154. Izumi Y, Benz AM, Katsuki H, Matsukawa M, Clifford DB, Zorumski CF. Effects of fructose-1,6-bisphosphate on morphological and functional neuronal integrity in rat hippocampal slices during energy deprivation. Neuroscience. 2003;116(2):465-75.
155. Veras FP, Peres RS, Saraiva AL, Pinto LG, Louzada-Junior P, Cunha TM, et al. Fructose 1,6-bisphosphate, a high-energy intermediate of glycolysis, attenuates experimental arthritis by activating anti-inflammatory adenosinergic pathway. Sci Rep. 2015;5:15171.
156. Lenglet A, Liabeuf S, Bodeau S, Louvet L, Mary A, Boullier A, et al. N-methyl-2-pyridone-5-carboxamide (2PY)-Major Metabolite of Nicotinamide: An Update on an Old Uremic Toxin. Toxins. 2016;8(11).
157. Sternak M, Khomich TI, Jakubowski A, Szafarz M, Szczepanski W, Bialas M, et al. Nicotinamide N-methyltransferase (NNMT) and 1-methylnicotinamide (MNA) in experimental hepatitis induced by concanavalin A in the mouse. Pharmacol Rep. 2010;62(3):483-93.

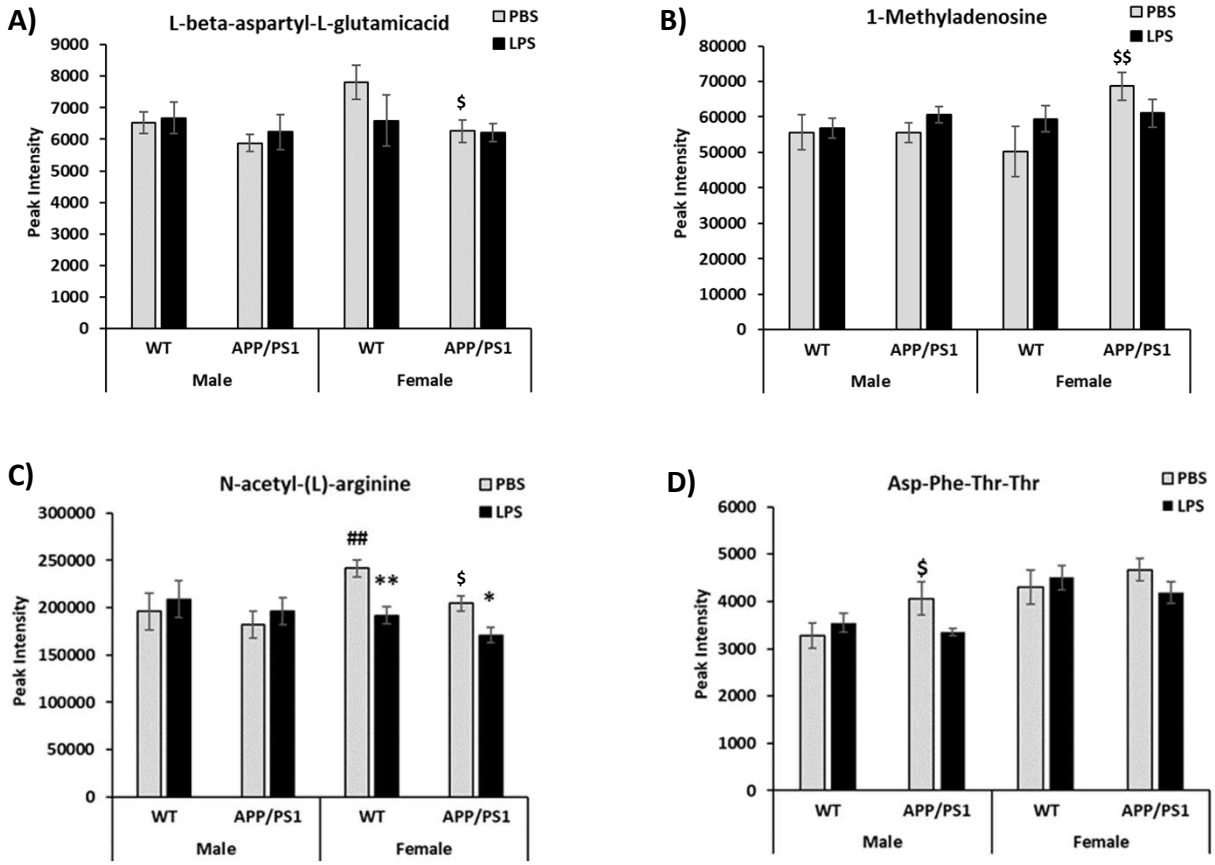

Supplementary. Fig. 2. Metabolites affected in APP/PS1 mice in the absence of immune stimulation. Levels of L-beta-aspartyl-L-glutamic acid, were particularly reduced in female APP/PS1 mice (A). B) 1-Methyladenosine, was more abundant in the hippocampus of female APP/PS1 mice compared to their WT female littermates (B). Significant Genotype X Treatment interactions were also found for N-acetyl-(L)-arginine ($F_{(1,34)}$=12.07, p=0.001), whose levels were significantly lower in PBS-treated APP/PS1 females compared to PBS-treated WT females (C), and for the hydrophobic tetrapeptide Asp-Phe-Thr-Thr ($F_{(1,34)}$=5.40, p=0.03), whose levels were significantly increased in PBS-treated APP/PS1 males compared to their PBS-treated counterparts (D). Data are expressed as Means $\pm$ SEM. Pairwise comparisons following 3-way ANOVAs: $^{\$}$, p<0.05; $^{\$\$}$, p<0.01 compared to WT PBS-treated (same sex); $^{\#\#}$, p<0.01 compared to PBS-treated males (same genotype); *, p<0.05; **, p<0.01 compared to PBS-treated mice of same sex and genotype.

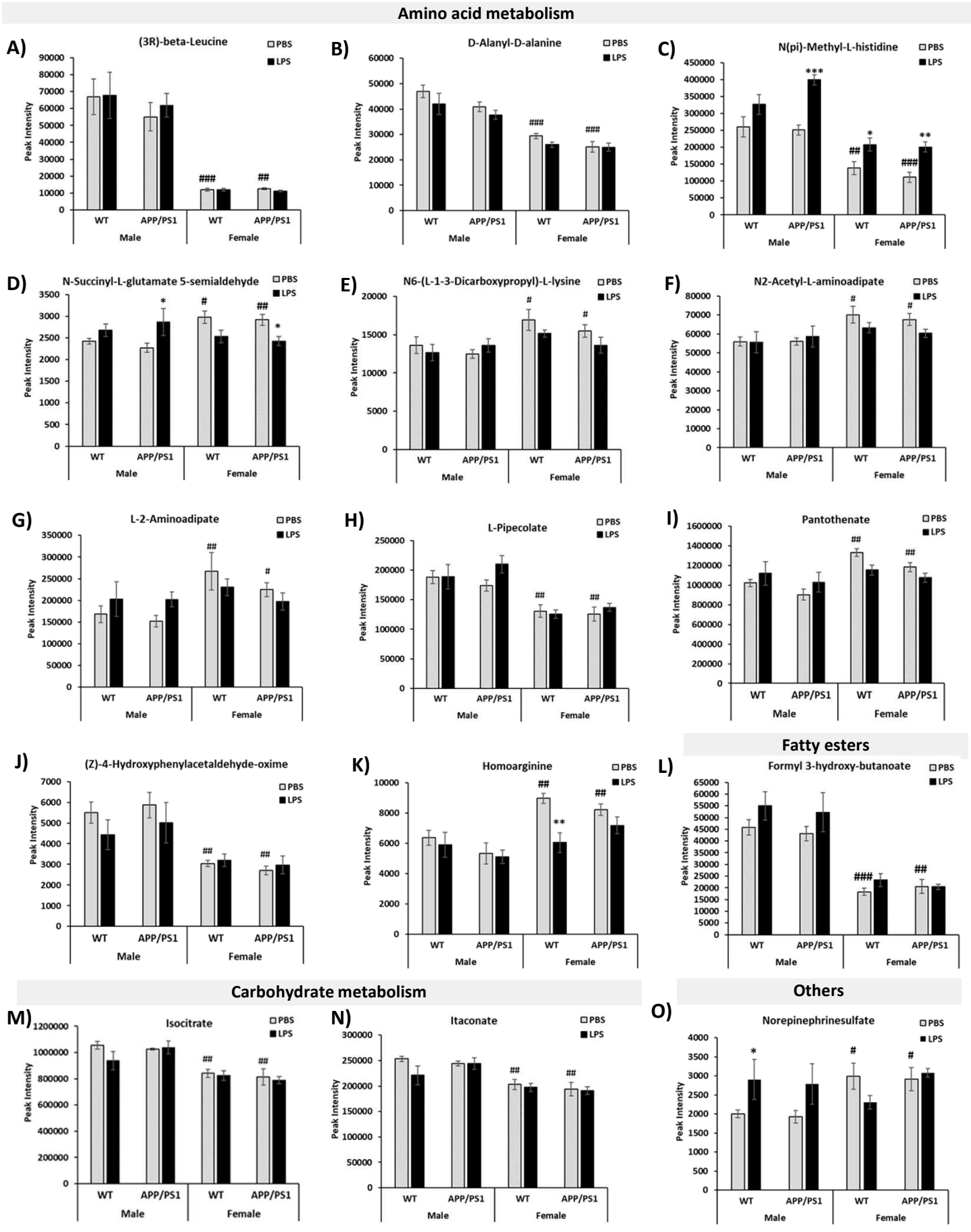

Supplementary Figure 3. Metabolites with sex differences in the hippocampus. Data are expressed as Means ± SEM. Post-hoc tests following 3-way ANOVAs: #, p<0.05, ##, p<0.01 compared to PBS-treated males (same genotype); **, p<0.01; ***, p<0.0001 compared to PBS-treated mice of same sex and genotype.

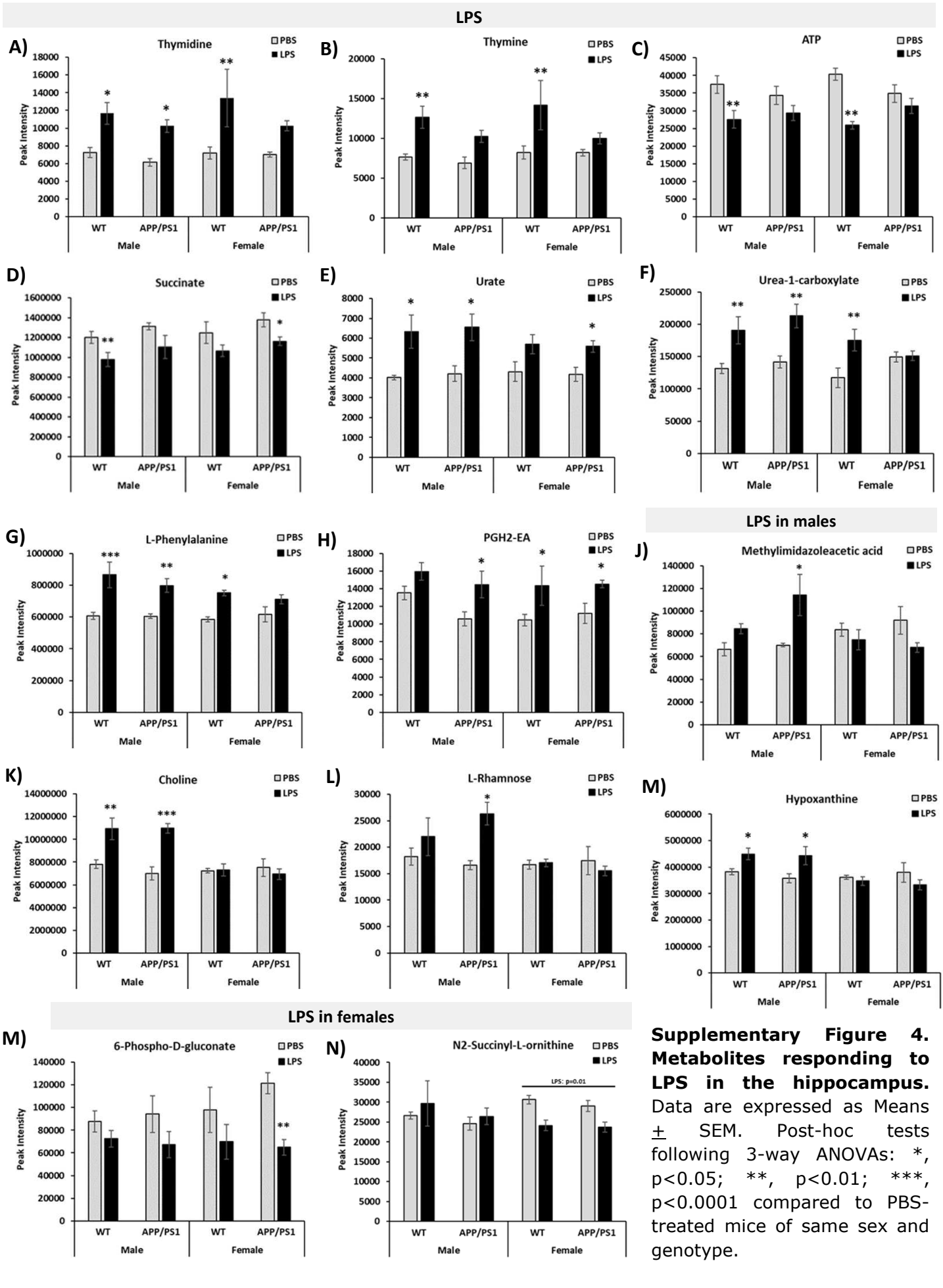

Supplementary Figure 4. Metabolites responding to LPS in the hippocampus. Data are expressed as Means ± SEM. Post-hoc tests following 3-way ANOVAs: *, $p<0.05$; **, $p<0.01$; ***, $p<0.0001$ compared to PBS-treated mice of same sex and genotype.

Supplementary table 3. Results of the two-way repeated measure ANOVAs on glial measures.

	% area stained by Iba1	Number of cells/mm²	Microglial soma area	% area stained by GFAP
Whole hippocampus				
Genotype	$F_{(1,35)}$=0.96; p=0.33	$F_{(1,35)}$=0.43; p=0.51	$F_{(1,35)}$=0.00; p=0.95	$F_{(1,33)}$=3.81; p=0.059
Sex	$F_{(1,35)}$=0.80; p=0.38	$F_{(1,35)}$=3.28; p=0.08	$F_{(1,35)}$=2.16; p=0.15	$F_{(1,33)}$=1.02; p=0.32
Treatment	$F_{(1,35)}$=2.26; p=0.14	$F_{(1,35)}$=1.39; p=0.24	$F_{(1,35)}$=0.20; p=0.66	$F_{(1,33)}$=0.16; p=0.69
Genotype X Sex	**$F_{(1,35)}$=4.14; p=0.049**	$F_{(1,35)}$=3.01; p=0.09	$F_{(1,35)}$=0.20; p=0.75	$F_{(1,33)}$=0.87; p=0.36
Genotype X Treatment	$F_{(1,35)}$=0.65; p=0.42	$F_{(1,35)}$=0.22; p=0.64	$F_{(1,35)}$=0.10; p=0.70	$F_{(1,33)}$=0.13; p=0.72
Sex X Treatment	$F_{(1,35)}$=0.71; p=0.40	$F_{(1,35)}$=0.23; p=0.64	$F_{(1,35)}$=0.75; p=0.39	$F_{(1,33)}$=0.66; p=0.42
Genotype X Sex X Treatment	$F_{(1,35)}$=0.98; p=0.33	$F_{(1,35)}$=1.75; p=0.19	$F_{(1,35)}$=0.42; p=0.52	$F_{(1,33)}$=0.06; p=0.80
CA1				
Genotype	$F_{(1,35)}$=1.08; p=0.31	$F_{(1,35)}$=0.07; p=0.79	$F_{(1,35)}$=0.02; p=0.90	$F_{(1,33)}$=4.13; p=0.0503
Sex	$F_{(1,35)}$=1.45; p=0.24	$F_{(1,35)}$=3.21; p=0.08	$F_{(1,35)}$=1.60; p=0.21	$F_{(1,33)}$=1.03; p=0.32
Treatment	$F_{(1,35)}$=3.30; p=0.08	$F_{(1,35)}$=0.19; p=0.66	$F_{(1,35)}$=0.15; p=0.70	$F_{(1,33)}$=0.16; p=0.69
Genotype X Sex	$F_{(1,35)}$=3.56; p=0.07	$F_{(1,35)}$=1.95; p=0.17	$F_{(1,35)}$=0.06; p=0.80	$F_{(1,33)}$=0.43; p=0.52
Genotype X Treatment	$F_{(1,35)}$=0.51; p=0.48	$F_{(1,35)}$=0.13; p=0.72	$F_{(1,35)}$=0.03; p=0.86	$F_{(1,33)}$=0.03; p=0.85
Sex X Treatment	$F_{(1,35)}$=1.15; p=0.29	$F_{(1,35)}$=0.50; p=0.48	$F_{(1,35)}$=0.42; p=0.52	$F_{(1,33)}$=0.20; p=0.66
Genotype X Sex X Treatment	$F_{(1,35)}$=0.89; p=0.35	$F_{(1,35)}$=1.76; p=0.19	$F_{(1,35)}$=0.52; p=0.48	$F_{(1,33)}$=0.68; p=0.42
CA2				
Genotype	$F_{(1,35)}$=0.82; p=0.37	$F_{(1,34)}$=0.45; p=0.51	$F_{(1,34)}$=0.34; p=0.56	$F_{(1,32)}$=0.18; p=0.67
Sex	$F_{(1,35)}$=0.73; p=0.40	$F_{(1,34)}$=0.66; p=0.42	$F_{(1,34)}$=2.01; p=0.16	$F_{(1,32)}$=0.13; p=0.72
Treatment	$F_{(1,35)}$=1.29; p=0.26	$F_{(1,34)}$=1.00; p=0.32	$F_{(1,34)}$=0.22; p=0.64	$F_{(1,32)}$=1.93; p=0.17
Genotype X Sex	**$F_{(1,35)}$=4.24; p=0.047**	$F_{(1,34)}$=2.26; p=0.14	$F_{(1,34)}$=0.04; p=0.84	$F_{(1,32)}$=0.03; p=0.87
Genotype X Treatment	$F_{(1,35)}$=0.02; p=0.90	$F_{(1,34)}$=0.10; p=0.75	$F_{(1,34)}$=0.09; p=0.77	$F_{(1,32)}$=0.00; p=0.99
Sex X Treatment	$F_{(1,35)}$=0.11; p=0.74	$F_{(1,34)}$=0.61; p=0.44	$F_{(1,34)}$=0.93; p=0.34	$F_{(1,32)}$=1.54; p=0.22
Genotype X Sex X Treatment	$F_{(1,35)}$=0.29; p=0.59	$F_{(1,34)}$=0.03; p=0.85	$F_{(1,34)}$=0.95; p=0.33	$F_{(1,32)}$=0.13; p=0.71
CA3				
Genotype	$F_{(1,36)}$=2.50; p=0.12	$F_{(1,36)}$=1.79; p=0.19	$F_{(1,36)}$=0.00; p=0.99	$F_{(1,33)}$=1.21; p=0.28
Sex	$F_{(1,36)}$=0.97; p=0.33	$F_{(1,36)}$=1.55; p=0.22	$F_{(1,36)}$=3.62; p=0.06	$F_{(1,33)}$=0.41; p=0.53
Treatment	$F_{(1,36)}$=1.77; p=0.19	$F_{(1,36)}$=3.08; p=0.09	$F_{(1,36)}$=0.01; p=0.93	$F_{(1,33)}$=0.24; p=0.63
Genotype X Sex	**$F_{(1,36)}$=7.37; p=0.01**	$F_{(1,36)}$=3.04; p=0.09	$F_{(1,36)}$=0.00; p=0.96	$F_{(1,33)}$=0.76; p=0.39
Genotype X Treatment	$F_{(1,36)}$=0.56; p=0.46	$F_{(1,36)}$=0.59; p=0.45	$F_{(1,36)}$=0.16; p=0.69	$F_{(1,33)}$=0.09; p=0.76
Sex X Treatment	$F_{(1,36)}$=0.98; p=0.33	$F_{(1,36)}$=0.03; p=0.85	$F_{(1,36)}$=0.68; p=0.41	$F_{(1,33)}$=1.15; p=0.29
Genotype X Sex X Treatment	$F_{(1,36)}$=0.47; p=0.49	$F_{(1,36)}$=0.05; p=0.82	$F_{(1,36)}$=1.08; p=0.30	$F_{(1,33)}$=0.01; p=0.93
Dentate Gyrus				
Genotype	$F_{(1,36)}$=1.33; p=0.26	$F_{(1,36)}$=0.17; p=0.68	$F_{(1,36)}$=0.04; p=0.83	$F_{(1,33)}$=3.43; p=0.07
Sex	$F_{(1,36)}$=0.82; p=0.37	$F_{(1,36)}$=3.69; p=0.06	$F_{(1,36)}$=2.82; p=0.10	$F_{(1,33)}$=0.15; p=0.70
Treatment	$F_{(1,36)}$=3.15; p=0.08	$F_{(1,36)}$=0.00; p=0.99	$F_{(1,36)}$=0.75; p=0.39	$F_{(1,33)}$=0.09; p=0.77
Genotype X Sex	$F_{(1,36)}$=2.81; p=0.10	**$F_{(1,36)}$=5.02; p=0.03**	$F_{(1,36)}$=0.01; p=0.92	$F_{(1,33)}$=0.68; p=0.41
Genotype X Treatment	$F_{(1,36)}$=0.14; p=0.71	$F_{(1,36)}$=0.45; p=0.50	$F_{(1,36)}$=0.50; p=0.48	$F_{(1,33)}$=0.94; p=0.34
Sex X Treatment	$F_{(1,36)}$=0.51; p=0.48	$F_{(1,36)}$=0.11; p=0.74	$F_{(1,36)}$=0.96; p=0.34	$F_{(1,33)}$=1.75; p=0.19
Genotype X Sex X Treatment	$F_{(1,36)}$=0.83; p=0.36	$F_{(1,36)}$=1.17; p=0.29	$F_{(1,36)}$=0.02; p=0.90	$F_{(1,33)}$=0.10; p=0.76

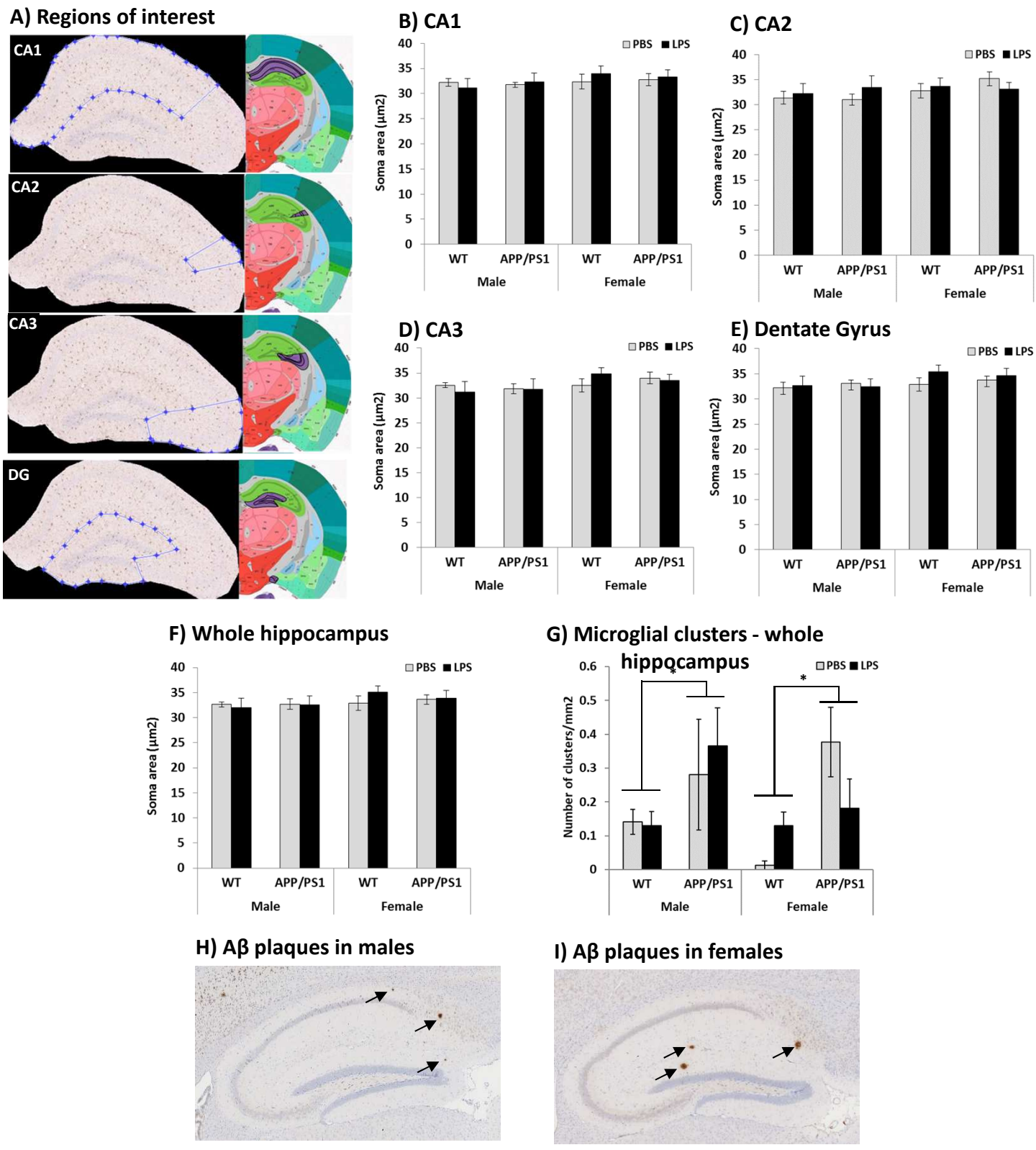

Supplementary Figure 5. Microglial soma size a morphometric marker of microglial activation was measured using Iba1 immunostaining at 4 hours after the PBS or LPS challenge. Illustration of the regions of interests used for microglia and astrocytes segmentation, delineated using a custom made Matlab tool. No differences were found in the whole hippocampus (B), CA1(C), CA2 (D), CA3 (E) or Dentate Gyrus (F) subfields. The number of microglial clusters was elevated in APP/PS1 mice ($F_{(1,35)}$=10.05, p=0.003; G), which displayed relatively few plaques (white arrows) at 4.5 months of age (H, I). *, p<0.05. Data are expressed as Means ± SEM.

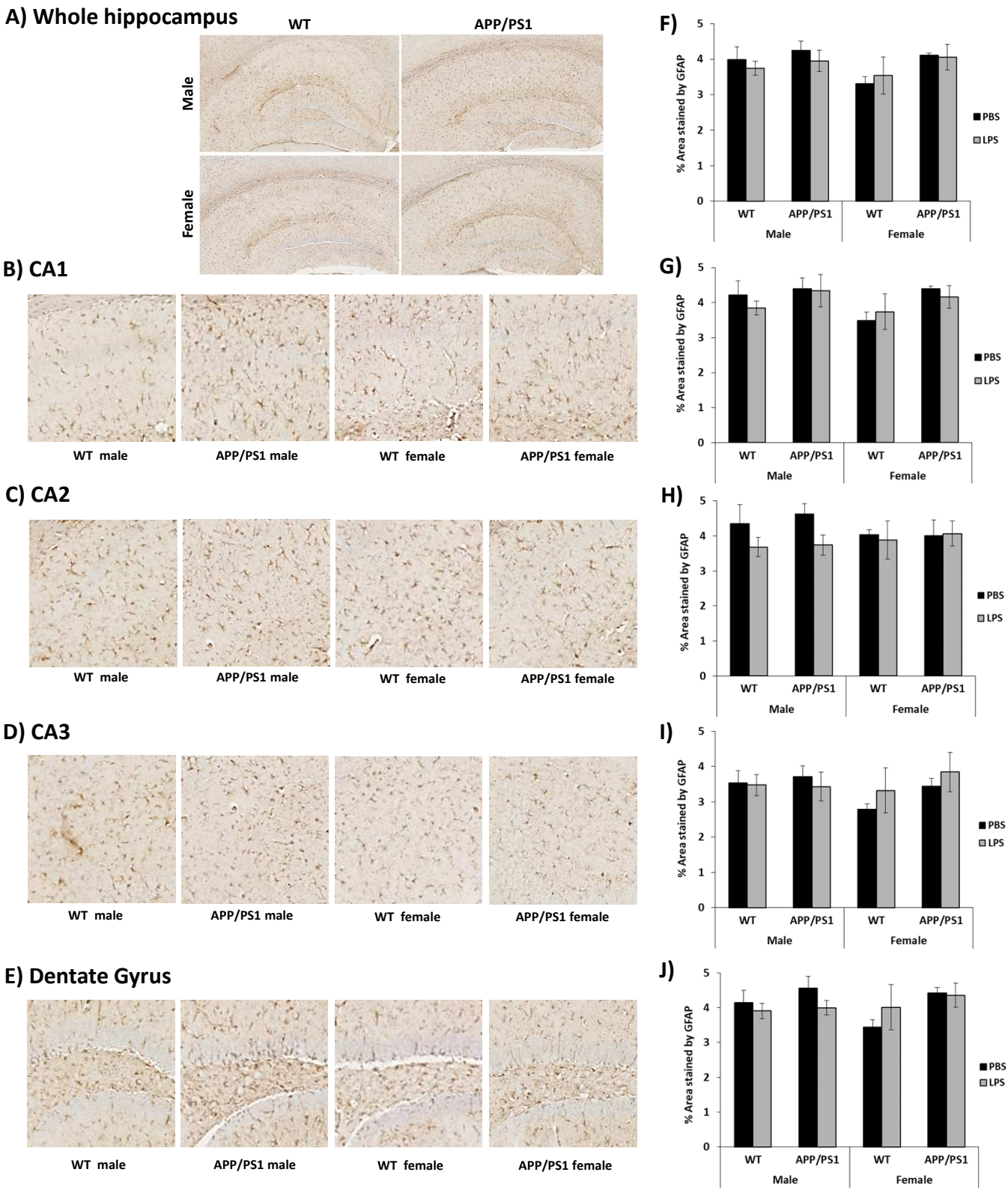

Supplementary Figure 6. The area occupied by astrocytes was quantified using GFAP immunostaining 4 hours after the PBS or LPS challenge. Representative image of GFAP positive astrocytes in the whole hippocampus (A), CA1(B), CA2 (C), CA3 (D) or Dentate Gyrus (E) subfields. No differences were found between any of the experimental conditions in these regions of interests: whole hippocampus (F), CA1(G), CA2 (H), CA3 (I) or Dentate Gyrus (J). Data are expressed as Means $\pm$ SEM.

Highlights:

- Hippocampal metabolic profile of females is more pro-inflammatory and pro-oxidant
- Comparable LPS-induced sickness behaviour in male and female WT and APP/PS1 mice
- Pro- and anti-inflammatory pathways both recruited 4h after systemic LPS
- Predominant anti-inflammatory metabolic response to LPS in female hippocampi